Mansoura University
Faculty of Engineering
Public Works Eng. Department

Leveling By Using Global Positioning System

By

Eng./ Mosbeh Rashed Mosbeh Kaloop

B.Sc. Civil Engineering - Mansoura University, 2002
Demonstrator in Public Works Department- Mansoura University

A Thesis

Submitted in Partial Fulfillment for the
Requirement of the Degree of Master of Science

Supervisors

Dr./Mahmoud El-Mowafi

Associate Professor
Public Works Department
Faculty of Engineering
Mansoura University

Dr./ Mostafa Mousa Rabah

Ass. Prof. in Geomatic Engineering in
Geodynamic Department, National Research
Institute of Astronomy and Geophysics,
Helwan, Cairo, Egypt

2005

Chapter (1)

INTRODUCTION

1.1 General

Determination of geoid has been one of the main research areas in science of Geodesy for decades. According to the wide spread use of GPS in geodetic applications, great attention is paid to the precise determination of local/regional geoid with an aim to replace the geometric leveling, which is very onerous measurement work, with GPS surveys. GPS technique provides the surveyor with three-dimensional coordinates including ellipsoidal heights (h) with respect to its reference ellipsoid "the geocentric WGS84 (World Geodetic System 1984)". As in GPS measurements, geodesists have chosen an oblate ellipsoid of revolution, flattened at the poles, to approximate the geoid in order to simplify survey data reduction and mapping. However, most surveying measurements are made in relation to the geoid, which is the equipotential surface of the earth gravity field, not ellipsoid because the equipment is aligned with the local gravity vector, which is perpendicular to the geoid surface, usually through the use of a spirit bubble.

Normally, "H" orthometric height is derived from leveling measurements, but these measurements are tiring applications. So, while having a geoid model in the region as the essential part of geodetic infrastructure, number of leveling measurements can be reduced using this procedure and by this way time and labor is saved. Geoid determination is modeling of the data in such a way that geoid height can be obtained digital or analog at a point whose horizontal position is known. Geoid models can be developed for local, regional or global

regions. Using satellite techniques, especially GPS, in geodetic measurements are increased importance of geoid. Because geoid is a natural tie between high precision geodetic coordinates and coordinates which obtained from satellites.
There are several geoid determination methods according to used data and models. GPS/Leveling method, which is also known as geometric method, is one of these methods. This method is appropriate for local precise geoid determination in respectively small areas. In this search, it is going to be given information about GPS/Leveling geoid determination method and mathematical models, which are used in geoid determination with this method.

1.2 Scope of the Thesis

The current thesis contains six chapters including this chapter. In the following a brief description for the contents of each chapter:

- Chapter (2) contains the global positioning system (GPS) observations, different observations techniques and their related errors. In addition, the common utilized techniques that one can apply to reduce these errors.
- Chapter (3) contains the definition of the datum and the relation between the different datums. It also displays the different methods used to calculate the geoid undulation (practical and mathematical techniques), description of the theory of mathematical techniques (regression, least square collocation and minimum surface curvature). Finally, a review about computations of geoid in Egypt is outlined.
- Chapter (4) presents the algorithms of the mathematical models of the different techniques that have been used in our developed programs.

- Chapter (5) demonstrates the computed results from these mathematical models as well as discussions for these results are made. In addition, a comparison between the results of the different techniques is done, where finally the best technique is derived. Therefore, we use this technique to calculate a geoidal undulation model for Egypt based upon the data what we have in our hand. Of course, the quality of the resulted model is strongly correlated to the quality and the distribution of the available data points.
- Chapter (6) outlines the summary and conclusion of the thesis and the recommendations for future work in this field.
- A list of the used reference in the research is introduced in Reference Chapter. In addition a list of appendices is outlined where Appendix (A) contains the table of geoid undulation for estimating the minimum surface curvature technique at the node of grid for the Egyptian map. Appendix (B) contains the table of geoid undulation for estimating the 2^{nd} degree of regression technique at the node of grid for the Egyptian map. Appendix (C) contains the table of geoid undulation for estimating the least square collocation technique at the node of grid for the Egyptian map. Finally, Appendix (D) contains the different programs used in this research.

Chapter (2)

PRECISE GPS POSITIONING

2.1 Introduction

The global positioning system (GPS) is a satellite based radio positioning system designed for accurate positioning information in three dimensions (Latitude, Longitude and Height), that is, vertical as well as horizontal information is provided. The satellites continuously send radio signals that can be received by suitable equipments. Computer programs are used to process the data and to determine the relative positions of points on the earth's surface. Positions can be determined to about a centimeter using GPS. Elevations determined by GPS observations differ from the elevations shown on topographic map. The topographic elevations, called orthometric heights, are determined by techniques that make use of a local horizontal surface. Most topographic elevations are refered to the height above mean sea level (MSL) determined by leveling but GPS elevations, called geometric heights, are referenced to the center of mass of the earth, not to sea level. An overview of GPS observation technique and its accuracy is introduced in this chapter.

2.2 General description of the global positioning system

The global positioning system GPS is a system of 27 satellites that orbit at approximately 20000 km above the surface of the Earth. The satellites are launched into six orbital planes, 60 degrees apart at an inclination of 55 degrees with respect to the equator. The constellation of GPS satellites provides all-weather, world-wide, and continuous measurements, providing line-of-sights to the satellites are available. These characteristics make GPS observations

advantageous for positioning and navigation, and remote sensing applications [V. Hoyle, 2005].

This system is composed of three segments, which are a space segment, a control segment and user segment. The space segment contains the satellites that broadcast the ranging signal. The control segment consists of the ground monitor stations that perform the satellite tracking, orbit determination and time synchronization. The user segment is made up of the GPS receivers that translate the satellite ranging signals into a point position solution [C.Liu, 1993] as shown in figure (2.1).

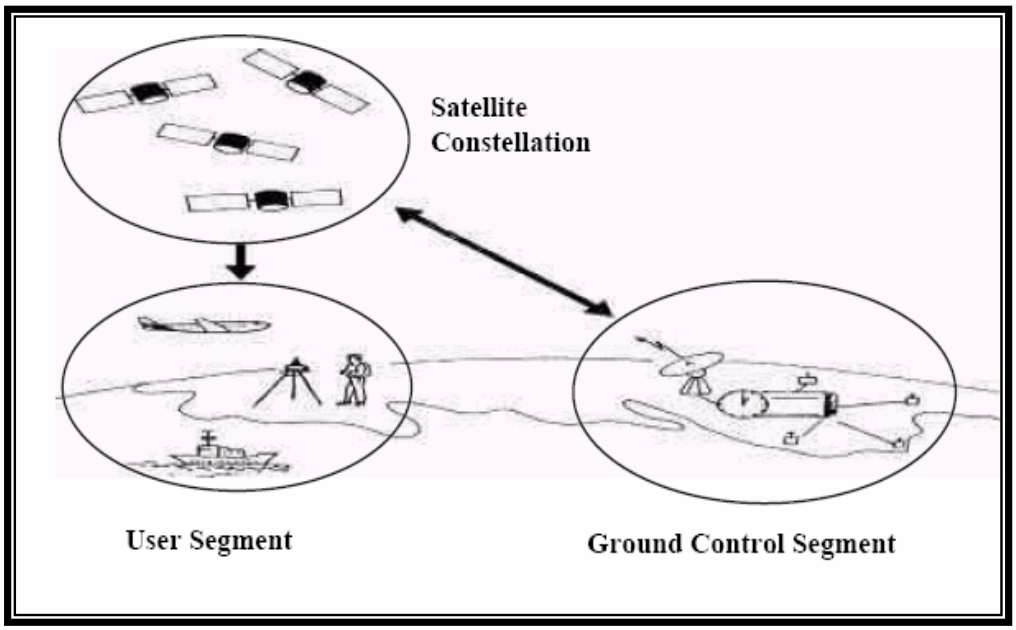

Figure (2.1) GPS elements

The primary task of GPS surveying is to measure the distances between 27 satellites in known orbits at a height of 20,000 km above the earth. Once ranges have been measured, the coordinates of positions on the earth are calculated by triangulation [Bradford W. Parkinson,1996]. Distances are measured based on

the amount of time required for an electromagnetic GPS signal to travel from the satellites to ground-based antennas and receivers. Antennas collect the satellite signal and convert the electromagnetic waves into electric currents that can be recorded by the receiver [Leick, A., 1990].

There are two main GPS surveying methods, kinematics and static surveying. The type and accuracy of positioning in kinematics and static surveying is dependent on the number of receivers available. There are two types of positioning, single point and relative. Single-point positioning is the determination of a ground position using one receiver and observable from one or more satellites. Single-point positioning relies on the pseudorange observable. The accuracy of the single-point positioning increases with the number of satellites available. Relative positioning is the determination of a ground position using two or more receivers and two or more satellites. Relative positioning determines the precise vector (baseline) between receiver's positions. When the coordinates of one of the receiver positions is known, we referred to it as a base station in the known coordinates and baseline can be used to determine the precise coordinates of the unknown points [Van Sickle J., 1996].

The GPS receiver records raw data on a 24-hour basis. The measurements are stored in the computer of the system and these are available to surveyors or other users, working with GPS in the area of observations. Then, they can use these GPS measurements for post-processing positioning computations.

The GPS satellites continuously transmit signals on the frequencies; L1=1575.42 MHZ and L2=1227.60 MHZ. The associated wavelengths of the

L1 and L2 carriers are approximately19 cm and 24 cm, respectively. GPS modernization a third frequency L5 (1176.45 MHZ) add to GPS satellite [Z.Liu, 2004]. This will lead to more accurate dual-frequency measurements, so the ionospheric error can be determined more accurately [M.C.Olynik, 2002]. These carriers are modulated with two types of code, namely the Clear Acquisition (C / A) code and the Precise (P) code. The L1 carrier is modulated with the C / A and P code, and L2 carrier is modulated with P code only as shown in figure (2.2). For comparisons of code and carrier measurements, Carrier wavelengths are much shorter than the C/A code chip length and consequently can be measured more accurately and used to achieve much higher positional accuracies than code measurements. Indeed the best relative accuracies achieved using code measurements are usually a few meter and using carrier measurement are usually a few centimeters. Table (2.1) summarizes advantages and disadvantages of code and carrier observations after EMR (1995).

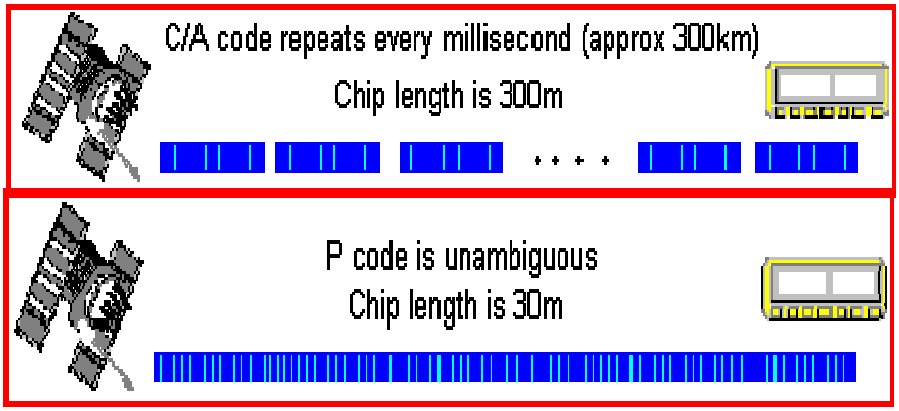

Figure (2.2) The C/A and P code

Table (2.1) Key advantages and disadvantages of Code and Carrier observation

	Code	Carrier
Advantages	Non-ambiguous simple	High accuracy potential
Disadvantages	Low accuracy	More complex

Two different kinds of codes with two different accuracies can be used. In this content two frequency signals can be used for the correction of ionospheric effects on GPS measurements. The concept of positioning with GPS is based on simultaneous ranging to at least four GPS satellite to determine the unknown coordinates of a point. From a geometric point of view, a unique solution can be obtained if the distances from three satellites with known coordinates are measured [C.Liu, 1993]. Because the GPS satellite clocks cannot be synchronized with the user clock, a fourth unknown (the clock bias) is introduced. Therefore, a minimum of four satellites is used to determine the three-dimensional position vector. The determination of point coordinates is affected by many errors discussed later in this chapter. The method of single

point positioning cannot generally meet precise positioning requirements. The differential GPS positioning method can, significantly reduce the above errors. Major types of possible positioning methods; as follow;

Single point versus relative positioning, positioning with GPS may take the form of single point positioning or relative positioning. In single point positioning coordinates of a receiver at an "unknown" point are sought with respect to the earth's reference frame by using the "known" positions of the GPS Satellites being tracked. Single point positioning is also referred to as absolute positioning, and often just as point positioning [EMR, 1995]. In relative positioning, the coordinates of a receiver at an "unknown" point are sought with respect to a receiver at a "known" point. The concept of single point positioning is illustrated in figure (2.3). Using the broadcast ephemerides, the position of any satellite at any point in time may be computed.

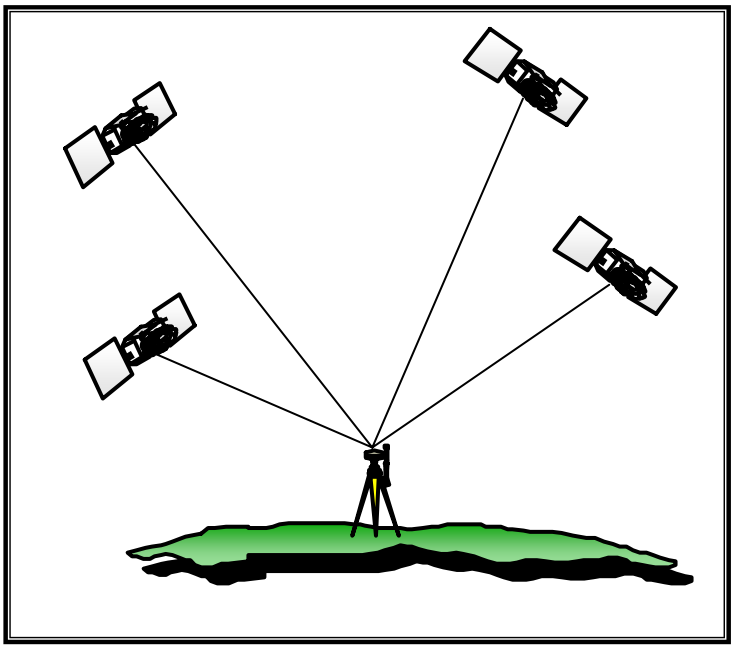

Figure (2.3) Single point positioning

The concept of relative positioning is illustrated in figure (2.4). Instead of determining the position of one point on the earth with respect to the satellites (as done in single point positioning), the position of one point on the earth is determined with respect to another "known" point. The advantage of using relative rather than single point positioning is that much higher accuracies are achieved because most GPS observation errors are common to the known and unknown site and are reduced in data processing [H.Abou-Halima, 2002].

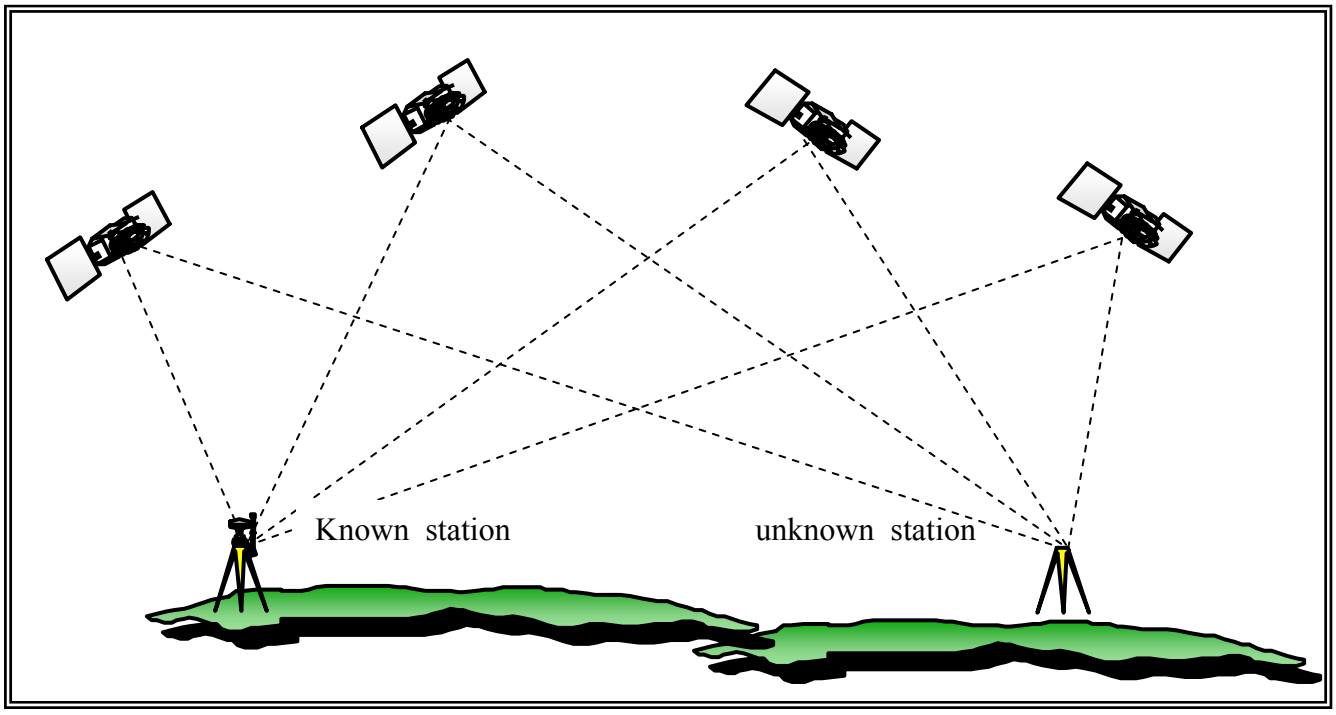

Figure (2.4) The Differential GPS

Static versus Kinematic Positioning, GPS positioning may also be categorized as static or kinematic. In static positioning, a GPS receiver is required to be stationary whereas in kinematic positioning a receiver collects GPS data while moving. The concepts of static and kinematic positioning for both single point and relative positioning cases are illustrated in figure (2.5). Note that for

kinematic relative positioning one receiver, referred to as a monitor, is left stationary on a known point while a second receiver, referred to as a rover, is moved over the path to be positioned [H.Abou-Halima, 2002].

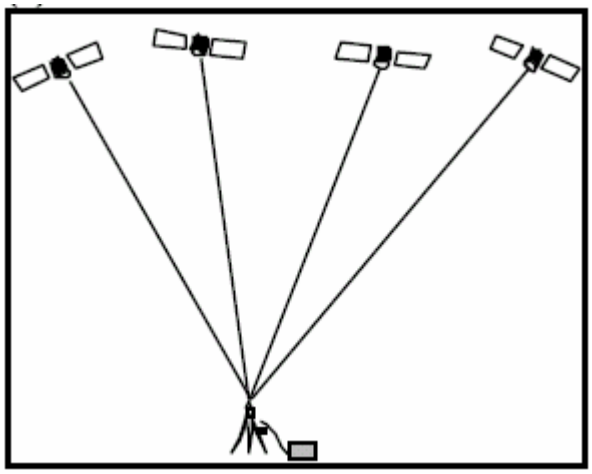

(a) Static single point positioning

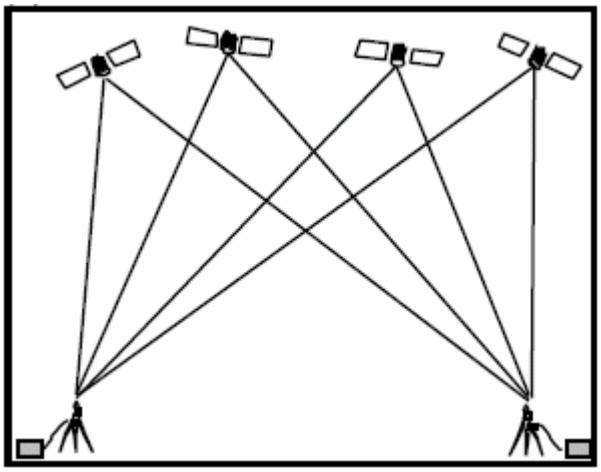

(b) static relative positioning

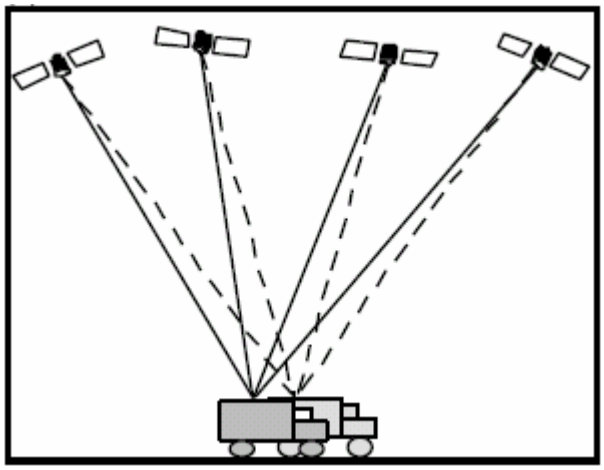

(c) Kinematic single point positioning

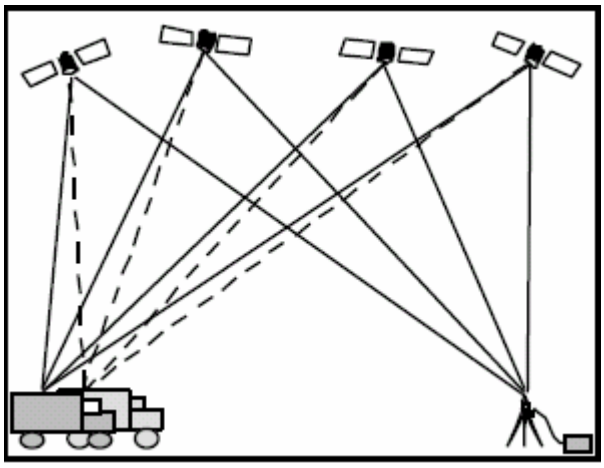

(d) kinematic relative positioning

Figure (2.5) Static and kinematic

Real-Time versus Post-Mission, GPS positions may be attained through real-time or post-mission processing as shown in figure (2.6). In real-time processing, positions are computed almost instantaneously, on site. In post-mission processing, data is combined and reduced after all data collection has been completed. Real-time relative positioning requires a data link to transmit corrections from a monitor receiver at a known point to a rover receiver at an unknown point as shown in figure (2.6a).

Post-mission processing for relative positioning requires physically bringing together the data from all receivers after an observation period as shown in figure (2.10d). Even with real-time point positioning, for many GPS applications it is still necessary to download data and enter it in a database specific to the user's application as shown in figure (2.6b). Very low accuracy code single point positioning is usually computed by GPS receivers in real-time, whereas very high accuracy carrier relative positioning is almost always dependent on post-mission processing. Real-time and post-mission processing options exist for methodologies which yield accuracies between these two extremes [EMR, 1995].

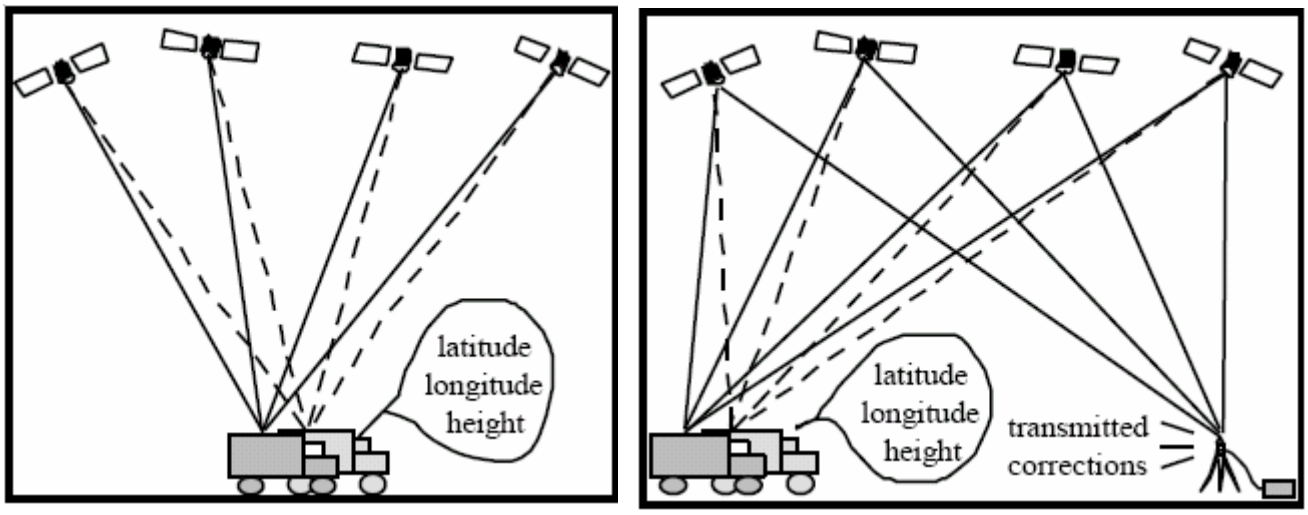

(a) Real-Time Point Positioning (b) Real-Time Relative Positioning

(c) Data Management For Relative Positioning (d) Post-Mission Processing For Point Positioning

Figure (2.6) Real-Time and Post-Mission Processing

2.3 GPS measurement models

The following three types of measurements can be obtained from most GPS receivers [Mark G. Petovello, 2003] :

[A] Pseudorange (code) measurements

These are derived from the satellite codes and are therefore classified according to code and frequency as L1-C/A, L1-P and L2-P.

[B] Carrier phase measurements

By measuring the phase of the incoming carrier (L1 and/or L2), the range to a satellite can be measured with an ambiguous number of cycles.

[C] Doppler measurements

The derivative of the carrier phase measurement is the Doppler shift caused by the relative receiver-satellite motion. The three types can be explained as following:

2.3.1 Pseudorange observation

This type is the time delay between the transmission time and the reception time of the satellite signals. The range between the receiver and satellite is obtained by multiplying the transit time by the speed of light [C.Liu, 1993]. The pseudorange observation equation can be written as:

$$P = \rho + d\rho + c\,(dt - dT) + d\,ion + d\,trop + \sum(P) \quad \ldots\ldots\ldots\ldots\ldots\ldots (2.1)$$

Where

P	is the Pseudorange observation (***m***)
ρ	is the range between the receiver and the satellite (***m***)
$d\rho$	is the orbit error (***m***)
c	is the speed of light in vacuum (***m/sec***.)
dt	is the satellite clock error (***sec***.)
dT	is the receiver clock error (***sec***.)
$d\,ion$	is the ionospheric delay (***m***)
$d\,trop$	is the tropospheric delay (***m***)
$\sum(P)$	is the measurement noise (***m***)

The code measurement noise $\sum(P)$ contains code receiver noise $\sum(P_{rx})$ and multipath $\sum(P_{mult.})$. It can be expressed as:

$$\sum(P) = f\{\sum(P_{rx}) , \sum(P_{mult.}) \} \quad \text{.....(2.2)}$$

Where:

$\sum(P_{rx})$ is the receiver pseudorange noise (***m***)

$\sum(P_{mult.})$ is the multipath effect in pseudorange (***m***)

2.3.2 Carrier phase observation

This type is the difference between the phase of the incoming carrier signal from the satellite and the phase of a carrier signal generated by receiver oscillator. The difference, which is the beat frequency, is due to the Doppler effect caused by the relative motion between the satellite and observation point [C.Liu, 1993]. The carrier phase measurement equation is given as:

$$K = \rho + d\rho + c\,(dt - dT) + Ai - d\,ion + d\,trop + \sum(K) \quad \text{.....(2.3)}$$

Where:

K Is the Carrier phase observation (***m***)

A is the range Carrier phase wavelength (***m/cycle***)

$\sum(K)$ is the Carrier phase noise (***m***)

i is the Carrier phase integer ambiguity (***cycles***)

$\rho, d\rho, dt, dT, d\,ion, d\,trop$ ..... are the same as in equation (2.1).

Similar to code measurement noise, the carrier phase measurement noise $\sum(K)$ is also a function of receiver noise $\sum(K_{rx})$ and multipath $\sum(K_{mult.})$, i.e.:

$$\sum(K) = f\{\sum(K_{rx}) , \sum(K_{mult.}) \} \quad \text{.....(2.4)}$$

Where:

$\sum(K_{rx})$ is the receiver carrier phase noise (***m***)

$\sum(K_{mult.})$ is the multipath effect in carrier phase (***m***)

From equations (2.1) and (2.3), it is seen that both pseudorange and carrier phase measurements are similar except for the ambiguity term ***Λn***, the sign of the ionospheric correction term d_{ion}, and the noise of $\sum(P)$ and $\sum(K)$. The two observations have different levels of accuracy. The carrier phase observation has a much lower receiver noise and multipath effect than the pseudorange observation and thus a higher accuracy, but the value of ***n*** cannot be known. It is not easy task to determine the ambiguity even in the case of static positioning [C.Liu, 1993].

2.3.3 Doppler frequency

It is simply the time derivative of the carrier phase. The Doppler frequency is measured on the pseudorange. The model for GPS the Doppler frequency measurement can be written as:

$$\dot{K} = \dot{\rho} + d\dot{\rho} + c\,(\dot{dt} - \dot{dT}) - \dot{d}\,ion + \dot{d}\,trop + \sum\dot{(K)} \quad \text{……..……(2.5)}$$

Where:

$(\dot{\ })$ denotes a time derivative.

As shown in equation (2.5), the Doppler frequency is not a function of the carrier phase ambiguity. Thus it is free from cycle slips and usually used for estimation of the receiver velocity. From the mathematical models of GPS observations as discussed before, it is noted that GPS measurements are subjected to a number of errors, which will be described in the following.

2.4 Error contributor and accuracy in GPS measurements

The accuracy of GPS in case of relative positioning depends on the distribution (positional geometry) of the observed satellites and on the quality of the observations. The GPS observables are affected by systematic errors and random noise. The errors sources can be classified according to (M.Rabah, 1998) into three groups as show figure (2.7)

(1) Satellite related errors like: orbit errors, satellite clock biased, satellite antenna offsets and satellite antenna phase center variations.

(2)Propagation medium related errors like: tropospheric and ionospheric refraction.

(3) Receiver environment related errors like: receiver clock offsets, interchannel biases, antenna phase center variations and multipath.

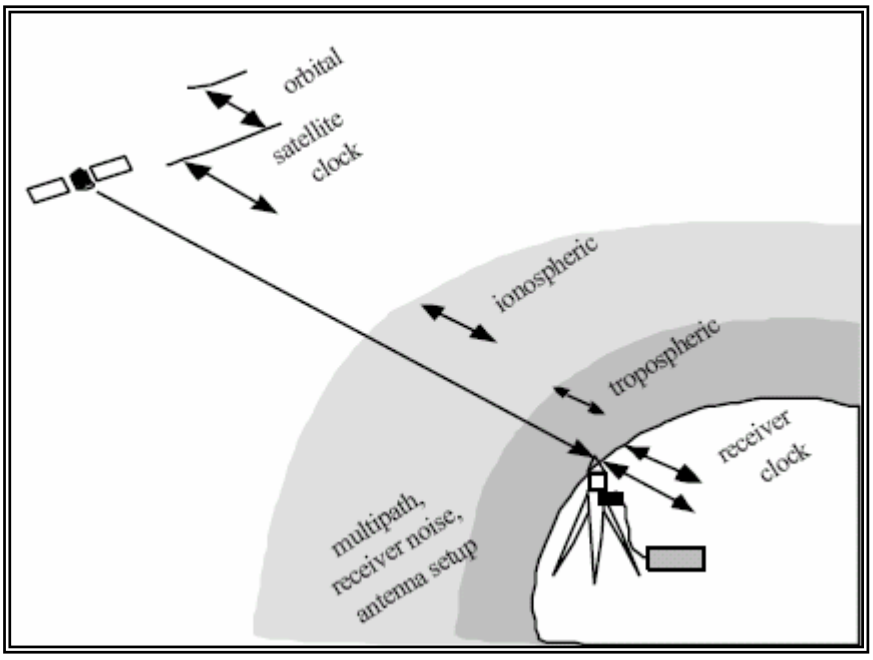

Figure (2.7) Common errors in GPS measurements

Some of the errors may have a systematic effect on the measured baselines producing significant scale errors and rotations. Due to the changeable geometrical distribution of the satellites and the resulting changeable systematic effects of the observation errors, repeated GPS surveys for the purpose of monitoring crustal deformations can also be significantly influenced (up to a few mm) [Van Sickle J., 1996]. In GPS, an array of antennae is positioned at selected points on the structure and on remote stable monuments as opposed to using reflectors and EDM. The baselines between the antennae are formulated to monitor differential movement. The relative precision of the measurements is on the order of +5 mm over distances averaging between 5 and 10 km.

When looking at GPS error sources, two classes of biases are found: those mainly influencing the height and those influencing the scale of a baseline or a network, in terms of precision positioning. The effect on baseline length can occur due to a bias in the absolute tropospheric delay, to neglect the ionospheric delay, or to incorrect heights of fixed reference stations, etc[Y.Ahn, 2005].

For example, if there is a bias in the absolute tropospheric delay, the baseline length can be affected by an amount of the same magnitude as shown in figure (2.8). For the signals transmitted on satellite A and satellite B satellite. Consequently, this error can be reflected in the baseline length.

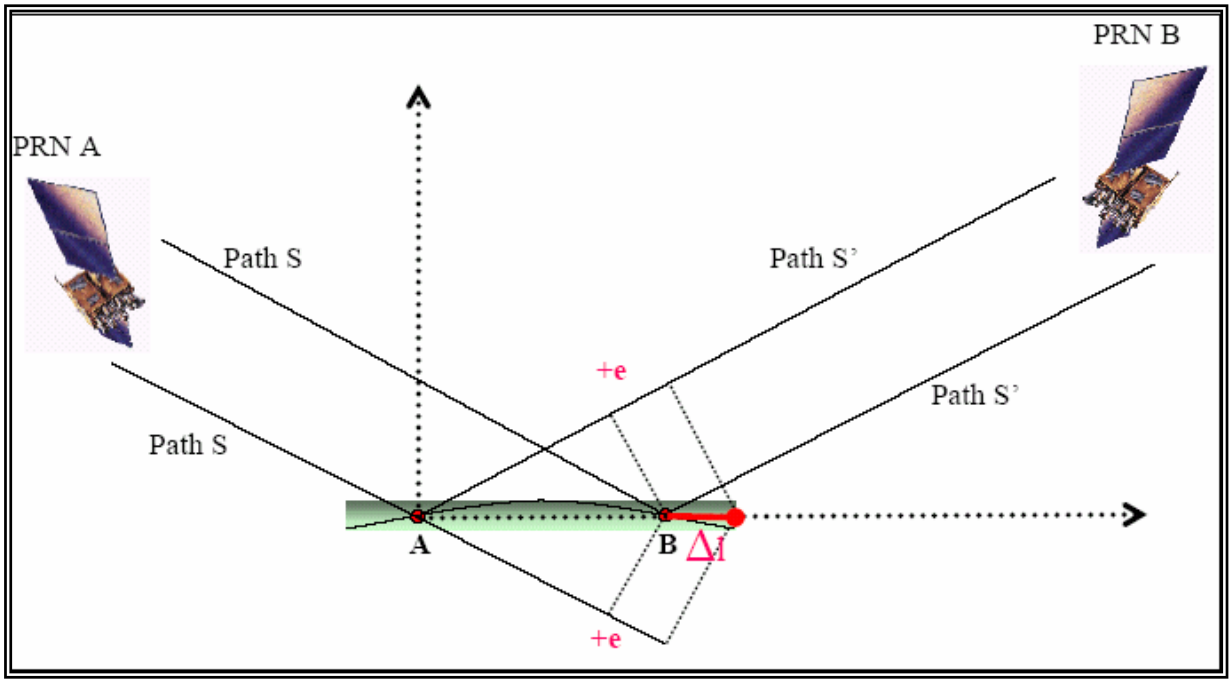

Figure (2.8) Effect of GPS errors on baseline length

The second class of GPS errors can affect the relative station heights. This can occur due to a different bias at each endpoint of a baseline. Such cases happen when there is a bias in the relative tropospheric delay, in the horizontal positions for fixed reference stations, in the satellite orbit, in the antenna phase center differences and in the multipath, etc.

Similarly, if there is a bias in relative tropospheric delay, it can have an effect of the same magnitude, but in a different direction, on the signals transmitted on satellite A and satellite B. Consequently, this error can be reflected in the station height, as shown in Figure (2.9) [Y.Ahn, 2005].

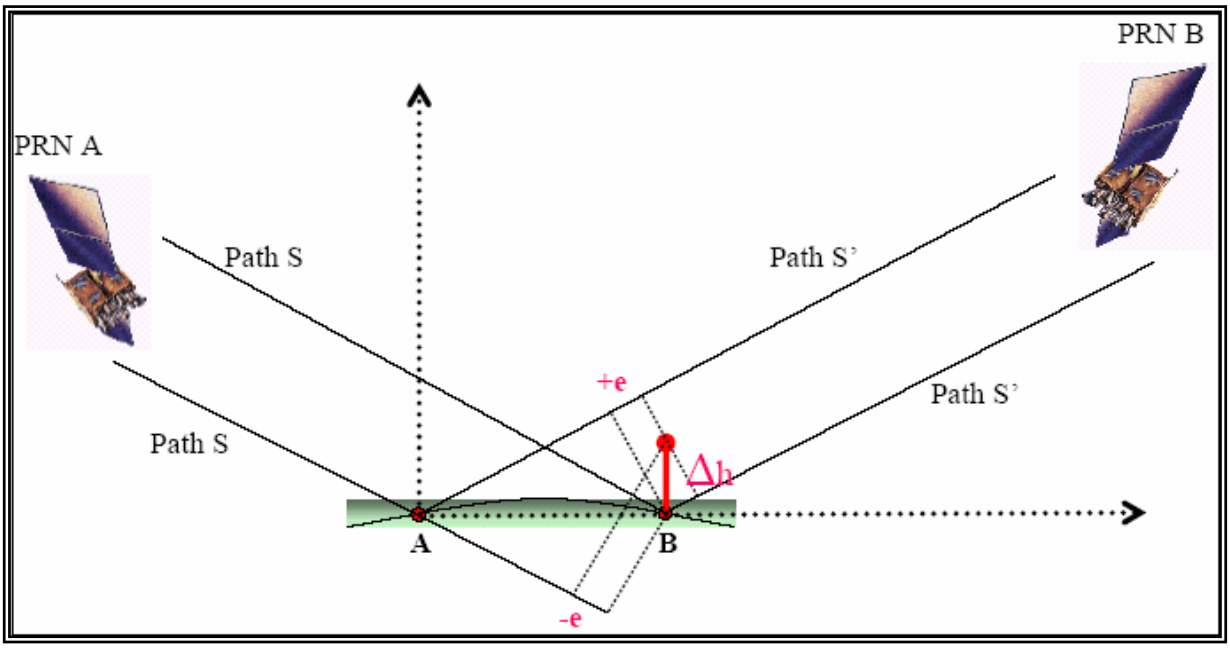

Figure (2.9) Effect of GPS errors on station height

The errors in GPS observation depend mainly on two factors:

(1)The user equivalent range error (noise and systematic)

(2) Geometry of the satellite used.

The most of errors are due to the effect of hardware, environmental and atmospheric error sources.

a) The satellite geometry: Satellite geometry has a direct effect on positioning accuracies. The best single point positioning accuracies are achieved when satellites have good spatial distribution in the sky (e.g. one satellite overhead and the others equally spread horizontally and at about 20 ° elevations). Sub-optimal geometry exists when satellites are clumped together in one quadrant of the sky. The geometry of satellites, as it contributes to positioning accuracy, is quantified by the geometrical

b) dilution of precision (GDOP). Satellite configurations exemplifying poor and good GDOP are illustrated in figure (2.10).

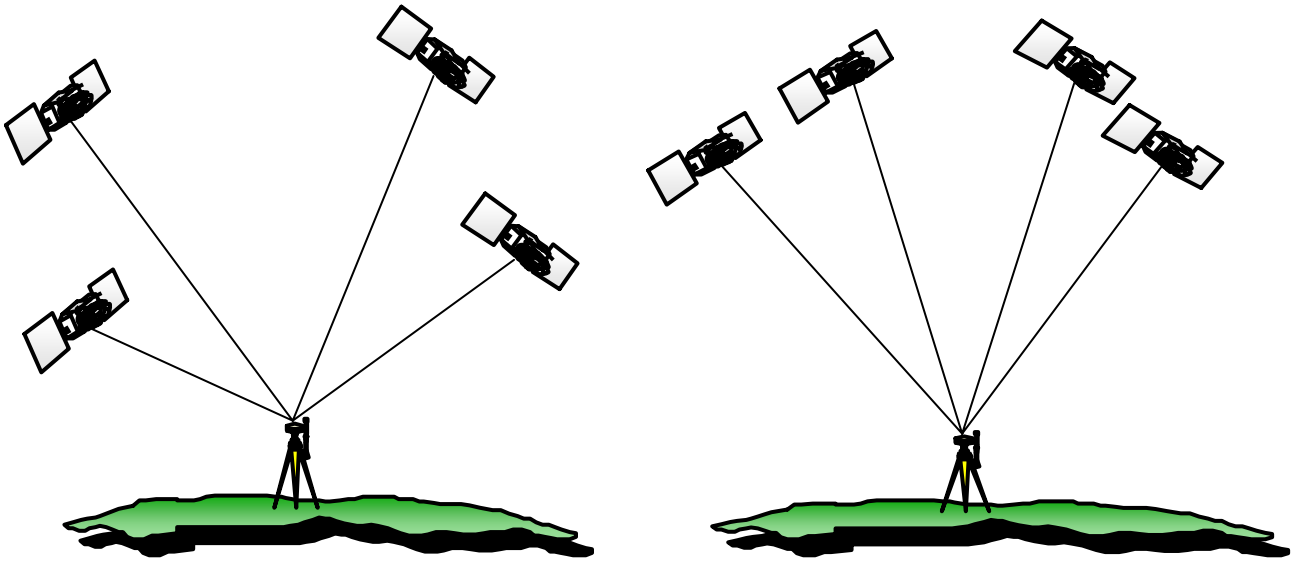

(a) Good geometric **(b) Poor geometric**

Figure (2.10) The geometric of satellite in observations

b)The satellite error: these error could be divided to two part clock and orbits error

<u>1)The clock error</u>, is the difference of satellite clock time with respect to true GPS time [M.C.Olynik, 2002]. The cause of these errors is primarily due to the satellite ephemeris and monitored clock. Tracking data for all observed satellites recorded at the GPS monitor stations is sent to the Master Control station which then uses this data to predict the parameters for the future. These predictions are then returned to the uplink stations where they are transmitted to the satellites. The latency of the tracking data and the prediction routines used at the Air Force Base therefore directly affect the satellite system errors [The GPS

Tutor]. When the difference from a satellite to two receivers is performed, the satellite clock error is removed [C.Liu, 1993].

2)The orbital error, this arises from the uncertainties of the predicted broadcast ephemerides and Selective Availability (SA) [C.Liu, 1993]. The broadcast ephemerides of the satellite are updated by GPS Control Segment. In order to generate the point position messages of the satellites, monitoring stations distributed around the world are required to continuously track all satellites in view. Then, this data is transmitted to the master station and processed to create up-to-date point position parameters. When two receivers are being positioned, both will be in error by nearly the same amount (the extent to which this is true is a function of the distance between the two receivers the closer they are, the more similar the error due to orbital bias). The Relative positioning is therefore an effective strategy for minimizing the effect of this error [G.El-Fiky,2003]. Post-processed ephemerides, which come in several forms, are more accurate than predicted ephemerides, with demonstrated accuracies well below the meter level to several centimeters [X.Shen, 2002].

c)The receiver error, this error can be divided into three parts receiver noise, antenna phase center and hardware delay.

1) Receiver noise, this depends on the signal to noise ratio of the satellite signal [G.El-Fiky, 2003]. Usually, manufacturers claim that the noise levels are respectively 1 m for C/A code pseudorange, 10 cm for p-code pseudorange and 5 mm for carrier phase [M.L.El Gizawy, 2003].

2) Antenna phase center error, at the receiver level, the antenna phase center offsets are of great concern for accurate ellipsoidal height estimates. GPS measurements are actually made with respect to the point in the antenna known

as the phase center, not the survey mark. Corrections must be applied to reduce the measurement to the unknown point. It has been shown that the antenna phase center is not fixed and varies depending on the elevation of the satellite and also the frequency of the propagated signal. For the combined height networks used in this work, complications arise from the mixing of different antenna types, which may produce errors in the ellipsoidal heights of up to 10 cm. Estimated tropospheric parameters are also highly correlated with antenna phase center patterns, which may be incorrectly interpreted in processing software, resulting in amplified errors, especially in the height component. Thus, it is important to use the same antenna and model for network surveys in order to reduce the errors caused by antenna phase center offsets. Although the mitigation of this error source seems simple compared to the complicated modeling of other error sources [G.Fotopoulos , 2003]. The phase center offsets and azimuthal phase dependencies can cause measurements variation of several cm. The receiver performance also depends on the technique used in retrieving the carrier phase. However, they are not significant and masked by other errors [G.El-Fiky,2003].

3) Hardware delay, since satellite signal travel along a different electronic path, multichannel receiver exhibit different signal propagation delays for each hardware channel. The instrument makers try to calibrate and to compensate these interchannel biases [G.El-Fiky,2003].

d) The Propagation error, this error can be divided to three part ionospheric, tropospheric and multipath delay.

1) Ionospheric error, the ionosphere is a layer of atmosphere, which is roughly 50 to 1000 km above the earth's surface. It is composed of a sufficient

concentration of free electrons to affect electromagnetic waves significantly. GPS signals traveling through the ionosphere are affected by refraction and dispersion [C.Liu, 1993]. The refractive group index of the ionosphere is greater than 1, which means that the group velocity of radio waves is smaller than the speed of light in vacuum. The refractive phase index of ionosphere is smaller than 1, so the phase velocity of radio waves is greater than the speed of light in vacuum. These cause delay on the measured pseudorange and advance on the measured carrier phase. Therefore, the ionospheric corrections are the opposite sign on pseudorange and carrier phase observations, respectively [M.C.Olynik, 2002]. The ionospheric effect is proportional to the Total Electron Content (TEC) along the propagation path and can be expressed mentioned by the equation B.Hofmann-Wellenhof, (1995):

$$\left[\Delta t = \left(\frac{1}{Cos\left(Z^{\backslash}\right)}\right) * \left(\frac{40.30}{f^2}\right) * TVEC\right] \quad \text{.....(2.6)}$$

and $$\sin\left(Z^{\backslash}\right) = \left(\frac{R_E}{R_E + h_m}\right) * \sin\left(Z_0\right) \text{..... (2.7)}$$

Where:

f	is the frequency
$Z^{\backslash}$	is the zenith angle at the ionospheric point (IP)
$TVEC$	is the total vertical electron content in el m $^{-2}$.
R_E	is the mean radius of the earth
h_m	is the mean value for the height of the ionosphere
Z_0	is the zenith angle at the observing site (it can be calculated it

for a known satellite position and approximate coordinate of the observation location) as shown in figure (2.11)

Differencing observations from one satellite between two stations can reduce ionospheric effect since the ionospheric delay is to same extent spatially correlated between the stations [Y.Ahn, 2005]. The technique is use the broadcast model for reducing the ionospheric about 50 % of this delay can be removed by application of above equation [C.Liu, 1993].

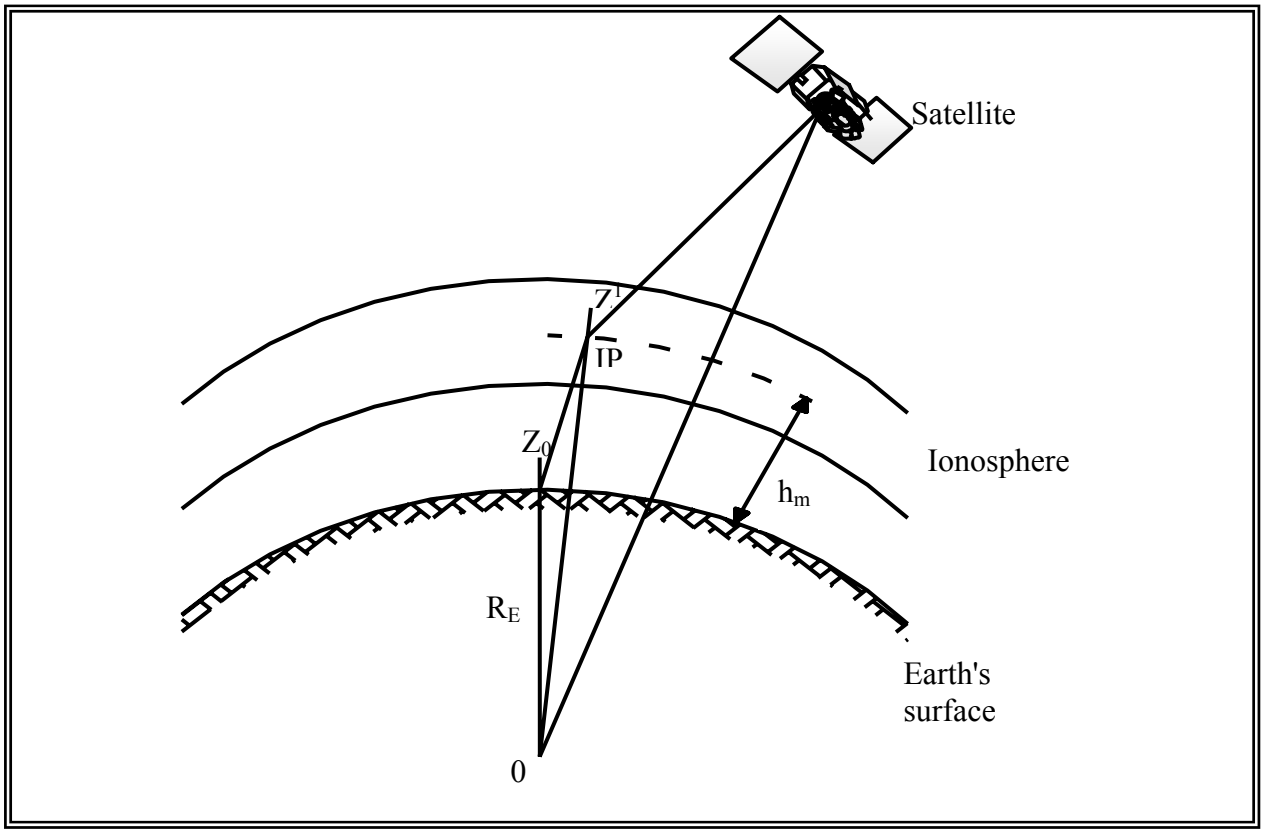

Figure (2.11) Geometry for the ionospheric path delay

2) Tropospheric Delay, the tropospheric delay is caused by the refraction of a GPS signal in lower atmosphere. The magnitude of tropospheric delay is

affected by a number of parameters, such as, the temperature, humidity, pressure, the height of the user, and the type of terrain below the signal path.
But most of them are affected by the mixture of a dry and wet component. The dry component contributes about 80 % to 90 % of the total tropospheric refraction and can be modeled with an accuracy of 1 % to 2 % at the zenith [C.Liu, 1993]. The wet component ranges from 10 % to 20 % of the total tropospheric refraction and cannot be estimated accurately due to variability of water vapor. Then the elevation angle of satellite are depended on the point accuracy and effective on the tropospheric delay, the angle don't less than 10^o, this is one major reason why satellites with elevation angles greater than 10^o are used for precise static and kinematic GPS positioning. After these we can decrease of tropospheric delay by Black model as following:

$$\Delta S = \Delta S_d + \Delta S_w \quad \text{……..(2.8)}$$

$$\Delta S_d = 2.34\, P_i * [\,(T-4.12) / T\,] * I\,(h=h_d, E) \quad \text{…….(2.9)}$$

$$\Delta S_w = K_w * I\,(h=h_w, E) \quad \text{…….(2.10)}$$

$$I\,(h=h,E) = \{\, 1 - [(\cos E)/(1+(1-1_c)h/r_s)]^2 \,]^{-1/2}$$

$h_d = 148.98\,(T-4.12)$ ***m*** above the station

$h_w = 13{,}000$ ***m***

$1_c = 0.85$

$K_w =$ ***0.28*** for summer in tropic or mid-latitudes

0.20 or spring or fall in mid-latitudes

0.12 for winter in maritime mid-latitude

0.06 for winter in continental mid-latitudes

0.05 for polar regions

r_s distance from the center of the earth to the station

P_i surface pressure in standard atmospheres

T surface temperature

3) Multipath, is the phenomena where the reception of signals is reflected by objects and surfaces in the environment around the antenna. Multipath error affects both pseudorange and carrier phase measurements. The amount of multipath error or code observation is much larger than carrier phase multipath error. Pseudorange multipath can reach up to one chip length of the Pseudo-Random Noise (PRN) code, while carrier phase multipath is less than 25 % the carrier phase wavelength. The multipath is also proportional to the ratio of the direct signal power to the reflected signal power [C.Liu, 1993]. Multipath effects are also much pronounced for low elevation satellites [G.El-Fiky,2003]. In static case multipath is non-gaussian in nature and shows sinusoidal oscillations with periods of a few minutes [C.Liu, 1993]. Effective ways to reduce this effect include the use of specially designed antenna and careful antenna mounting. New receiver technology is being developed to effectively filter out multipath effects sign advanced signal processing [G.El-Fiky, 2003]. The magnitude of errors as they affect a single satellite-receiver range is summarized in Table (2.2). All the errors are presented in Table (2.2), when combined using scientific laws of error propagation, forms the user equivalent range error. It is this value, which when multiplied by the DOP (dilution of precision), yields an estimate of achievable accuracies for single point positioning [EMR, 1995].

Table (2.2) Magnitude of errors (EMR, 1995 – M.Rabah, 1998)

Error	Magnitude
Satellite clock	3.028m (assuming broadcast corrections used)
orbital	<± 0.005 ppm
ionospheric	8.176 m (at zenith)
tropospheric	1.813m (at zenith)
receiver clock	9.084m (depends on type of receiver oscillator)
multipath C/A code carrier	 50cm to 20m (depends on GPS equipment and site) up to a few cm (depends on GPS equipment and site)
receiver noise C/A code carrier	 10cm to 2-3m (depends on receiver type) 0.5-5 m (depends on receiver type)

Positioning accuracies are determined by the mapping of these range accuracy measures into the position domain through a measure of satellite geometry called the Dilution of Precision (DOP). Equation 2.11 shows the form of how DOP relates to position error for single-point positioning [V.Hoyle, 2005].

Position Error = DOP * range measurement error ……(2.11)

For differential carrier phase positioning, a relative dilution of precision or RDOP value can be derived for a period of processing time. This value can then be multiplied by the double-difference measurement error to obtain a relative position error for the solution.

2.5 Differential GPS Technique

The more accuracy we can obtain by the differential GPS (DGPS). The type of DGPS are static (a method of GPS surveying using long occupations (hours in some cases) to collect GPS raw data, then postprocessing to achieve sub-centimeter precisions and FastStatic. A method of GPS surveying using occupations of up to 20 minutes to collect GPS raw data, then postprocessing to achieve sub-centimeter precisions. Typically the occupation times a variation is based on the number of satellites (SVs) in view:

4 SVs take 20 minutes*

5 SVs take 15 minutes*

6 or more SVs take 8 minutes*

(Collected at a 15 second epoch rate))[Geometrics program].

Kinematic (a method of GPS surveying using short Stop and Go occupations, while maintaining lock on at least 4 satellites. Can be done in real-time or postprocessed to centimeter precisions)[Geometrics program] but the static type more accurate, which the observation point we stopping in it more time, these given more accurate and remove more error. The static surveying method is most commonly used since the only basic requirement is a relatively unobstructed view of the sky for the occupied points. Conventional static surveys require observation periods depending on the baseline length, the

number of visible satellites, the geometric configuration, and the method used. The accuracy is correlated with the baseline length and amounts of 1and 0.1 ppm for baselines up to some 100 km and even better for longer baselines [G.Fotopoulos, 2003]. DGPS observations (' between-satellite', or 'between-receiver', and both 'between-receiver' and 'between-satellite') are used to eliminate or effectively reduce the common errors. The single 'between-receiver' difference as shown in figure 2.12 can be performed by differencing the GPS observations from two receivers to one satellite. The single difference equations for the pseudorange, carrier phase and Dopller frequency are :-

$$\Delta P = \Delta\rho + d\Delta\rho - c\Delta dT + \Delta d\,ion + \Delta d\,trop + \Delta\sum(P)$$

$$\Delta K = \Delta\rho + d\Delta\rho - c\Delta dT + \Lambda\Delta n - \Delta d\,ion + \Delta d\,trop + \Delta\sum(K)$$

. . . . . .

$$\Delta K = \Delta\rho + \Delta d\rho + c\Delta\, dT - \Delta d\,ion + \Delta d\,trop + \Delta\sum(K)$$

Where:

Δ denotes a single difference operator between receivers.

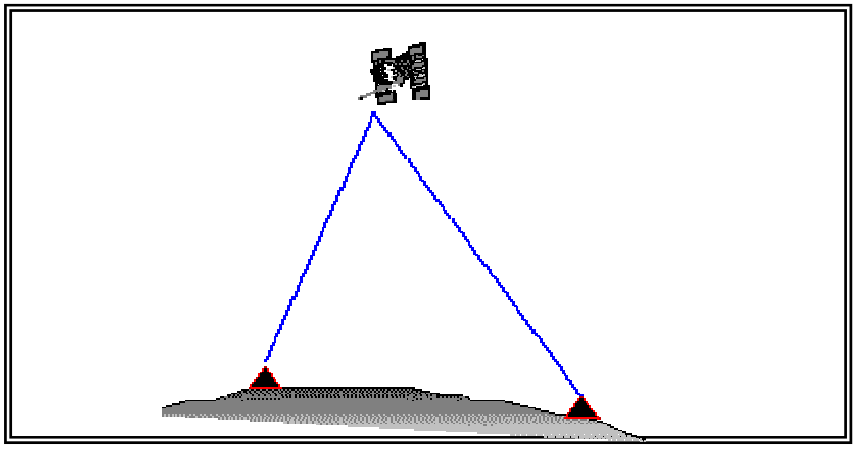

Figure (2.12) Single differencing between receivers

In the single difference observable, the satellite clock error has been vanished and the residual orbital and atmospheric effects have been reduced and can be

neglected for stations separated less than 30 km under normal atmospheric conditions. The relative receiver clock error, however ,may be significant and must be estimated, along with the parameters of position, velocity and carrier phase ambiguity. To eliminate the receiver clock error ,double difference between receivers and between satellites (show in figure(2.13)) can be employed. The equations are as follows [1]:-

$$\blacktriangledown\Delta P = \blacktriangledown\Delta\rho + d\blacktriangledown\Delta\rho + \blacktriangledown\Delta d\,ion + \blacktriangledown\Delta d\,trop + \blacktriangledown\Delta\sum(P)$$

$$\blacktriangledown\Delta K = \blacktriangledown\Delta\rho + d\blacktriangledown\Delta\rho + \Lambda\blacktriangledown\Delta n - \blacktriangledown\Delta d\,ion + \blacktriangledown\Delta d\,trop + \blacktriangledown\Delta\sum(K)$$

. . . . . .

$$\blacktriangledown\Delta K = \blacktriangledown\Delta\rho + \blacktriangledown\Delta d\rho - \blacktriangledown\Delta d\,ion + \blacktriangledown\Delta d\,trop + \blacktriangledown\Delta\sum(K)$$

Where

$\blacktriangledown\Delta$ represents the double difference operator between two stations and two satellites.

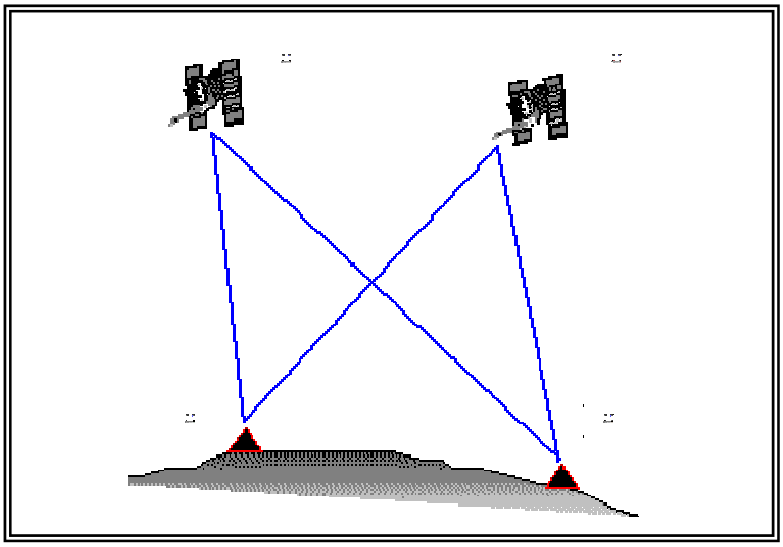

Figure (2.13) Double differencing between receivers and satellites

From the above equations, the double differenced observables have cancelled out both the receiver and satellite clock errors and have further reduced the

orbital and propagation effects [C.Liu, 1993]. The most GPS applications using double DGPS positioning technique is considered as the best processing method. It is also noted that the double difference of carrier phase observation contains the double difference ambiguity term. In order to achieve high positioning accuracy, the integer ambiguity must be correctly resolved before the beginning of the mission and then fixed in kinematic survey. Table (2.3) summarizes; what are required to find the accurate ellipsoidal height.

Table (2.3) Summary of carrier GPS positioning methods (EMR, 1995)

Method	Basic Concepts	Min. # Rcvrs	Obs. Time	Accuracy (3D rms)	Comments
Static	simultaneous site occupation	2	= 1 h	1 cm + 1 ppm to 10 ppm	complexity varies
Kinematic (carrier based)	moving rover positioned with respect to static monitor, need initial ambiguity resolution	2	--	10 cm to 1 m	Logistically difficult since must maintain lock while moving
Semi-Kinematic (also called Stop & Go)	rover stopped temporarily on points to be positioned with	2	~1 min. per point	a few cm	limited to baselines under ~10 km, must maintain

	respect to monitor				lock while moving between points
Pseudo-Kinematic	each rover site occupied twice, at least one hour apart, to exploit change in satellite geometry	2	1-3 min.	a few ppm	double site occupation essential, logistically cumbersome
Rapid Static	uses sophisticated techniques and extra Information to resolve ambiguities	2	3 to 5 min.	a few cm	generally for baselines under 10 km, need "extra" measurements

2.6 Data processing

Data processing as described first is followed by a description of final reporting. The complexity of data processing corresponds with the complexity of the GPS technique used. Single point positioning is the simplest, followed by differential positioning and then carrier techniques [EMR, 1995].

Most receiver purchases or rentals are accompanied by software for GPS processing. As well, several GPS processing packages are available commercially. Fortunately most of these packages are quite automated. Nevertheless, it is important for users to have a general idea of what is involved

in GPS processing. Most single point positioning solutions are computed within the receiver and display. The only post-processing activities which may be involved include downloading this data and combining it in a database or a geographically referenced information system. For differential solutions using code observations, the data from the monitor site and all the rover sites must be loaded onto one computer. At the start of the processing program, the known monitor receiver WGS84 coordinates should be entered. The program will then match the times of the code observations made at each remote site with those made at the monitor site. By using the satellite ephemeris data, the known receiver coordinates and the code measurements, the program will compute the coordinates for each remote site. Note that by using the differential method following a radial network configuration, there are no checks on the solution unless a rover site is occupied twice, and the differences in the solutions are compared. Processing for conventional static GPS surveys is more complex and may require combining several sessions of observations [V.Hoyle, 2005]. All data for one session must be loaded onto a computer. As well, the appropriate "known" three-dimensional WGS84 coordinates of the control points should be entered in the processing program. Most software will also require that approximate coordinates for all other sites occupied during the session be entered. Such approximate values may be read off the same receiver used in the field, or may be scaled from a map. For each session processed, most software will require one point be held fixed three dimensionally. Ideally this point will be a control point with know WGS84. If a control point is not included in a specific session, coordinates of a site in common with an adjoining session which was tied to a control point should be used. In the GPS processing

algorithm, models may be used to correct some of the biases in the observations. Then all the observations, the ephemeris data and the known coordinates will be combined together in an optimal way (know as an adjustment) to arrive at a solution. In this process, an attempt will be made to resolve all carrier phase integer ambiguities. If this can be correctly done, the resultant solution will be of higher accuracy. The solution will consist of coordinate differences between each station included in the session and the related accuracy information. Much of the orbital errors described in Section (2.4), including those introduced by selective availability, may be significantly reduced if a precise ephemeris is used instead of a broadcast ephemeris. The broadcast ephemerides are based on predictions of where a satellite is in the sky at a given time. More precise determinations of the satellite's position are attained by tracking the satellites at stations around the world, combining this data and computing the position of where the satellites were in the sky. Using post-computed precise ephemerides can significantly improve accuracies for precise surveys [EMR, 1995, V.Hoyle, 2005].

Precise ephemerides are available from the Geodetic Survey Division and the U.S. National Geodetic Information Center. To combine several sessions of information together into one solution, a network adjustment should be carried out using software designed for this purpose. The network adjustment combines all the coordinate differences from all the sessions of observations in an optimal manner. A few GPS manufacturer software packages also provide network adjustment capabilities. As well, several independent packages which can adjust GPS networks are available commercially. Note that for a network adjustment to be effective, the survey design requirements spelled out for conventional

static GPS surveys in planning and preparation for the GPS working should be followed. The initial network adjustment carried out should be minimally constrained (i.e. only one three-dimensional control point should be held fixed) to enable examination of GPS results without the influence of existing control. The processing results of conventional static GPS may be checked by comparing redundant baselines, and through statistical tests in the adjustment process. Techniques for processing semi-kinematic and rapid static data are still evolving and have similarities with both differential processing and conventional static processing. Processing software has not been dealt with in any detail here as it is usually included with receiver rental or purchase and tends to be quite complicated [EMR, 1995].

Chapter (3)
THE GEOID UNDULATION

3.1 Introduction

The geoid height (or geoidal undulation) can be defined as the separation of the reference ellipsoid with the geoid surface measured along the normal ellipsoid (figure (3.1)). The combined use of GPS, leveling, and geoid height information has been used as key procedure in various geodetic applications. Although these three types of height information are considerably different in terms of physical meaning, reference surface definition, observational methods, accuracy, etc., they should fulfill the simple geometrical relation-ship [C. Kotsakis, M. G. Sideris, 1999]

$$N = h - H \quad \text{.....(3.1)}$$

Where N is the geoid undulation

h is the ellipsoidal height

H is the orthometric height

The GPS technique has benefits of high accuracy and simultaneous 3-D positioning in Geodetic aims, however, GPS derived ellipsoidal heights must be transformed to orthometric heights (by using the relation in equation (3.1)) to have any physical meaning in a surveying or engineering applications.

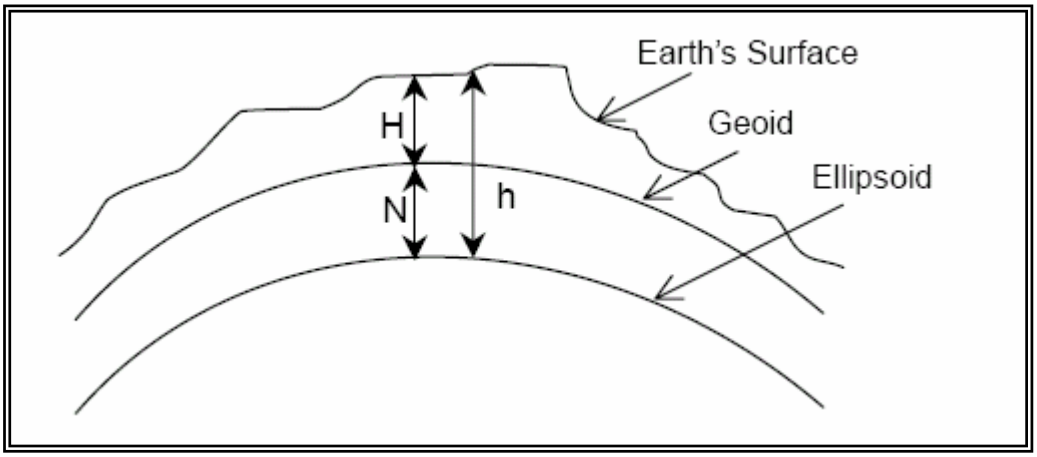

Figure (3.1): Orthometric, geoid, ellipsoid height

This chapter explains the datum define the earth, how compute it, comparison between the different methods and review the methods used to compute the geoid in Egypt.

3.2 The geoid

The geoid is an equipotential surface of the earth that coincides with the undisturbed mean sea level. Therefore one might say that it describes the actual shape of the earth. The geoid is also the reference surface for most height networks since leveling gives the heights above the geoid. In geodesy, these heights are called orthometric heights (H), but they are the ordinary heights above the sea level [Lars Harrie, 1993] as shown figure (3.2).

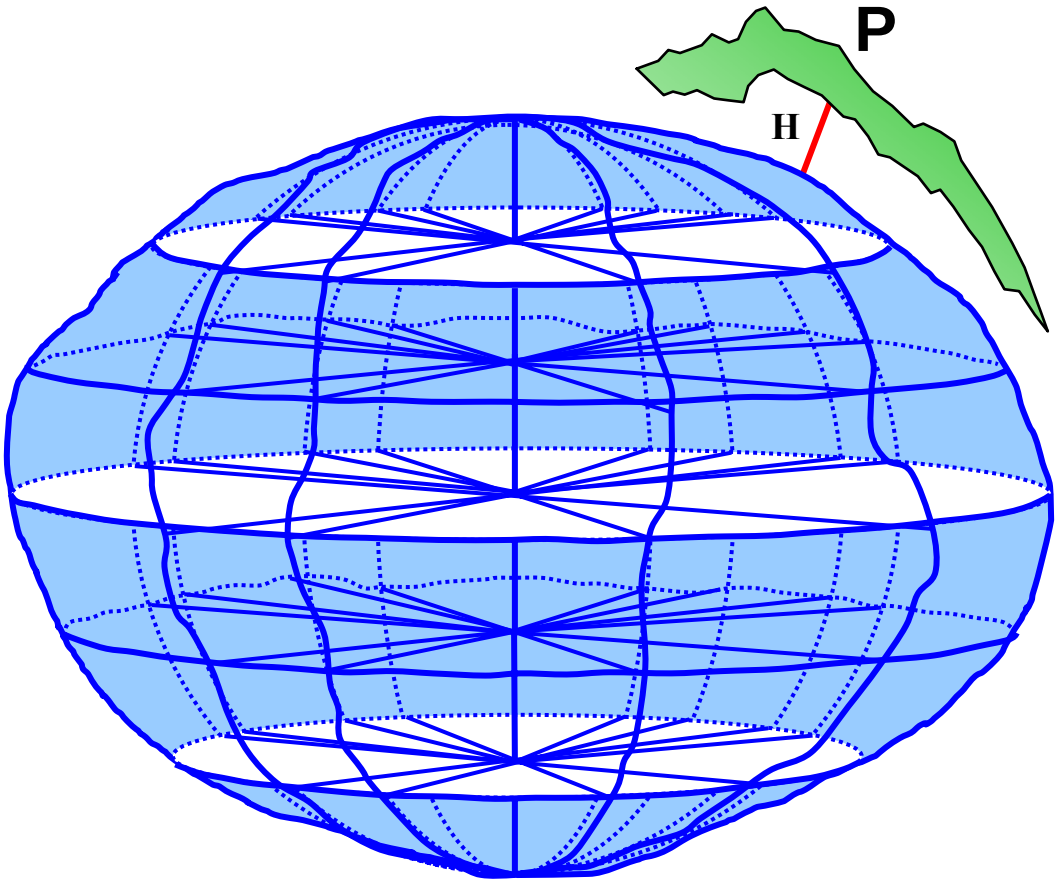

Figure (3.2): The shape of the geoid in the world

The geoid is determined by using several techniques based on a wide variety of using one or more of the different data source such as: Gravimetric method using surface gravity data, Satellite positioning based on measuring both ellipsoidal heights for stations with known orthometric heights, Geopotential models using spherical harmonic coefficients determined from the analysis of satellite orbits, Satellite altimetry using satellite-borne altimetric measurements over the ocean, Astrogeodetic method using stations with measured astronomical and geodetic coordinates, and Oceanographic leveling methods used mainly by the oceanographers to map the geopotential elevation of the

mean surface of the ocean relative to a standard level surface [A.A.Saad, 2002]. The global goidal modals are explained as the following

3.2.1 EGM96 and OSU91A global geopotential models

The Earth Geopotential Model (EGM96) and the Ohio State University (OSU91A) are examples of the recent global geopotential models representing the earth gravitational potential as spherical harmonic coefficients. Both models are complete to degree and order 360. Therefore, the shortest wavelength of these models is one degree, and their resolution is one-half degree (about 50 km). the calculated geoid over Egypt was calculated by EGM96 model (figure 3.3), while the geoid over the whole world is shown in figure (3.4).

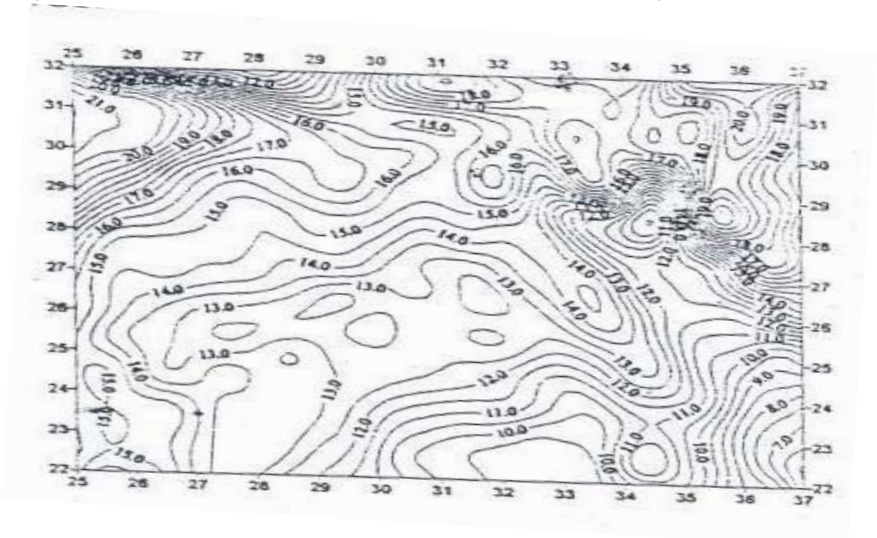

Figure (3.3) The geoid undulation of EGM96, over Egypt contour values in meters

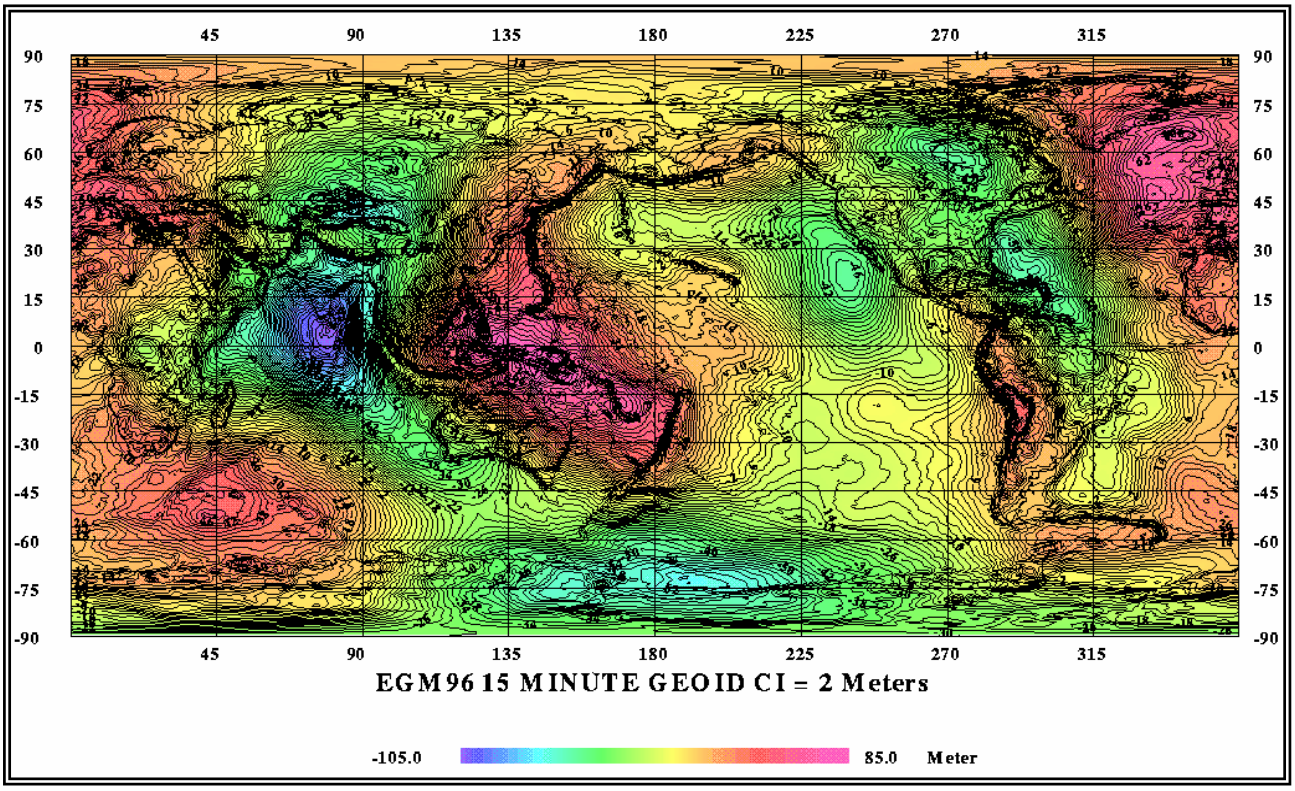

Figure (3.4) The contour map of geoid over the world

Smith and Milbert [1997a] stated that there is an error in the order of one meter in geoid undulation determination using OSU91A model and Geodetic Reference System (GRS80) as the chosen reference field. This effect is due to the difference between the normal potential of GRS80 and the potential of the geoid, and in the case of OSU91A model, it is due to the fact that it is implemented value for the gravitation-mass constant does not equal the corresponding value of the GRS80. In the case of EGM96-based geoid undulations computed by NIMA, a constant bias of 0.41 m was taken into account [Smith and Milbert, 1997b].

3.3 The ellipsoid

The ellipsoid is the mathematical figure generated by the revolution of an ellipse about one of its axes. The ellipsoid is dividing into two types; local and international ellipsoid according to the study and the country as shown figure (3.5).The World Geodetic System 1984 (WGS84), which is used in this study, is designed to be a geocentric coordinate reference system. The center of the ellipsoid is at the center of mass of the earth. Its minor axis aligned with the mean axis of rotation of the earth. Furthermore, the origin of longitude is at the conventional zero meridian (Greenwich). The semimajor axis (***a***) and the flatting (***f***) of WGS84 are:

a = 6378137 meter ***f = 1/298.257223563***

In **Egypt**, the **Helmert 1906** ellipsoid (***a = 6378200*** meter, ***1/f = 297.3***) is used to define the local (non-geocentric) geodetic datum [E.Farag, 2000]

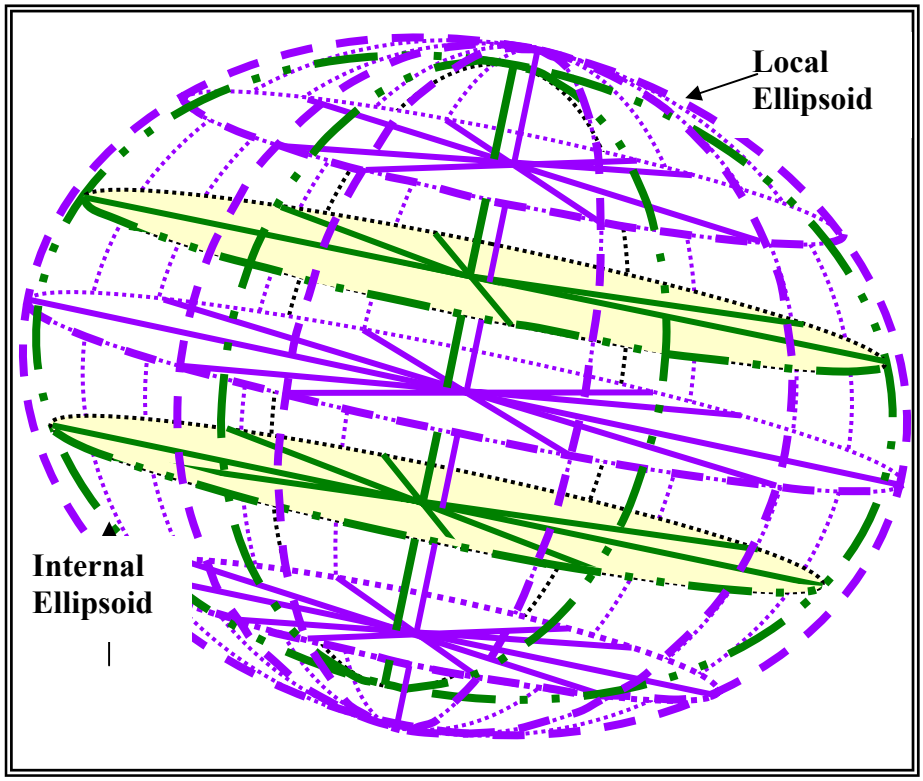

Figure (3.5): The shape of ellipsoidal reference system

The Global Positioning System (GPS) is used to observe the three-dimensional system above the ellipsoidal model. But, the heights obtained from GPS are typically heights above an ellipsoidal model of the earth. These GPS ellipsoidal heights are not consistent with leveled heights above mean sea level, often known as orthometric height. The conversion from ellipsoid to orthometric height requires a geoid height model. Through the use of careful GPS survey procedures coupled with high-resolution geoid models, surveyors have obtained orthometric heights with accuracy commensurate with that of leveling.

3.4 The relation between the geoid and ellipsoid

The geoid defines the astronomic coordinate system while the reference ellipsoid defines the geodetic coordinate system. The relationship between these two systems is relative and can be fully described at any point in space by specifying the magnitude of the linear separation and the angular deviation between the two systems at the same point [E.Farag, 2000]. The separation denoted by N, is known as goidal undulation, separation or geoid height (positive or negative depending on the relation in equation (3.1)). The deflection of the vertical component in the prime vertical plane is usually denoted by η and the deflection of vertical component in the meridian plane is usually denoted by ζ. The mathematical expression for ζ, η, N is:

$$\eta = (\Lambda - \lambda) \cos\varphi$$
$$\zeta = \varphi - \Phi$$
$$N = h - H$$

Where (φ, λ, h) are the geodetic latitude, longitude and ellipsoidal height and (Φ, Λ, H) are the astronomic latitude, longitude and orthometric height at the same point. Figure (3.6) illustrates the relation between the two systems.

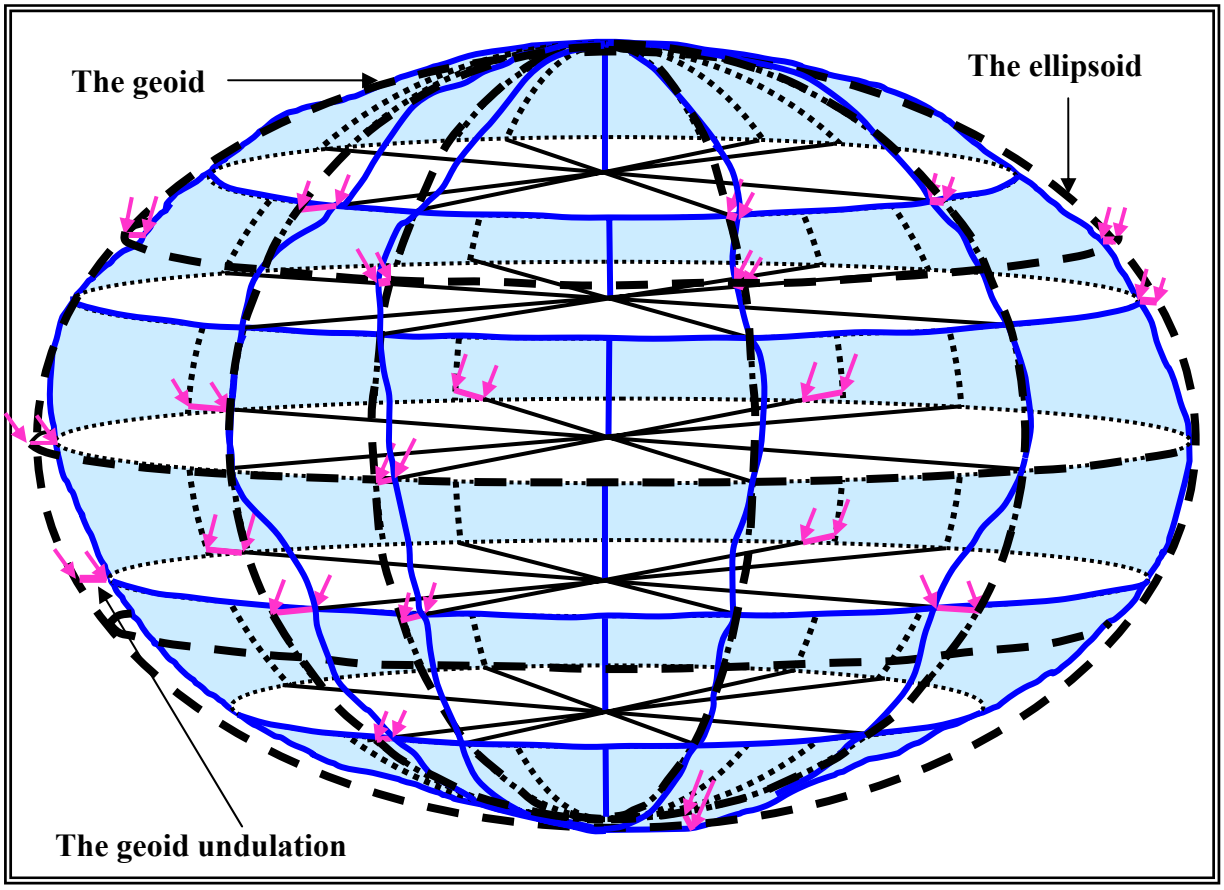

Figure (3.6): The relation between the geoid and ellipsoid

3.5 The geoid computation methods

Two types of observations can be used for the determination of the geoid:

- ***Geometric method (GPS/leveling)***

The simplest method is to use GPS/leveling points, where both the geodetic and orthometric heights are given. From these data, the point geoid height can be calculated with a simple subtraction according to equation (3.1). Orthometric heights can be derived from a surveying technique called “precise leveling” or "Trigonometric leveling" or by both. Precise leveling represents the highest development of the methods of ordinary leveling; precaution is being taken in

the construction of the instruments and in the field work to reduce errors to minimum. In Trigonometric leveling, differences of elevation are computed from vertical angles and horizontal distances. The precise leveling is much more precise than trigonometrically leveling. But this solution can not provide high-resolution geoid, due to the distribution of the GPS/leveling points.

- ***Gravimetric solution***

Gravity is defined as the force acting on a body at rest on the earth's surface. It is the resultant of gravitational (attraction) force and the centrifugal force of the earth's rotation [Heiknan and Moritz, 1967]. The relationship (attraction, centrifugal force and gravity) forces are shown in figure (3.7).

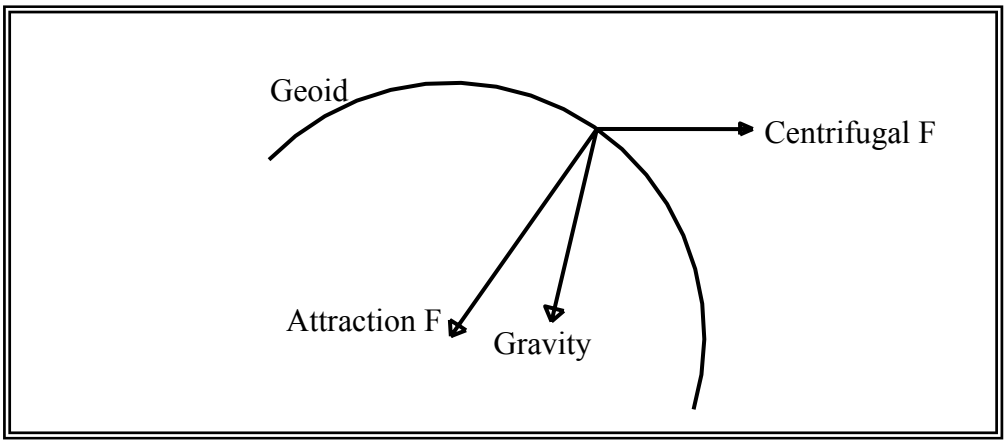

Figure (3.7): Relation between the geoid, attraction centrifugal force and gravity

The gravity vector is normal to the equipotential surface (geoid) passing through the same point. The magnitude (g) of the gravity vector is called gravity, it is physical dimensions are given in Gal or mGals. The numerical

value of gravity varies on the earth's surface from about 978 Gal at the equator to about 983 Gal at the poles [D.Sobhy, 1986].

According to K.Prijatna (1998) precise geoid computation in the any region is influenced by the following facts:

1- Physical terrain or bathymetry.

2- Establishment of a high resolution mean of free air gravity anomaly data covering the entire area and its surroundings.

3- Needs for a Digital Terrain Model (DTM) in order to correct for the train effect.

4- Unified national vertical datum, such a reference does not exist.

5- Insight into the oceanographic and tidal setting in the region.

But the gravimetric observations require expensive and sensitive instruments and time consuming observation procedures like the leap-frog method. In addition the observations must cover a large area for reliable geoid modeling to obtain high accuracy in the region.

3.6 Formulas for geoid computation

Geoid determination is one of the most fundamental problems in geodesy. In the precise geoid determination studies, GPS/leveling data is used to measure the quality of gravimetric or astrogeodetic geoid, and to combine with one of them. Therefore, it is an important data set[A. Ustun1, 2002].The precise model of the geoid not only enable us to transform satellite-derived heights to physically meaningful heights, based on the earth’s gravity field, but also plays an important role in geophysics and oceanography [S. A. Benahmed Daho,2001].

3.6.1 Practical methods

3.*6.1.1 Gravity method*

The classical Gauss-Listing definition of the geoid is given as an equipotential surface of the earth's gravity field that coincides with the mean sea level. Today, it is well known that this is not a strictly correct definition as mean sea level departs from the equipotential surface by amount up to two meters due to various oceanographic phenomena, such as variable temperature, salinity and instantaneous sea surface topography (G. Fotopoulos ,2003). Recently, many methods have been developed for determining the geoid, including astronomical leveling, gravimetric geoid determination using Stokes' or Molodensky's approach, and optimal operational schemes for combining heterogeneous data such as least-squares collocation. The focus of this section is to provide a general overview of the main errors affecting the determination of the geoid heights in practice. Fotopoulos (2003) discussed formulations and techniques for precise geoid determination in details. One practical procedure for regional geoid determination, which provides insight into the main errors inhibiting the accuracy of the computed geoidal height values (N) or relative geoidal heights (ΔN), is the classic "remove-compute-restore" technique (G. Fotopoulos, C. Kotsakis, and M.G. Sideris, 1999).

The procedure is summarized as follows:-

1) Remove a long-wavelength gravity anomaly field (determined by a global spherical harmonic model) from terrain-reduced gravity anomalies that are computed from local surface gravity measurements and digital elevation data.

2) Compute "residual co-geoid undulations" $N_{\Delta g}$ .This can be done by a spherical Fourier representation of Stokes' convolution integral using the residual gravity anomalies.

3) Restore a long-wavelength geoid undulation field N_{GM}(determined by a global spherical harmonic model) to the residual co-geoid undulations, and add a topographic indirect effect term N_H (computed from digital elevation data) to form the final geoidal undulations.

The above three steps can be combined in a single formula as follows:

$$N = N_{GM} + N_{\Delta g} + N_H \quad \text{.....(3.2)}$$

The computation of the long-wavelength geoid component N_{GM} is usually made on a grid, within the appropriate geographical boundaries for the region of interest. Currently, the most widely used global geopotential model is EGM96 (Lemoine et al., 1998), complete to degree and order 360. The coefficients of the global geopotential models are determined from measurements of satellite orbits, satellite altimetry and gravity anomalies (K.Prijatna, 1998). In spherical approximation, its contribution is computed according to the following formula (Heiskanen and Moritz, 1967):

$$N_{GM}(\phi,\lambda) = R\sum_{n=0}^{360}\sum_{m=0}^{n}(Cnm\cdot Cos(m\lambda) + Snm\cdot Sin(m\lambda))Pnm(Sin\phi) \quad \text{..... (3.3)}$$

Where

Pnm are fully normalized Legendre functions, ***Cnm*** and ***Snm*** are the fully normalized unit less coefficients of the geopotential model, and R is the mean radius of the earth.

The medium-wavelength contributions to the total geoid heights can be computed from the available local gravity anomaly data according to Stokes' formula (Heiskanen and Moritz, 1967)

$$N_{\Delta g}(\phi_P,\lambda_P)=\frac{R}{4\Pi\gamma}\int_{\lambda}\int_{\phi_Q}\Delta g(\phi_Q,\lambda_Q)\cdot S(\psi_{PQ})\cdot Cos\phi_q.d\phi_Q.d\lambda_Q \quad \ldots\ldots\ldots\ldots\ldots\ldots(3.4)$$

Where

$\boldsymbol{S\ (\psi_{PQ})}$ is the Stokes' function, $\boldsymbol{\psi_{PQ}}$ is the spherical distance between the computation point (P) and the running point (Q), γ is normal gravity, and Δg is the local gravity anomaly data. Δg are residual Faye anomalies which, when Helmert's second condensation method is used for the terrain effects, are obtained from the following equation:

$$\Delta \boldsymbol{g} = \Delta \boldsymbol{g_{FA}} + \boldsymbol{C} - \Delta \boldsymbol{g_{GM}} \quad \ldots\ldots\ldots\ldots\ldots\ldots\ldots\ldots\ldots\ldots\ldots\ldots\ldots\ldots\ldots\ldots\ldots\ldots(3.5)$$

Where

Δg_{FA} are the free-air anomalies, C is the classic terrain correction term (Heiskanen and Moritz, 1967; Mainville et al., 1994), and Δg_{GM} is the removed long-wavelength contribution of the global geopotential model, which is computed from the expression:

$$\Delta g_{GM}=G\sum_{n=2}^{360}(n-1)\sum_{m=0}^{n}(Cnm\cdot Cos(m\lambda)+Snm\cdot Sin(m\lambda))Pnm(Sin\phi) \quad \ldots\ldots.(3.6)$$

The shorter wavelength information for the regional geoid model is usually obtained from the computation of the indirect effect term N_H, induced by using Helmert's second condensation method for the gravity data reduction on the geoid surface. There are numerous ways of modeling the effects of the topography.

The geoid undulation may be computed by another method using the following spherical harmonic expansion [A.A.Saad, 2002]:

$$N = \frac{GM}{r\gamma} \sum_{n=2}^{360} \left(\frac{a}{r}\right)^n \sum_{m=0}^{n} \left(C_{nm} Cos \cdot m\lambda + S_{nm} Sin \cdot m\lambda\right) \bullet P_{nm}\left(Sin\phi\right) \quad \text{.....(3.7)}$$

Where

- ***n*** The maximum degree of the model.
- ***m*** The maximum order of the model.
- ***γ*** The normal gravity of the reference ellipsoid.
- ***r*** The geocentric radial distance of the computation point projected on the ellipsoid.
- ***G*** The Newtonian gravitational constant.
- ***M*** The mass of the Earth.
- ***A*** The semi-major axis.
- ***Φ*** The geocentric latitude.
- ***λ*** The geocentric longitude.

Finally, it is obvious that this method given the accurate geoid since it is taken the most variables that affected on the geoid. But the errors in the observations, the cost and the time must be taken when the geoid for wide area is computed.

3.6.1.2 GPS method

The GPS observations methods and the errors explained in chapter (2), must be taken when the geoid by GPS method is compute. According to figure (3.6) the geoid undulation is determined by knowing the following parameters [M.EL-Tokhey, 1986]:-

1- The height of the satellite above the instantaneous sea surface (L).

2- The relationship between the instantaneous sea surface and the geoid.

3- The height of the satellite position related to the geodetic datum.

The geoid undulation with taken the above knowledge is:

$$N = h - L - \delta h \quad \text{.....(3.8)}$$

Where

L: is the distance measured by the satellite altimetry technique. And these observations must be adjusted from the errors.

h: is the ellipsoidal height referred to the chosen geocentric ellipsoid.

δh: is the deviation between the instantaneous sea level and the mean sea level (MSL) is considered as the separation between the geoid and the instantaneous sea level as Shown in figure (3.8).

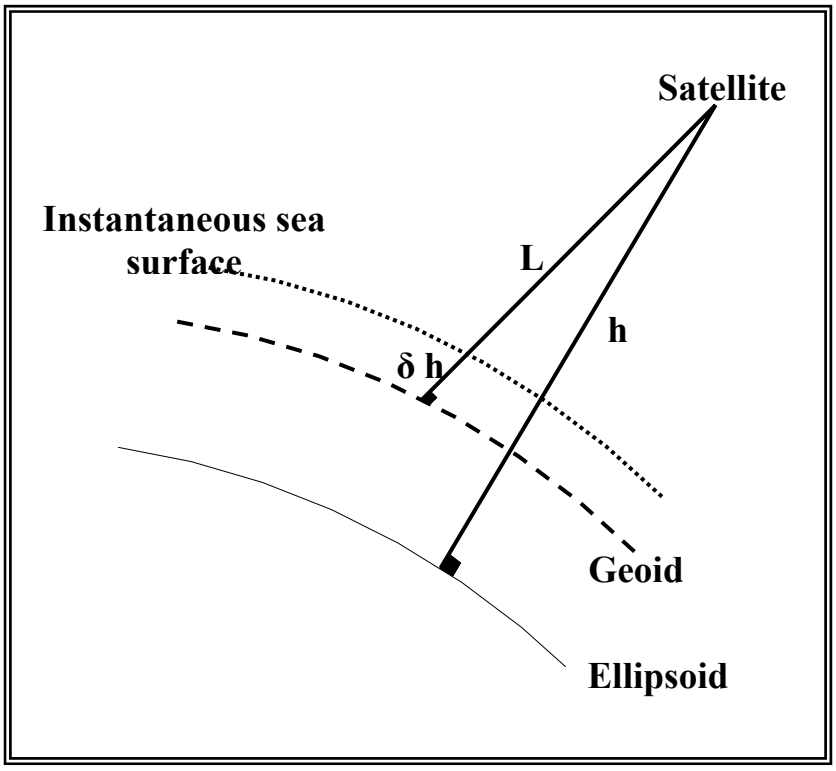

Figure (3.8) Altimeter Geometry

3.6.1.3 Precise method

The precise leveling is known to be the most accurate method to use for relative height determination (M-El-Mowafy, 1983). Although leveling measurements are very precise (i.e., at the mm-level depending on the order or class of leveling), it is often the regional or national network adjustments of vertical control points that leads to the greatest source of systematic error (G. Fotopoulos, 2003).The precise leveling technique is used to supply the precise value for any method to compute orthometric height (***H***). Using the precise level shown in figure (3.9) and Invar rods in leveling routes, and when we used the first order to computed the orthometric height, these very high accurate to determine it. From the value of both the geodetic and orthometric heights can be computed them the geoid undulation and geoid model based on GPS (E.Farag, 2000).

But the errors in this method is greater than other methods, these errors are explained in (M-El-Mowafy, 1983), there for, another methods must be searched to compute the geoid given the orthometric height by highly accurate and less errors.

Figure (3.9) The precise level

3.6.2 The mathematical techniques

Among the geoid modeling techniques, fitting a surface, which is based on the reference points that have been chosen in the most critical locations for representing of the geoid, is one of the most common method. Representing geoid heights as an analytical surface and deriving the geoid undulation values in new points, which are measured with GPS technique, according to the mathematical formulation of this surface constitutes the basic idea of this technique. However, in Egypt, determined geoid model with surface fitting just works in the coverage area of the reference points properly. The model doesn't give reliable results for the extrapolation points. Researches show that this method gives better results where the geoid have a regular trend and well distributed reference points. There are different kinds of interpolation techniques used for modeling the geoid heights. In some part of these techniques, the a-priori heights derived from measurements assumed as if they

are exact values, in another part of the techniques, an adjustment procedure is carried out and random errors are filtered before using the mathematical expressions for interpolation [Erol and Celik, 2004].

The mathematical techniques are solving the most problems in the practical methods to compute the geoid and estimated the value of the geoid for low observed data available as notes in Egypt.

From available data in Egypt which are very low as shown the (S.Powell, 1997 report) we can compute the geoid undulation in Egypt. As the mathematical techniques are the best solution to compute the empirically or adjusted value of the geoid undulation suppose the few data available. The mathematical methods use the least square techniques to solve the mathematical equations and to obtaine from it the parameters of the mathematical equations and the standard deviation. These mathematical techniques are applied to compute the geoid undulation or other, which are;

1- Multiple regression equation
2- Least square collocation
3- Minimum curvature surface

The first and second techniques are using to compute the geoid undulation but the third technique is used to compute other problems but doesn't used to compute the geoid undulation, special in Egypt.

According to Erol and Celik, (2004) the important factors that affecting the accuracy of GPS/leveling geoid model are:-

- Distribution and number of reference stations (GPS/leveling stations). These points must be distributed homogeneously to the coverage area of the model and have to be chosen to figure out the changes of geoid surface.

- The accuracy of GPS derived ellipsoidal heights (h) and the heights derived from leveling measurements (H).
- Characteristic of the geoid surface area.
- Used method while modeling the geoid

Researches showed that there is not unique model works properly for realizing the geoid surface of different areas.

3.6.2.1 Multiple regression equation

The multiple regression equation (MRE) is the mathematical technique used in solution some problems in all branches of science. This traditional technique only accommodates coordinate transformations relating to two datum's. In many instances, particularly for many classical local datum's there are known datum and change it to realized unknown datum. For example the ellipsoidal datum is known datum and the geoid datum is unknown datum.

Various methods have been proposed to address this problem, and one of the most popular is the multiple regression formula. In this branch, the best technique used are the polynomial techniques, that given best solution in some searches in this problem and another. In simple terms they are polynomial functions, which represent the variations, as a function of position, of the difference of latitude, longitude and height (or X, Y and Z coordinates) [H.EL-Shmbaky, 2004].

Depending on the degree of variability in the distributions, approximation may be carried out using 2^{nd}, 3^{rd} , higher degree polynomials. In the case of geoid undulation used any degree that limitation from the less distortion in the check

points. For example in Turkey, the fifth degree is given the best solution as shown in (Erol and Celik, 2004).

Polynomial approximation functions themselves are subjected to variations, as different approximation characteristics may be achieved by different polynomial functions. The simplest of all polynomials is the general polynomial function [EUG,1998].

The polynomial technique can be classified into two models, the first is a real number polynomial model and the second is a complex number polynomial model.

The first model is the general model, the formula is:

$$N=A_0+A_1U+A_2V+A_3U^2+A_4UV+A_5V^2+\ldots\ldots\ldots\ldots\ldots\ldots A_{nn}U^nV^n \quad \ldots\ldots.(3.9)$$

Where

$A_0,\ldots,A_{nn}$ the coefficients

N the unknown (in this search the geoid undulation)

U,V the available data (in this search the coordinates of points)

This model is using in most research with mean value which used U and V relative to central evaluation points.

The second model is fewer coefficients in the same degree of the first model. It is taken low data with higher degree of polynomial. The general formula is:

$$N=(A_1+i.A_2)(U+i.V)+(A_3+i.A_4)(U+i.V)^2+(A_5+A_6)(U+i.V)^3 \ldots\ldots\ldots\ldots\ldots\ldots.(3.10)$$

The polynomial models are the simplest beside other models. Which models from the above give best solution? Those to define by the distortion at check points.

3.6.2.2 Least square collocation

The adoption of the least square collocation (LSC) technique for geoid determination requires the solution of a set of linear equations with dimension equal to the number of observations (Moritz, 1978). In its simplest form least square collocation can be considered as a direct extension of least square prediction. In this technique can be determine the quantities at the computation points are not generally the same as those being measured at the data points. Furthermore, the general collocation model is also able to take into account measurement errors at the data points and the possible requirement to compute certain parameters during the prediction process (P.A.Cross, 1983).

But at the first it must be known how data can be prepared from old observations especially if the precision of this data was not known. So, the process has two steps, the first step is to make the collocation adjustment.

First step: The covariance matrix

Let there are old observations at points 1, 2, 3,……., n points, and the covariance matrix between these measurements relative to the distance between these points (d_{ij}) will be calculated. Dividing all the distances between every pair of points to equal distance (r_k). So, for the distance (r_1) the covariance between every pair of points can be calculated according to the following equation:

$$C_1 = \frac{1}{n_1}\sum U_i U_J \quad \text{……..(3.11)}$$

Where

C_1 The covariance between i,j

n_1 The total number of pairs which satisfy the distance $r_{i,j}$

U_i, U_j The measurements at points i,j

For the general case for every distance r_k the general equation is as follows:

$$C_k = \frac{1}{n_k} \sum U_i U_J \quad \text{.....(3.12)}$$

After that, a histogram can be drawn showing the relation between the distance and the covariance between points as shown in figure (3.10).

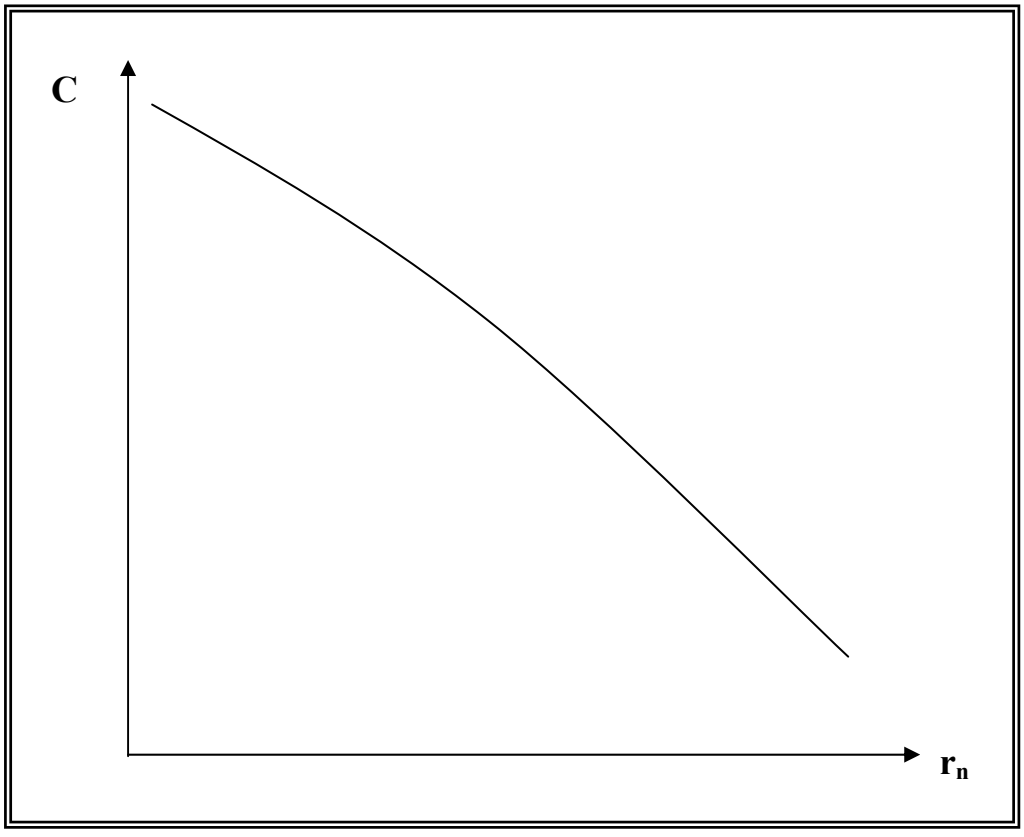

Figure (3.10): The relation between the distance and covariance

The curve function can be expressed as

$$C_{i,j} = ae^{(-br_{ij})} \quad \text{.....(3.13)}$$

Using least square method to calculate parameters a, b. after that the covariance matrix can be written as follows

$$\begin{bmatrix} C_{11} & C_{12} & ..... & .... & C_{1n} \\ C_{21} & C_{22} & ..... & ..... & C_{2n} \\ C_{31} & C_{32} & ..... & .... & C_{3n} \end{bmatrix} \quad \text{.....(3.14)}$$

It can be expressed as

$$\begin{bmatrix} C_{s1} & C_{s12} \\ C_{s21} & C_{s2} \end{bmatrix} \quad \text{.....(3.15)}$$

Where

C_{s1}	The covariance matrix of the original data
C_{s2}	The covariance matrix of the computational points
C_{s21}, C_{s12}	The covariance matrix between data points and the computational points.

From the above process it can be noticed that the covariance between points like Q, L and M at which there is no any observations, can be expected [P.A.Cross,1983].

Second steps: General case of least square collocation

In order to calculate the equation for the least square collocation, first the observation equation which contains parameters and observations will be linearised by Toylor's series is as follows

$$B\,(l + v) + A\,\Delta = b \quad \text{.....(3.16)}$$

With C is the original covariance matrix of the original observations

Where

$\boldsymbol{B}$	The coefficient matrix of observations.
$\boldsymbol{l}$	The observations at data points
$\boldsymbol{v}$	The vector of errors
$\boldsymbol{A}$	The design matrix of parameters.
Δ	The vector of unknown parameters
$\boldsymbol{b}$	The vector of constants.

Let a new set observations l_e may be written as

$$\boldsymbol{l_e + v_e = (-Bl + b) + Bv} \quad \text{.....(3.17)}$$

Where

$\boldsymbol{l_e = (-Bl + b)}$

$\boldsymbol{v_e = (Bv)}$

So using equation (3.15) and substituting in equation (3.14) and rearrange the equation. A special case can be appeared (observation equation) in the least square technique as following

$$\boldsymbol{v_e + A\Delta = l_e} \quad \text{.....(3.18)}$$

And the equation of the covariance matrix for the equivalent observation as follows

$$\boldsymbol{C_{le} = (BCB^T)} \quad \text{.....(3.19)}$$

The above equation can be obtained from the low of error propagation [Mikhail E.M., 1976].

So, every equation in the main system can be written as follow

$$\boldsymbol{A\Delta - l_e + GS + n = 0} \quad \text{..... (3.20)}$$

Where

$$v_e = GS + n \quad \text{……..……(3.21)}$$

And

S	The signal of original data and the computation data = $[S_1 \mid S_2]$
n	The noise in the observations
S_1	Signals for original data points
S_2	Signals for computation points
G	The coefficient matrix for signals = $[I / 0]$

So, the parameters can be calculated as follows

$$\Delta^{\backslash} = [A^T(C_n+C_{s1})^{-1}A]^{-1} A^T(C_n+C_{s1})^{-1} l_e \text{……..……(3.22)}$$

But we can notice that

$$C_{le} = (C_n+C_{s1}) \text{… ……..……(3.23)}$$

Vector of signals (S)

$$S^{\backslash} = C_s\, G^T(C_n+C_{s1})^{-1}(l_e - A\Delta^{\backslash}) \text{……..……(3.24)}$$

Vector of noise (n)

$$n^{\backslash} = C_n(C_n+C_{s1})^{-1}(l_e - A\Delta^{\backslash}) \text{……..……(3.25)}$$

Covariance matrix for signals

$$C_{s\backslash} = C_s\, G^T(C_n+C_{s1})^{-1}\, G\, C_s - C_s\, G^T(C_n+C_{s1})^{-1}A[A^T(C_n+C_{s1})^{-1}A]^{-1}A^T(C_n+C_{s1})^{-1}\, G\, C_s$$

……...(3.26)

Covariance matrix for noise

$$C_{n\backslash} = C_n(C_n+C_{s1})^{-1}C_n - C_n(C_n+C_{s1})^{-1}A[A^T(C_n+C_{s1})^{-1}A]^{-1}A^T(C_n+C_{s1})^{-1}C_n \text{…..(3.27)}$$

[P.A.Cross, 1983].

3.6.2.3 Minimum curvature surface

The method of minimum curvature surface (MCS) is an old and over-popular approach for constructing smooth surface from irregularly spaced data. The

surface of minimum curvature corresponding to the minimum of the Laplacian power or, in alternative formulation, satisfies the biharmonic differential equation. Physically, it is model the behavior of an elastic plate. In the one dimensional case, the minimum curvature loads to the natural cubic spline interpolation. In the two-dimensional case, a surface can be interpolated with biharmonic splines or gridded with an iterative finite difference scheme.

In most of the practical cases, the minimum-curvatur technique produces a visually pleasing smooth surface. However, in case of large changes in the surface gradient, the method can create strong artificial oscillations in the unconstrained regions. Switching to lower-order methods, such minimizing the power of the gradient, solves the problem of extraneous inflections. On the other side, it also removes the smoothness constraint and leads to gradient discontinuities [H.EL-Shmbaky, 2004].

The mathematical formula for (MCS) is seeking for a two-dimensional surface *f(x,y)* in region D, which corresponding to the minimum of the Laplacian power:

$$\iint_D \left|\nabla^2 f(x,y)\right|^2 dxdy \quad \text{.....(3.28)}$$

Where ∇^2 denotes the Laplacian operator $\nabla^2 = \frac{\partial^2}{\partial x^2} + \frac{\partial^2}{\partial y^2}$

Alternatively, seeking *f(x,y)* as the solution of the biharmonic differential equation :

$$(\nabla^2)^2 f(x,y) = 0 \quad \text{.....(3.29)}$$

Equation (3.27) corresponding to the normal system of equations in the least square optimization problem, [Nikos Drakos, 1997].

Poisson equation can be expressed as follows:

$$(\nabla^2)^2 f(x,y) = f(x,y) \quad \text{……..……..(3.30)}$$

The solution of this differential equation can be solved as follows:

If ***y=f(x)*** is a function of one variable, then by Taylor theorem:

$$y_1 = y_0 + hy_0^{'} + \frac{h^2}{2!}y_0^{''} + \frac{h^3}{3!}y_0^{'''} + ...$$

$$y_3 = y_0 - hy_0^{'} + \frac{h^2}{2!}y_0^{''} - \frac{h^3}{3!}y_0^{'''} + ...$$

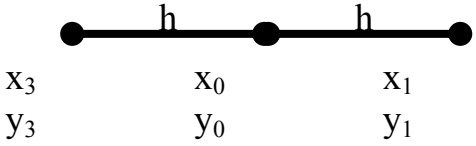

Figure (3.11): The grid arms

As shown in figure (3.11).

By adding the two equations and neglecting the higher orders one can get

$$y_1 + y_2 = 2y_0 + h^2 y_0^{''}$$

With an error less than $\left|h^4 y_0^4 / 12\right|$

$$\therefore y_0^{''} = \frac{1}{h^2}[y_1 + y_3 - 2y_0]$$

Or

$$\frac{d^2y}{dx^2} = \frac{1}{h^2}[y_1 + y_3 - 2y_0]$$

Similarly for a function of two variables as shown in figure (3.12)

$$\left.\begin{aligned} \frac{d^2\varphi}{dx^2} &= \frac{1}{h^2}[\varphi_1 + \varphi_3 - 2\varphi_0] \\ \frac{d^2\varphi}{dy^2} &= \frac{1}{h^2}[\varphi_2 + \varphi_4 - 2\varphi_0] \end{aligned}\right\} \text{……..……..} \quad (3.31)$$

Where φ_0 is the value of the function *f(x,y)* at the point (x_0 , y_0). It is needed to solve numerically the following partial differential equations:

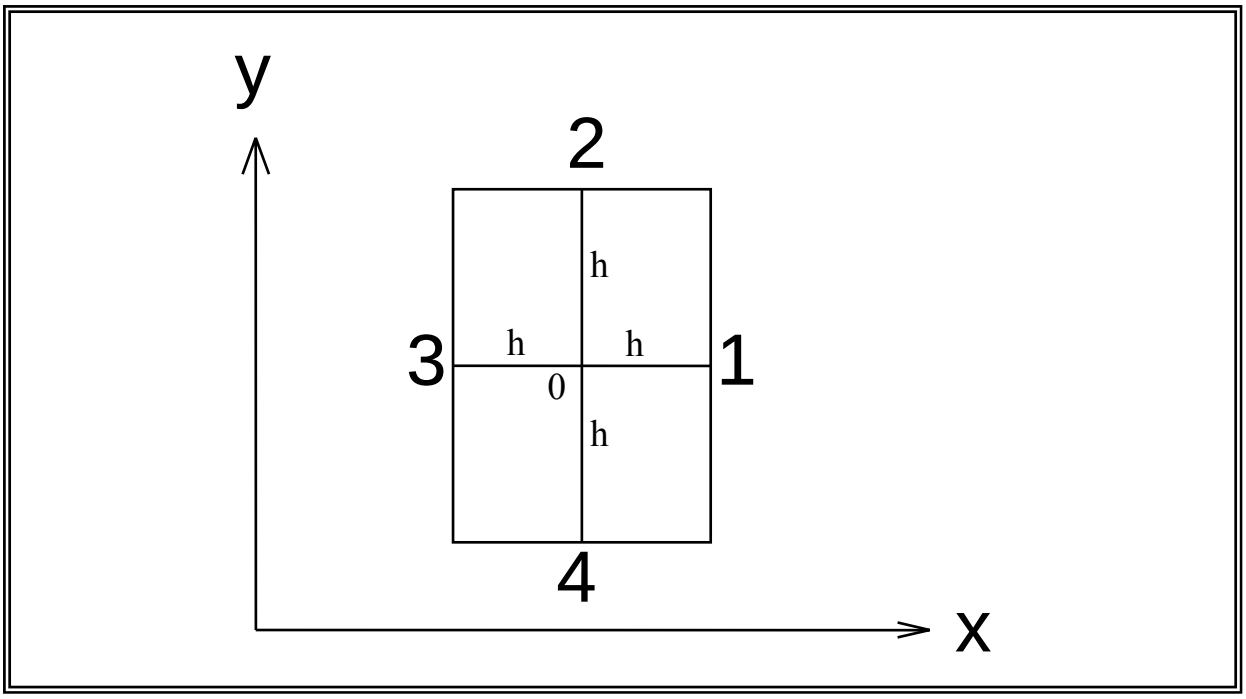

Figure (3.12): The grid for two variables

1- Laplace's equation : $\nabla^2\varphi = 0, i.e. \frac{\partial^2\varphi}{\partial x^2} + \frac{\partial^2\varphi}{\partial y^2} = 0$ ……..(3.32)

Inside any closed boundary.

2-Poisson's equation $\nabla^2\varphi = f(x,y), i.e. \frac{\partial^2\varphi}{\partial x^2} + \frac{\partial^2\varphi}{\partial y^2} = f(x,y)$ ……..(3.33)

inside any closed boundary.

Replacing $\frac{\partial^2\varphi}{\partial x^2}$ & $\frac{\partial^2\varphi}{\partial y^2}$ by their equivalent expression from (3.32), (3.33) we get the following difference equations:

** For Laplace's equation :

$$\varphi_1 + \varphi_2 + \varphi_3 + \varphi_4 - 4\varphi_0 = 0 \quad \text{……..(3.34)}$$

** For Poisson's equation :

$$\varphi_1 + \varphi_2 + \varphi_3 + \varphi_4 - 4\varphi_0 = h^2 f(x_0, y_0) \text{ .....(3.35)}$$

Now dividing the area inside the boundaries into a network or lattice of squares of side (h). The corners of these squares are called nodes of the network. A

difference equations must be written (3.32), (3.33) according to the considered problem for each node. These linear equations can then be solved by any method. It must be known the values of $\varphi(x,y)$ at the boundaries to solve the considered problem [A.Sedeek,1992].

3.7 Review of some previous trials to determine the geoid in Egypt

Some previous trials for orthometric height determination have been conducted, for small areas in Egypt, by many researchers, depending on utilizing local geoid models, or global geopotential model. In the first test, conducted by Baraka & Eman in [1991], the field surveys were performed in 1991 by Egyptian Survey Authority (ESA) and Survey Research Institute (SRI).28 GPS stations were observed, from which a subset of 14 stations were known to be first order vertical control GPS stations, and cover an area of 72 x 72 km. All such GPS stations have both orthometric and ellipsoidal heights. The used geoid is the geopotential model developed by the National Geodetic Survey (NGS) of order 360, with relative accuracy of 2-3 PPM, for points separated by 10 km. the results of this test notified that error in orthometric height from about 12 cm to 37 cm was reached, on absolute basis [M.M.Nassar, 2002]. Concerning the second test, conducted by Shaker et al., in [1996], two test areas were chosen. The first one was in Helwan (12 stations), and the second one was in Al-Abour city (7 stations). In areas, spirit leveling and GPS measurements were conducted. The geoid was determined by two different ways, the first one was through geometric satellite technique, while the other one is gravimetric geoid. The results, in terms of accuracy, declared that the leveling still yields better results and the GPS-geoid method supplied an accuracy of orthometric heights,

in absolute sense, from 0.891 m to 0.899 m. these results were improved when using the relative height difference approach, 1.3 cm to 1.2 cm, when one station with known ellipsoidal, orthometric height and geoidal undulation, was employed as a reference [M.M.Nassar, 2002].

The third test, performed by El-Tokhey and El-Maghraby in [1995] was conducted over a network covering a triangle of 60 km side length with 23 stations, from which (5) stations were known in the Egyptian datum. These stations were observed by GPS, and most of them were connected to each other and to national benchmarks by spirit leveling. The method of least squares collocation with the remove-restore technique was used to obtain geoid undulations where the data were reduced to the OSU91A global geopotential model. The researchers achieved an accuracy of 6 PPM for baseline of about 20 km in length, depending on the reference station as a base station for every new station to be determined. Using the local geoid to determine the orthometric height differences, without referring every new station to the reference station, the accuracy of the estimated orthometric height differences is about 15 PPM for baseline length of about 15 Km.

The last test was performed by Nassar et al in [2000a], three different GPS-leveling networks, covering different areas and locations within the Egyptian territory, where used in this test. The first network is New Cairo city data set (containing the first, third, and fifth new communities), comprises 99 third order GPS stations with known spirit leveling elevations, established in 1995 by the Survey Group of Ain Shams University, with base lines ranging in lengths between 1 Km and 11 Km. the second network is the Great Cairo network (known as Cairo Engineering network data set), composed of 23 first order GPS

stations with known orthometric heights, established by Cairo Engineering Company in 1993, with base line length ranging between 5 Km and 10 Km. the third network is Finnmap GPS first order data set (located basically along the Nile valley and the eastern desert), composed of 31 first order GPS stations with known orthometric heights, established by ESA-Finnmap joint project of 1:50000 topographic maps for the eastern desert in 1989, with base line lengths ranging between 60 Km to 900 Km. the used geoid model in this test, is the EGM96 global geopotential model of order 360, which was proved to be the best global model fitting the gravity field of Egypt [Nassar el. al,1999]. The obtained results of this test on relative bases indicated that, the GPS-EGM96 can provide orthometric height differences with accuracies satisfying the ordinary spirit leveling specifications over Egypt, for short base lines up to 10 Km [M.M.Nassar, 2002].

The accuracy improvement of the determined orthometric height differences, using the ASU-GEOID2000 new local geoidal model for Egypt, reached about 100 % from the corresponding results obtained from the geoidal model based on the ASU93 geoid data and using the remove-restore technique, and also 100 % as compared to the corresponding obtained results when using the EGM96 global geopotential model representing the gravity field in Egypt nowadays, for base lines of about 30 Km on the average [M.M.Nassar, 2002].

The EGM96 global model represents the most precise geopotential model to be used for geoid determination in Egypt [A.A.Saad, 2002].

A.A.Saad and G.M.Dawood used 240 gravity stations to estimation the geoid of Egypt. The data used consists of the 150 ENGSN97 stations, 67 stations of the National Gravity Standard Base Network of 1977 (NGSBN77), and some

gravity stations observed by the Survey Research Institute (SRI). All point gravity measurements have been corrected first to the terrain effect before generating the 5' x 5' free-air gravity anomaly grid. A total of 95 precise GPS stations with known orthometric heights, have been collected. They include the Egyptian National High Accuracy Reference Network (HARN) observed by the Egyptian Survey Authority to form the New Egyptian Datum 1995 (NED-95). From the above data he obtained SRI2000B geoid model as showing figure (3.13) is the most precise geoid model for Egypt [A.A.Saad, 2002].

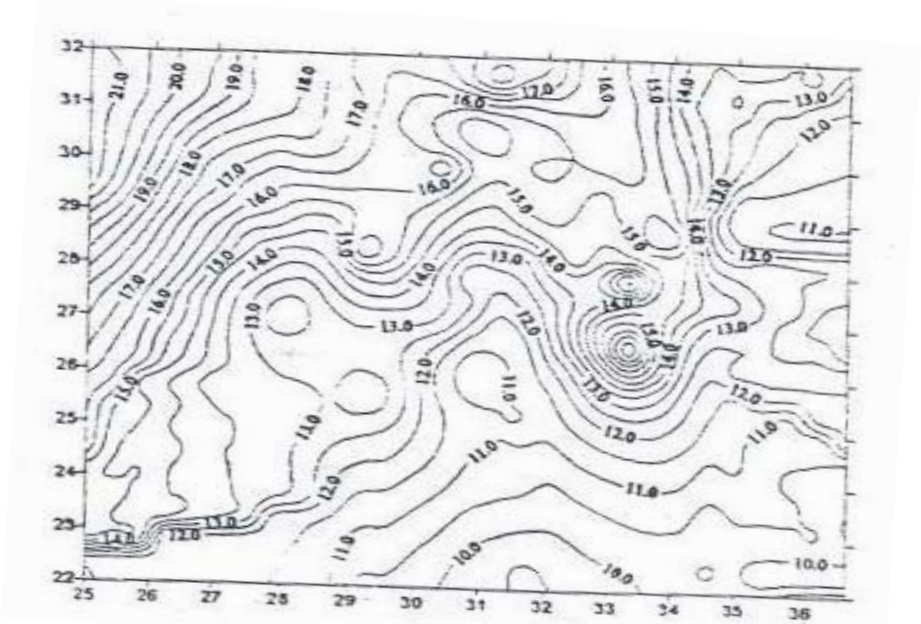

Figure (3.13) The geoid undulation in meters of SRI2000B GEOID

E.Farage study the geoid undulation by gravity observation over the area between longitude 30^0 and 33^0 E and latitude 28.5^0 and 31.5^0 N. And the geoid undulation computed by following equation

$$N_{GrV} = N_{GM} + N_g \quad \text{.....(3.36)}$$

Where

N_{GM} represents the contribution of the adopted geopotential model as a global trend (long wavelength feature of the geoid).

N_g represents the contribution of the smoothed gravity anomalies as a regional trend (short wavelength feature of the geoid).

Two software programs were used to calculate the above two parts. The first program evaluates the long wavelength feature of the geoid undulation N_{GM} at the required points using the adopted model EGM-96. The second program calculates the short wavelength feature of the geoid undulation at the required points using the Stokes' formula. The statistical values for the developed gravimetric geoid of study area for Egypt are given in table (3.1) [E.Farag,2000].

Table (3.1) Statistics of gravimetric geoid undulation N_{GrV} at study area

Statistic	The geoid undulation N_{GrV} for gravimetric method (m)
Minimum	13.75
Maximum	18.77
Average	15.9
RMS	1.05

A.H.EL-SHazly computes the leveling of the points by using the GPS observations only in the some region in Egypt as showing figure (3.14). most of the areas are located in the western desert. The areas are in EL-Wadi El-Gadid, Aswan, and Al-Fayom Governorates. The Cairo-Alexandria desert road also indicates gentle geoid slope. Also the area north of Cairo and the area at the eastern boundaries are with nearly flat geoid. Accordingly, the concept of using GPS leveling without geoid can be applied at these areas depends on the accuracy required and the available leveling information. In other words, one

has to collect all the information about the new projects and decides the method of obtaining orthometric heights based on the required accuracy [A.H.EL-SHazly, 2005]. He applied the no geoid model on Borgg El-Arab City, using 48 points are observed by GPS and the results of this case study as shown table (3.2).

Table (3.2) Comparison of errors in orthometric heights determined by GPS leveling based on global models and leveling orthometric heights for 48 points at Borg El-Arab City.

Geoid Model	Min.(cm)	Max.(cm)	Mean (cm)	STD (cm)
No Geoid	-11.2	8.6	2.2	5.4
GRACE	-11.7	8.6	-0.1	5
EGM96	-7.4	17.6	4.7	5.9
GPM98A	-10.7	3.6	-4.7	3.9

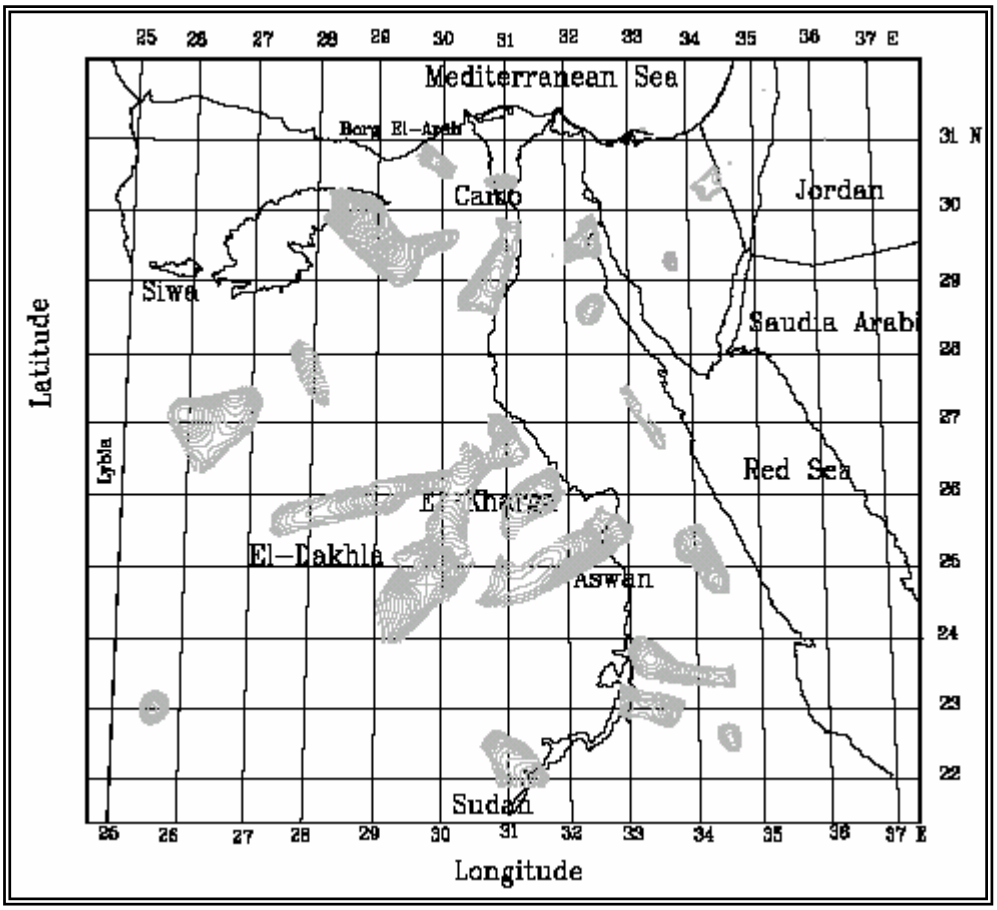

Figure (3.14) Areas with gentle geoid slope in Egypt, contour interval 2 cm

M.Amin, S.M.Elfatary, and R.M.Hasouna are using the gravity data to compute a gravimetric geoid for the newly developed Toshka sector in South Egypt. The Least-Squares collocation solution utilized scattered heterogeneous data types as input, using the remove-Restore technique. The input data included gravity anomalies, gravity disturbances and vertical deflection components, while the available GPS/Leveling. geoidal height data were devoted for the evaluation of the gravimetric geoid accuracy. The dominant data type was the gravity disturbances, and hence, this data was used to predict the empirical covariance

function. The RTM topographic effect was accounted for, using an appropriate DTM for the area under investigation. The long wavelength contribution was properly accounted for, using the locally fitted geopotential model EGM96EGCT. The results show that the mean collocation standard error is about 5 cm, while the comparison at the independent GPS/Leveling. Check points gives an external accuracy of about 16 cm [M.Amin, 2005]. The results as shown figure (3.14).

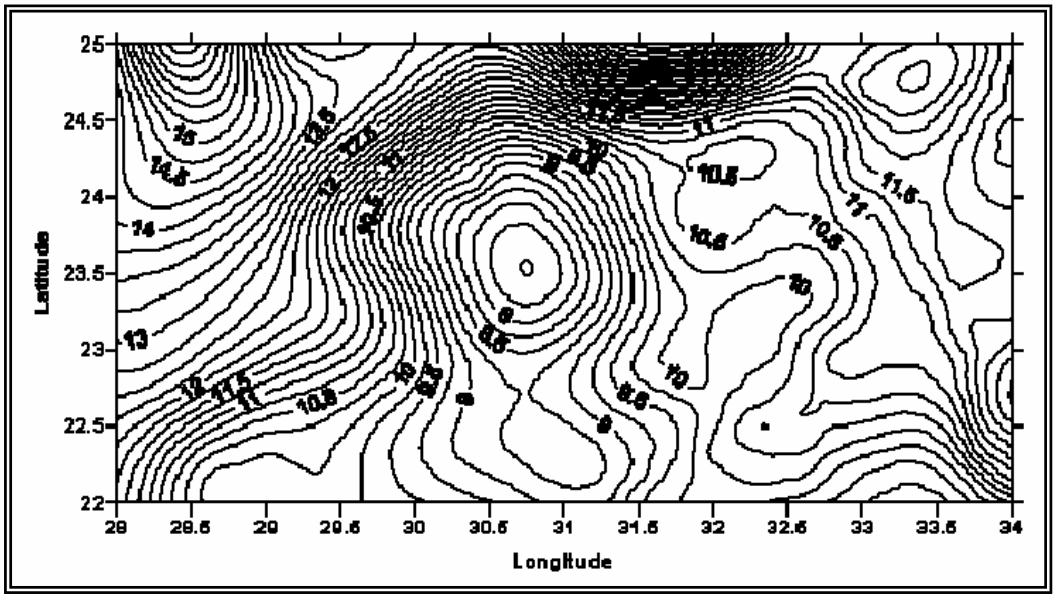

Figure (3.15) Contour map for the 5'x5' Toshka geoid (Interval: 0.25 m)

G.M.Dawod and S.S.Esmail are using A precise GPS control network have been established on both banks along the forth reach of the Nile, that is from Delta barrage to Assiut barrage extending about 408 km. Consists of 168 control points, of them 130 stations have observed orthometric heights, which station separation ranges from 0.2 km to 9.2 km with an average equals 5.7 km. The network has been observed and processed in the optimum way to insure the

quality of precise geodetic control networks, i.e., at least 1 ppm level of precision. It has been tied to the HARN and NACN national networks through 20 tie stations. The distances from GPS stations to NACN points range from 4.5 km to 34.2 km with an average equals 19.7 km. As previously stated, those stations have no observed orthometric heights. From that, they estimated precise orthometric heights of national GPS geodetic control networks based on utilizing the recent national geoid models and the GPS network currently being established along the Nile. It has been concluded that the accuracy of the estimated orthometric heights ranges from 0.06 meter and 0.42 meter with an average of 0.18 meter, which is seven times more-accurate than the OSU91A-based heights published by ESA right now [G.M.Dawod, 2005].

Saad and Dawod (2002) have developed two precise geoid models for the entire Egyptian territory. The first geoid, called SRI2001A, is a gravimetric geoid model utilizing the most recent and accurate first-order gravity measurements, and is based on the GRS80 reference datum. The EGM96 global geopotential spherical harmonic model is used to provide the long wavelength of the Earth gravitational field, along with a local DEM in the remove-compute-restore FFT processing technique. The obtained geoid undulations range from 5.42 m to 22.40 m with a mean value of 14.54 m and RMS equals 2.96 m. A GPS/Levelling data set of 195 precise stations has been used to generate a geometric-satellite geoid model. A second-order polynomial, as a function of the distance from the network origin, is found to be the best fitting function to integrate gravimetric undulations and GPS/Leveling undulations. Therefore, a combined GPS/Gravity geoid for Egypt, SRI2001B, has been generated. This geoid model, depicted in Figure (3.16), has a minimum undulation value of

9.437 m and a maximum value of 21.39 m with an average of 13.62 m and RMS of 2.62 m. The values of the estimated undulations from the SRI2001B model have been compared against the pure GPS undulation of some independent GPS/Leveling stations. The differences range between –0.01 m and –0.28 m, with an average equals –0.10 m, and RMS of 0.49 m [G.M.Dawod, 2005].

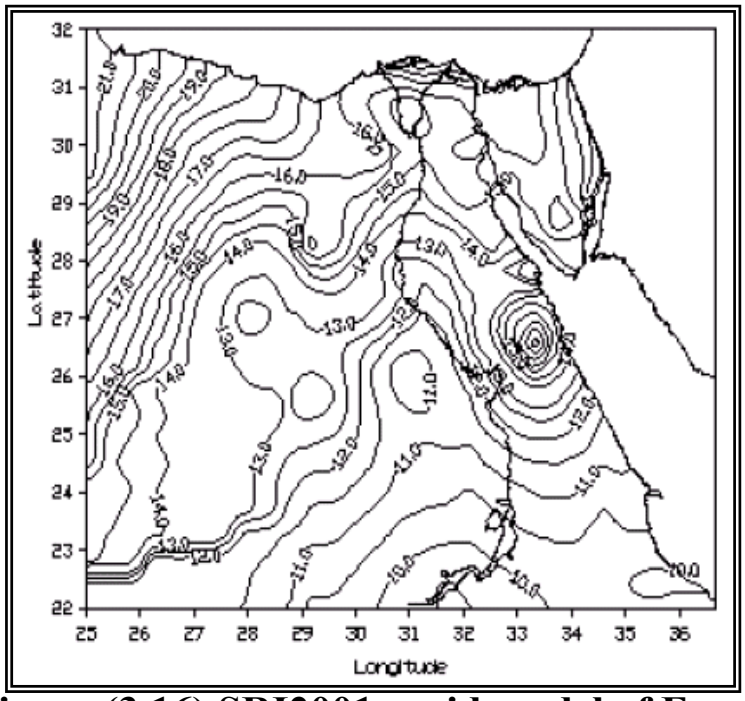

Figure (3.16) SRI2001 geoid model of Egypt

Chapter (4)
THE MATHEMATICAL MODELS AND DEVELOPED PROGRAM MODULES

4.1 Introduction

Normally one refers to the height as the height above the national vertical datum, normally Mean Sea Level at particular coastal point measured over a particular period. Levels have been normally derived by conventional surveying methods and their values are related to the geoid surface. Hence, in order to derive heights above the geoid by GPS, it is necessary to know the height of the ellipsoid above the geoid where over wide areas of the world this relation is not known with a great precision. Nowadays, various mathematical models of the geoid determination are existed. Most of them have been derived for individual countries or parts of the world or the entire world based upon satellite and terrestrial gravity data. Others are derived based on astronomical and geometrical observations and others utilized a combination of all type of the available data. In this chapter, the used algorithms of the mathematical models are outlined as well as the methodology that we utilize them in developing the programs. In this time most surveyor are using the GPS technique since its available and less time and cost beside another observations technique.

4.2 Polynomial Technique Program

4.2.1 Real polynomial technique

The mathematical formula of the polynomial model for general case is outlined in equation (4.1) [Erol and Celik, 2004]:

$$N = \sum_{i=0}^{n} \sum_{j=0}^{i} A_{ij} * \lambda^{i-j} * \phi^{j} \qquad (4.1)$$

And an example for two degrees polynomial model is expressed in equation (4.2):

$$\boldsymbol{N = A_{00} + A_{10}\lambda + A_{11}\Phi + A_{20}\lambda^2 + A_{21}\lambda\Phi + A_{22}\Phi^2} \qquad (4.2)$$

Where:

- $\boldsymbol{N}$ the geoid undulation
- $\boldsymbol{A_{ij}}$ the parameter
- $\boldsymbol{\Phi}$ geodetic latitude
- $\boldsymbol{\lambda}$ geodetic longitude
- $\boldsymbol{n}$ the degree of polynomial model.

By considering the coordinates (Φ,λ,h) as an observation equation for every data point, so a system of equations can be written for every point and hence we will have n equations for n points where the parameters (A_{00}, A_{10}, A_{11}, A_{20}, A_{21}, A_{22}, A_{30},……A_{nn}) are the unknown. Thus by using the Least Square Technique to solve this system of equations, where the above system can be reconstructed in a matrix form as follows [H.EL-Shmbaky, 2004].

:

$$\boldsymbol{A_{(n,n)}V_{(n,1)} + B_{(n,m)}\Delta_{(m,1)} = F_{(n,1)}} \qquad (4.3)$$

Where

A	The coefficients matrix of residuals
V	Vector of residuals
B	Design matrix of parameters
Δ	Vector of parameters
F	Vector of constants
n	Number of observations = Number of equations
m	Number of parameters = Number of unknowns

The degree of freedom "***r***" can be calculated by

$$r = n-m \qquad (4.4)$$

Matrix "***A***" which represents the differentiation of equations for n observations point has the following form:

$$A_{(n,n)} = \begin{bmatrix} \frac{\partial f_1}{\partial V_1} & \frac{\partial f_1}{\partial V_2} & \cdots & \cdots & \frac{\partial f_1}{\partial V_n} \\ \frac{\partial f_2}{\partial V_1} & \frac{\partial f_2}{\partial V_2} & \cdots & \cdots & \frac{\partial f_2}{\partial V_n} \\ . & . & & & \\ . & . & & & \\ . & . & & & \\ . & . & \cdots & \cdots & . \\ . & . & \cdots & \cdots & . \\ \frac{\partial f_n}{\partial V_1} & \frac{\partial f_n}{\partial V_2} & \cdots & \cdots & \frac{\partial f_n}{\partial V_n} \end{bmatrix} \qquad (4.5)$$

In this method the ***A*** matrix equally the unity matrix as follow

$$A_{(n,n)} = -[I] \qquad (4.6)$$

Matrix "***B***" which represents the differentiation of unknown parameters for n points can be taken the ***B*** matrix as following form

$$B_{(n,m)} = \begin{bmatrix} \frac{\partial f_1}{\partial \Delta_1} & \frac{\partial f_1}{\partial \Delta_2} & .... & .... & \frac{\partial f_1}{\partial \Delta_m} \\ \frac{\partial f_2}{\partial \Delta_1} & \frac{\partial f_2}{\partial \Delta_2} & .... & .... & \frac{\partial f_2}{\partial \Delta_m} \\ . & . & .... & .... & . \\ . & . & .... & .... & . \\ \frac{\partial f_n}{\partial \Delta_1} & \frac{\partial f_n}{\partial \Delta_2} & .... & .... & \frac{\partial f_n}{\partial \Delta_m} \end{bmatrix} \qquad (4.7)$$

The matrix "***F***" for ***n*** observations points can be take the follow

$$F_{(n,1)} = \begin{bmatrix} F_1 \\ F_2 \\ F_3 \\ . \\ . \\ . \\ . \\ F_n \end{bmatrix} \qquad (4.8)$$

Matrix "Δ" for ***n*** observations points can be taken the following:

$$\Delta_{(m,1)} = \begin{bmatrix} \Delta_1 \\ \Delta_2 \\ \Delta_2 \\ . \\ . \\ . \\ . \\ \Delta_m \end{bmatrix} \qquad (4.9)$$

And the "***V***" matrix for ***n*** observations points can be take the follow

$$V_{(n,1)} = \begin{bmatrix} V_1 \\ V_2 \\ V_3 \\ . \\ . \\ . \\ . \\ V_n \end{bmatrix} \qquad (4.10)$$

For example, the solution of the first degree by the LSA method is outlined in the following equation form derived from the general polynomial method, given in equation (4.1) as:

$$N = A_{00} + A_{10}\lambda + A_{11}\Phi$$

Assume the number of the observations is ***n*** observations then

$$N1 = A_{00} + A_{10}\lambda 1 + A_{11}\Phi 1$$

$$N2 = A_{00} + A_{10}\lambda 2 + A_{11}\Phi 2$$

$$N3 = A_{00} + A_{10}\lambda 3 + A_{11}\Phi 3$$

$$\cdots\cdots\cdots\cdots\cdots\cdots$$

$$Nn = A_{00} + A_{10}\lambda_n + A_{11}\Phi_n$$

The number of parameters is three parameters, namely (A_{00}, A_{10}, A_{11}).

Then the Degree of Freedom $r = n-3$

Then the equations to general least square can written as follow:

$$f_1 = A_{00} + A_{10}\lambda_1 + A_{11}\Phi_1 - (N_1 + V_1)$$

$$f_2 = A_{00} + A_{10}\lambda_2 + A_{11}\Phi_2 - (N_2 + V_2)$$

$$f_3 = A_{00} + A_{10}\lambda_3 + A_{11}\Phi_3 - (N_3 + V_3)$$

$$\cdots\cdots\cdots\cdots\cdots\cdots\cdots\cdots\ldots$$

$$f_n = A_{00} + A_{10}\lambda_n + A_{11}\Phi_n - (N_n + V_n)$$

However, ***A*** matrix is the unit matrix as mention in equation (4.6), and the **B** matrix is given as follow:

$$B_{(n,1)} = \begin{bmatrix} 1 & \lambda_1 & \phi_1 \\ 1 & \lambda_2 & \phi_2 \\ . & . & . \\ . & . & . \\ 1 & \lambda_n & \phi_n \end{bmatrix}$$

And the parameters Δ matrix is taken as in the following:

$$\Delta_{(3,1)} = \begin{bmatrix} A_{00} \\ A_{10} \\ A_{11} \end{bmatrix}$$

The constant vector matrix (***F***) can be calculated by using the following equations:

$$F_1=N_1-A_{00}-A_{10}\lambda_1-A_{11}\Phi_1$$

$$F_2= N_2-A_{00}-A_{10}\lambda_2-A_{11}\Phi_2$$

$$F_3= N_3-A_{00}-A_{10}\lambda_3-A_{11}\Phi_3$$

$$\ldots\ldots\ldots\ldots\ldots\ldots\ldots\ldots$$

$$F_n= N_n-A_{00}-A_{10}\lambda_n-A_{11}\Phi_n$$

Then the ***F*** and ***V*** matrix is depicted in equation (4.8) and (4.10) respectively. The aforementioned algorithm is used by MATLABB to find the required solution of the above system of equation by LSA. In addition, the developed program will compute the distortion between the check points (known point from the S.Powell report) and the value output from the program. The steps of program as follow:

1- Inputting the known data (Φ, λ, N) from the S.Powell report where the coordinates of points are WGS84 geodetic coordinate.
2- Building ***A*** matrix according to eq. (4.5)
3- Calculating ***B*** matrix according to eq. (4.7)
4- Calculating ***F*** matrix according to eq. (4.8)
5- Building Covariance matrix and calculating the equivalent weight matrix (We).
6- Calculating least square matrices operations using general least square algorithm.
7- Running the Fisher test at 98% confidence interval.
8- Inputting the check points from the S.Powell report.

9- Calculating the geoid undulation by the polynomial method as well as the distortion between known geoid undulation and the calculate geoid undulation.

In the above program module, two trials are made; the first trial with using the coordinates of points as outlined above, while the second with using the average of the coordinates of points according to the following equation:

$$N = \sum_{i=0}^{n} \sum_{j=0}^{i} A_{ij} * (\lambda - \lambda_o)^{i-j} * (\phi - \phi_o)^{j} \qquad (4.11)$$

Where

$\boldsymbol{\Phi_o}$	The mean of the geodetic Latitude for known points
$\boldsymbol{\lambda_o}$	The mean of the geodetic longitude for known points

In the second trials, the only difference between it and the first trials that: the input known data are (Φ, λ, N) from the S.Powell report where the coordinates of points are WGS84 geodetic coordinate, then mean values of the ellipsoidal coordinates are calculated, and the rest of the program as indicated in the first trials.

Alternative solution can also be made by using the Cartesian coordinates according to the next form of equation:

$$N = \sum_{i=0}^{n} \sum_{j=0}^{i} A_{ij} * X^{i-j} * Y^{j} \qquad (4.12)$$

Where: the (***X, Y***) is the Cartesian coordinates for the known points which is obtained by converting the geodetic coordinates to Cartesian coordinates if they are not available in the Cartesian format.

By solving it by the same program module as follows:

1- Inputting the known data (***X, Y, N***) from the S.Powell report after converting the geodetic coordinates of points to Cartesian coordinates.
2- Building ***A*** matrix according to eq. (4.5)
3- Calculating ***B*** matrix according to eq. (4.7)
4- Calculating ***F*** matrix according to eq. (4.8)
5- Building Covariance matrix and calculating the equivalent weight matrix (We).
6- Calculating least square matrices operations using general least square algorithm.
7- Running the Fisher test at 98% confidence interval.
8- Inputting the check points from the S.Powell report.
9- Calculating the geoid undulation by the polynomial method as well as the distortion between known geoid undulation and the calculate geoid undulation.

As alternative solution, the mean value of the Cartesian coordinates can be used according to the following equation:

$$N = \sum_{i=0}^{n} \sum_{j=0}^{i} A_{ij} * (X - X_o)^{i-j} * (Y - Y_o)^{j} \qquad (4.12)$$

Where: the (X_0,Y_0) is the mean of the Cartesian coordinates for known points and the most solution steps are still the same only the following steps are updated:

1- Inputting the known data (Φ, λ, N) from the S.Powell report where the coordinates of points are WGS84 geodetic coordinate.
2- Converting the geodetic to Cartesian coordinates.

3- Calculating the mean of the Cartesian coordinates.

4.2.2 Complex Polynomial technique

Another form of the polynomial can be used; it is called the complex method. The advantage of the complex polynomial technique is that the dependence between the coefficients for geodetic coordinates is taken into account in the formula, resulting in fewer coefficients for the same order polynomial [EUG, 1998]. Equation (4.13) gives a general least square format for the complex polynomial [EUG, 1998].

$$
\begin{aligned}
N \;=\; & (A_1+iA_2)\,(\Phi+i\lambda) + (A_3+iA_4)\,(\Phi+i\lambda)^2 && \{\text{to } 2^{nd} \text{ order}\} \\
& +(A_5+iA_6)\,(\Phi+i\lambda)^3 && \{\text{to } 3^{rd} \text{ order}\} \qquad (4\text{-}13) \\
& +(A_7+iA_8)\,(\Phi+i\lambda)^4 && \{4^{th} \text{ order}\}
\end{aligned}
$$

The same above steps of the program module were design to compute the solution of the complex polynomial technique.

4.3 Least Square Collocation Program

The purpose of using the Least-Square Interpolation Technique in the geoid undulation determination is to supplement the GPS/Leveling observations, which are made at only a relatively few points, by dense points which their values of geoid undulation are estimated across a surface covering a specific region.

A trial was made to compute the geoid undulation in Egypt by using least square collocation technique as in the following:

- In the first step of the program module, the Egypt map is divided to grids $0.50^{'}$ x $0.50^{'}$ as shown figure (4.1).
- The second step: the covariance matrix between the data points and the computation points are designed. Then the distances between data points and the geoid undulation are computed (or difference between the orthometric and ellipsoidal heights); the equations which describe this relationship are explained in the following steps:

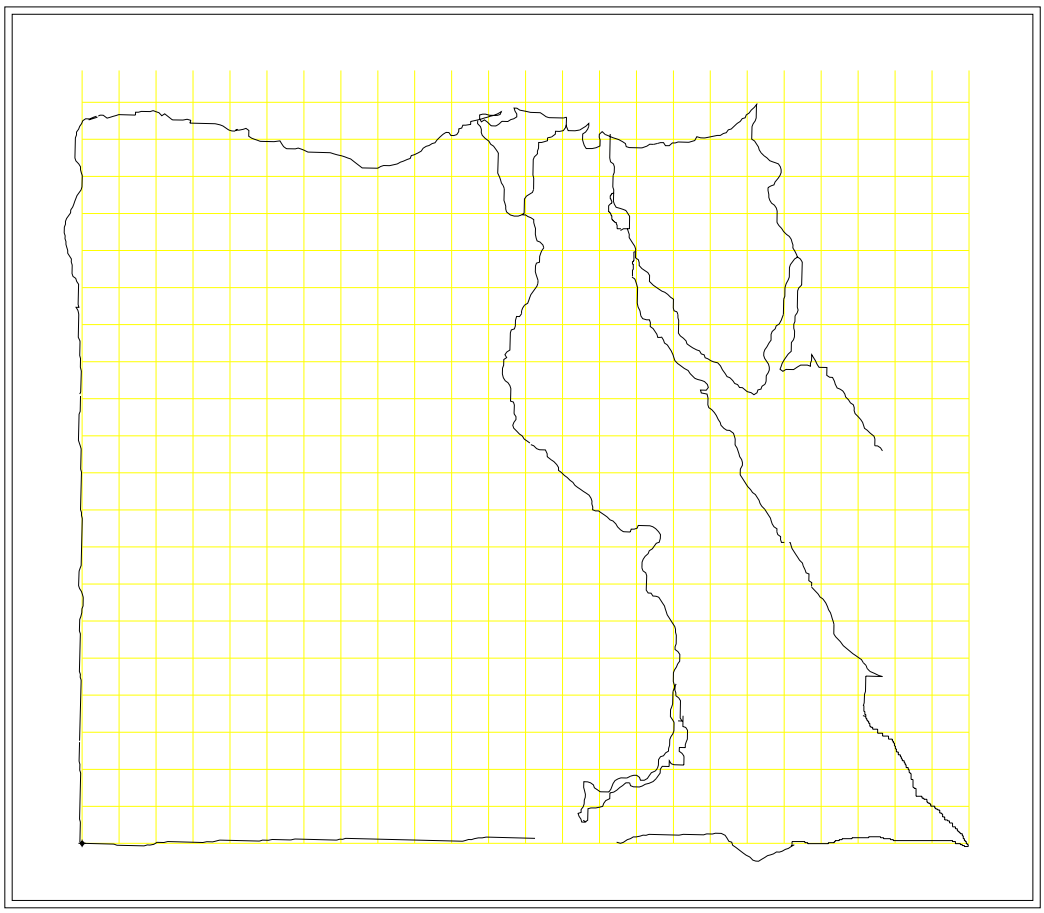

Figure (4.1): The Grid of Egypt

⇒ The difference between the ellipsoid and Orthometric height at any station is described in the following equation (as shown in figure (4.2)):

$$N = h - H \qquad (4.14)$$

⇒ The covariance between each pair of stations under the condition of distance (r) is:

$$C_{ij} = \Sigma N_i N_j / 2 \qquad (4.15)$$

⇒Solving the following equation using general least square technique:

$$C_{ij} = ae^{-br}{}_{ij} \qquad (4.16)$$

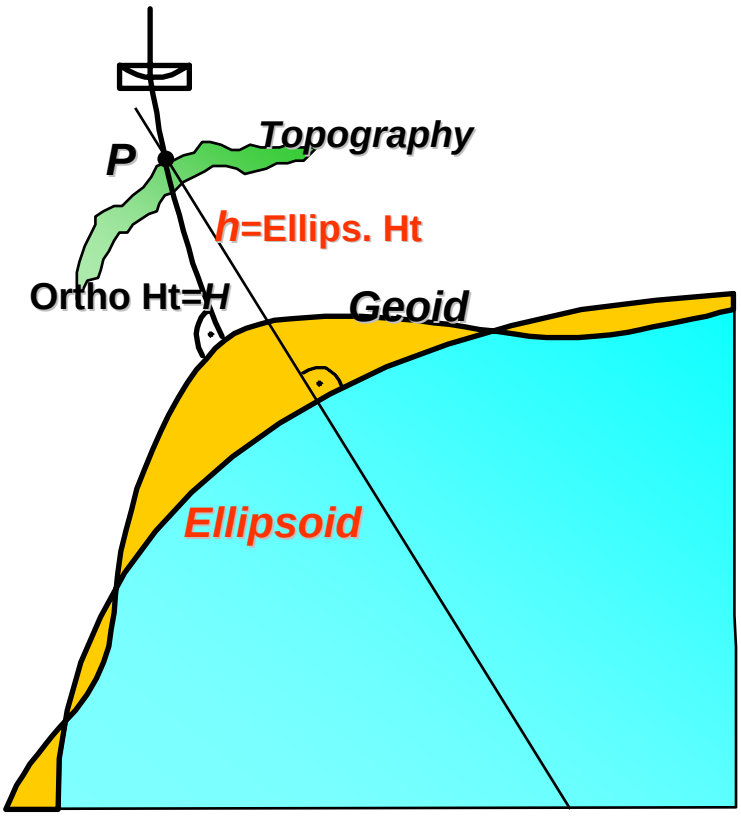

Figure (4.2): The relation between geodetic and orthometric heights

Where: ***a, b*** are unknown parameters and C_{ij} are observations of geoid undulation.

Then the covariance equation will equal

$$C_{ij} = 1.00000000008583\, e^{-0.99999999983886\, r_{ij}} \quad (4.17)$$

The illustration of Equation (4.17) is depicted in figure (4.3). From this equation, the covariance matrix between data and computation points can be determined by the following matrix:

$$C_S = \begin{bmatrix} C_{S_{11}} & C_{S_{12}} \\ C_{S_{21}} & C_{S_{22}} \end{bmatrix} \quad (4.18)$$

Where:

C_{S11} Is a covariance matrix of data points, it's a square matrix of (***n,n***) dimension where ***n*** the number of data points.

C_{S12} , C_{S21} Are the covariance matrix between data and computation points, $C_{S21} = (C_{S12})^T$. C_{S12} is not square matrix but (***n,q***) dimension where q is the number of computation points.

C_{S22} Is covariance matrix of computation points and has (***q,q***) dimension.

After that, rearrange the equation in this form

$$BS + N = b \quad (4.19)$$

Where:

$B=[I|0]$ the unit matrix has a (***n,n***) dimension, and the null matrix has a (***n,q***) dimension.

$S=[S_{11}|S_{22}]^T$ S_{11} is the data vector (n,1) dimension, and S_{22} is the

computation vector (q,1) dimension.

b is the vector of constants (n,1) dimension.

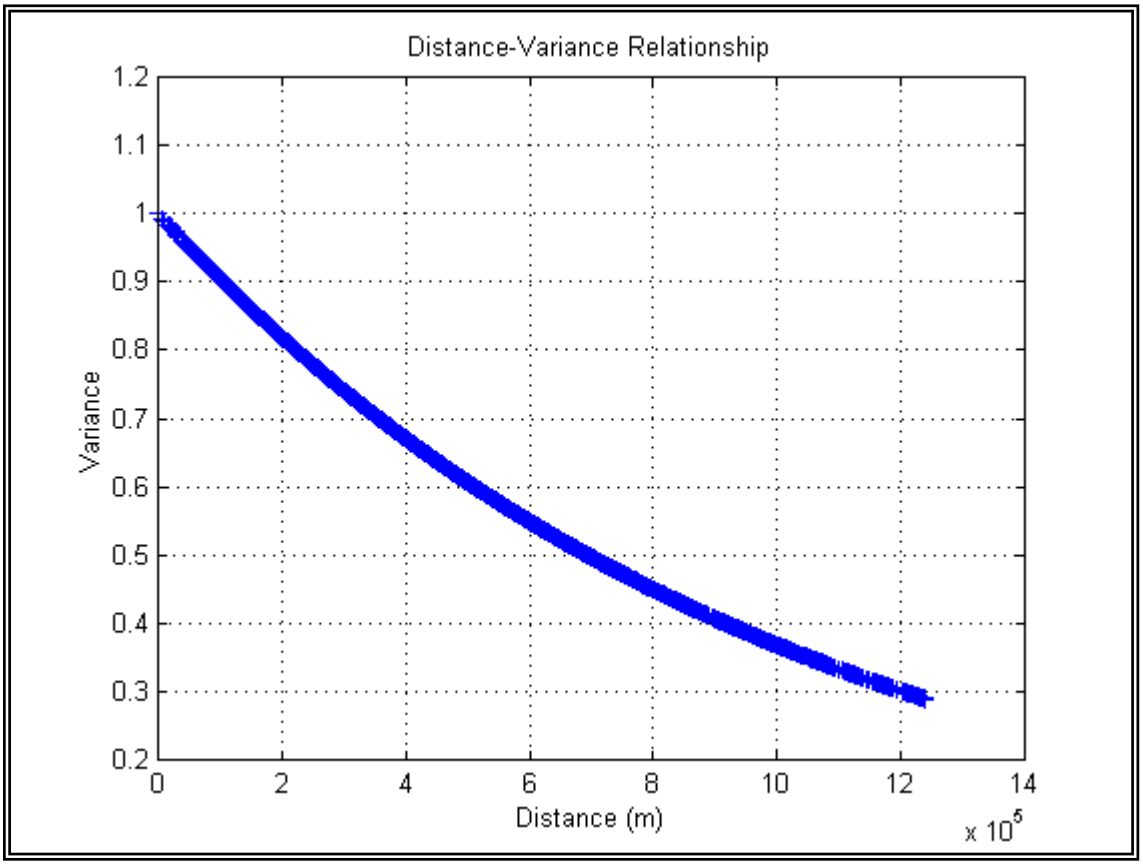

Figure (4.3): The (Distance – Covariance) relationship

Then the computation value of geoid undulation at the grid nodes can be obtained from the following equations as a special case of least square collocation where the system is modeled by the signal ***S*** and noise ***n***.

$$\left.\begin{aligned} S^{\backslash} &= C_s\, B^T (C_n + C_{s11})^{-1} b \\ C_{s\backslash} &= C_s\, B^T (C_n + C_{s11})^{-1}\, B\, C_s \\ n^{\backslash} &= C_n (C_n + C_{s11})^{-1} b \end{aligned}\right\} \qquad (4.20)$$

(90)

$$C_{n\backslash} = C_n(C_n+C_{s11})^{-1}C_n$$

Where: C_n is the covariance matrix of observations.

Based upon the above algorithm, the LSC program is developed and its execution steps can be described in the following:

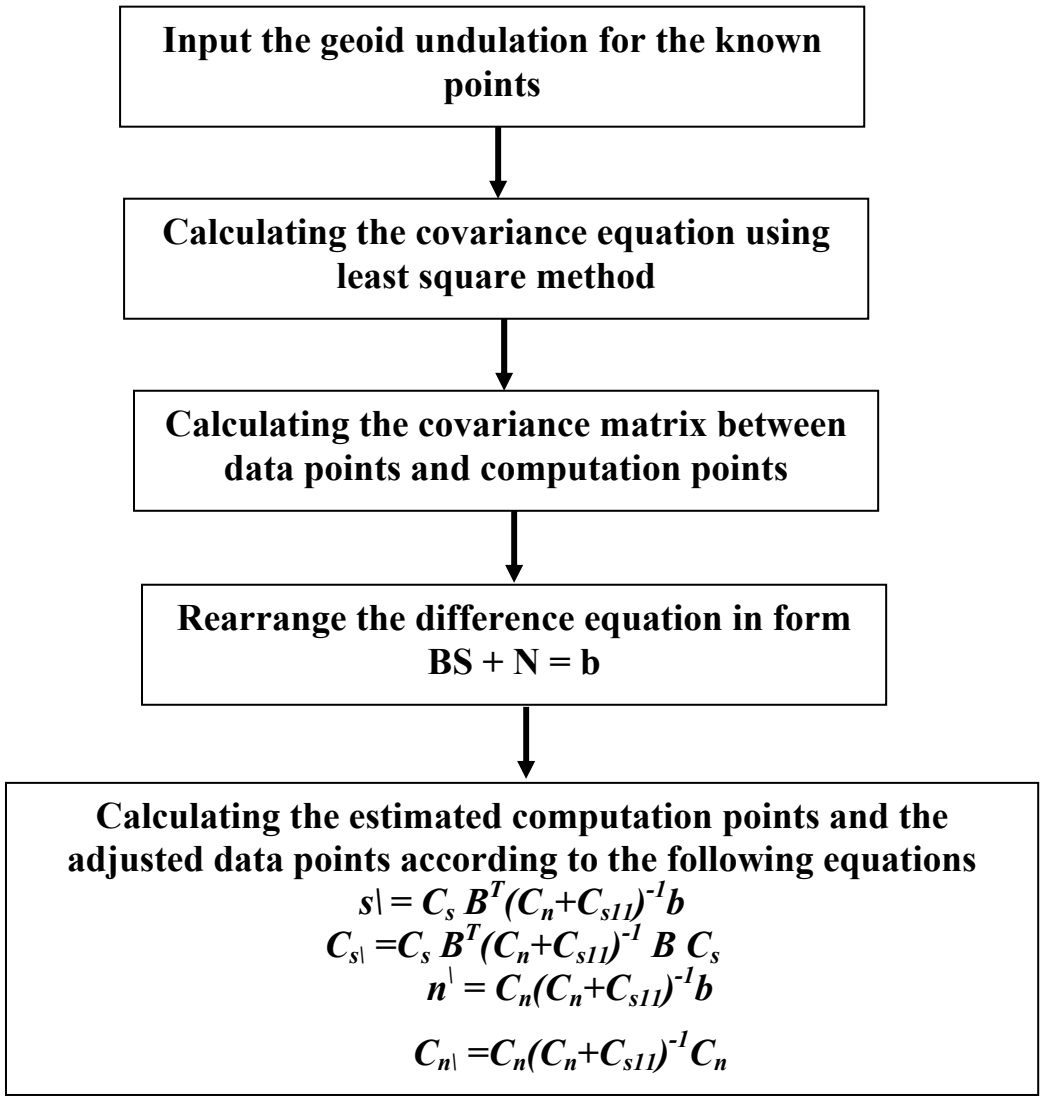

Figure (4.4): Flow chart of LSC technique

1- Input the available coordinates of data and grid points.

2- Calculate the Cartesian coordinates for the data and grid points.
3- Input the geoid undulation at the data points.
4- Calculate the distances between stations and covariance.
5- Calculate value of constant parameters in the equation (4.16) by least square technique.
6- Calculate the covariance matrices between different points (data & computation).
7- Build the general covariance matrix as equation (4.18).
8- Output the Solution of collocation without parameters and printing the results.

4.4 Minimum Curvature Surface (MCS)

Shmbaky, 2004 introduced some obstacles to realize the conversion process of the system of Laplace and Possion equations to be in a programmable algorithm by using least square method.

In this chapter, an explanation for how one can convert the system of Laplace and Possion equations to a programmable by MATLAB program is demonstrated; details are presented in appendix (D). By using the same divided grids in the LSC program:

- The four arms about the nodes may be not completed. So, equation (4.21) can be rearranged as follows to be suitable in our special case such as:

$$\frac{2\varphi_a}{k_1(k_1+k_2)}+\frac{2\varphi_c}{k_1(k_1+k_2)}+\frac{2\varphi_b}{l_1(l_1+l_2)}+\frac{2\varphi_4}{l_1(l_1+l_2)}-(\frac{2}{(l_1l_2)}+\frac{2}{(k_1k_2)})\phi_0=\begin{cases}0, Laplace\\ h^2 f_0, Poisson\end{cases}$$

(4.21)

Where:

K_1, K_2 , l_1, l_2 are the ratio from the complete grid arm (h) shown in figure (4.3), and f_0 is a function of unknown value φ_0 .

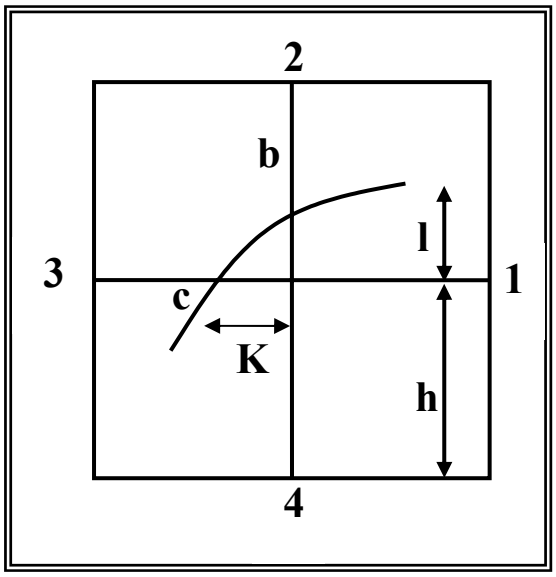

Figure (4.5): The case of uncompleted of grid arms

It can be noticed from this formula that, the position effect of stations on the neighbor nodes.

- When using the grid and there are no information about true difference at the boundaries of the grid to be used in the solution. But unified least square technique will overcome this obstacle and the boundaries difference will be predicted and adjusted according to the available data.
- The number of node, this obstacle can be solution it by built a program using MATLAP program asking the user about the number of unknown nodes before started solution. unified least square can be applied to equations with Laplace equation as equation (4.22).

$$A_{(n,m)}\, V_{(m,1)} = F_{(n,1)} \qquad (4.22)$$

Where:

- ***n*** The number of equations
- ***m*** The number of unknown and known station
- ***F*** The constant vector equal to observation difference
- ***V*** The vector of residual

Which ***V*** = no. of unknown nods / no. of difference coordinates for known stations.

After we known that, can be design the MCS program as follow

1- Collecting geographical coordinates data
2- Entering the number of grid nodes
3- Collecting the data matrix for original grid which contains the length of node arms, number of neighbors nodes on the grid and the value of distortion.
4- Calculating the number of equations
5- Calculating the degree of freedom
6- Constructing A matrix as in equation (4.22)
7- Beginning the iteration process
8- Calculating equivalent weight matrix (We)
9- Constructing F matrix as equation (4.22)
10- Calculating least square operation
11- Calculation the posterior covariance
12- Running the Fisher test at 99 % confidence interval for posterior variance

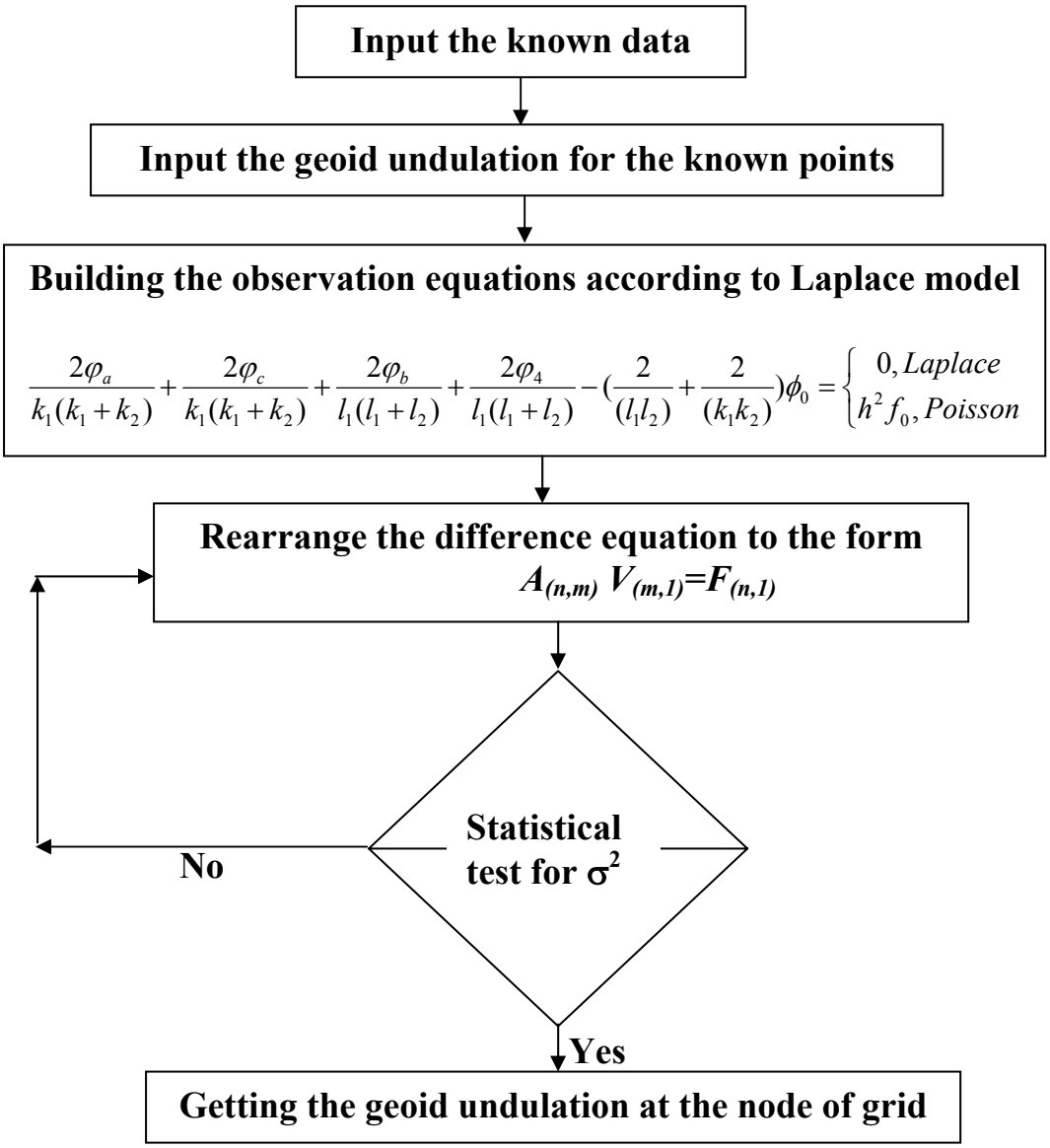

Figure (4.6): Flow chart of MCS technique

4.5 Circulation for secondary programs

Besides above programs, secondary soft were we used like EXCELL and SURFER programs. Rearrangement of raw data made by EXCELL program and contour maps for data made by SURFER program are description in the following flow chart.

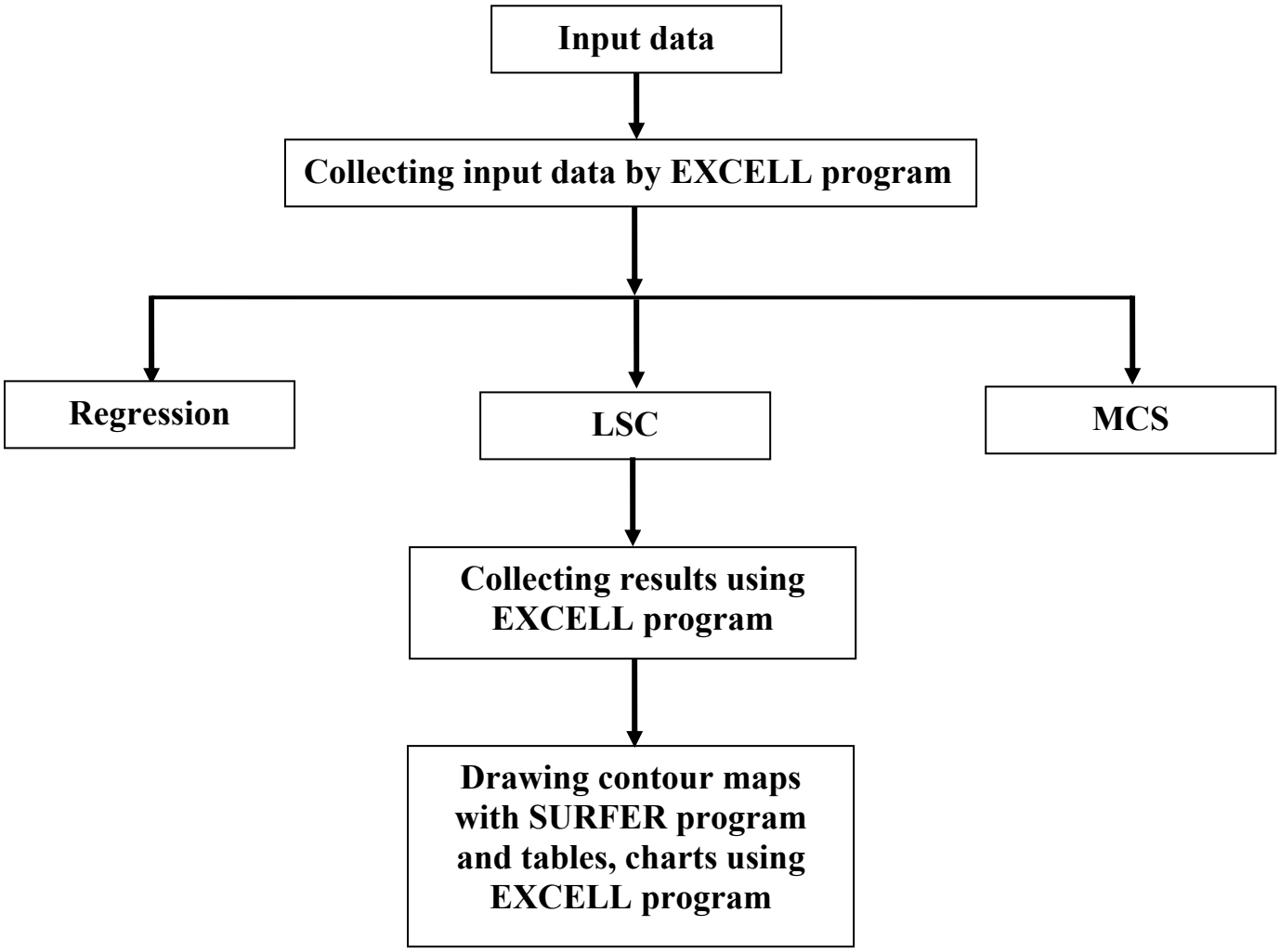

Figure (4.7) Flow chart for analysis process

Chapter (5)

RESULTS AND DISCUSSION

5.1 Introduction

The determination of the geoid has been one of the prime objectives of geodesy. The knowledge of the geoid with respect to some reference ellipsoid, either on a global or local scale is valuable to geodesy, surveying and geophysics for a number of purposes such as the reduction of measured distances to a reference surface and the processing of satellite observations. The geoid heights are essential for verification of global datums and transformation of local datums to the world datum. Also the combination of an accurate geoid model with GPS co-ordinates plays a dominant role in achieving high accuracy leveling results. Spirit leveling is tedious, time consuming and costly in conventional surveying exercise. The knowledge of the geoid is also essential in geophysical explorations (reconnaissance survey), in control surveys, in large scale mapping, in engineering surveys, in height control and in understanding of the Earth's crustal structure.

In this chapter a trail to compute the geoid undulations from the GPS data, and by using mathematical models, including the Linear regression model, the Least Squares Collocation (LSC) and the minimum curvature surface (MCS) techniques, as shown in figure (5.1). Comparisons between the best models with world geoid models are also discussed.

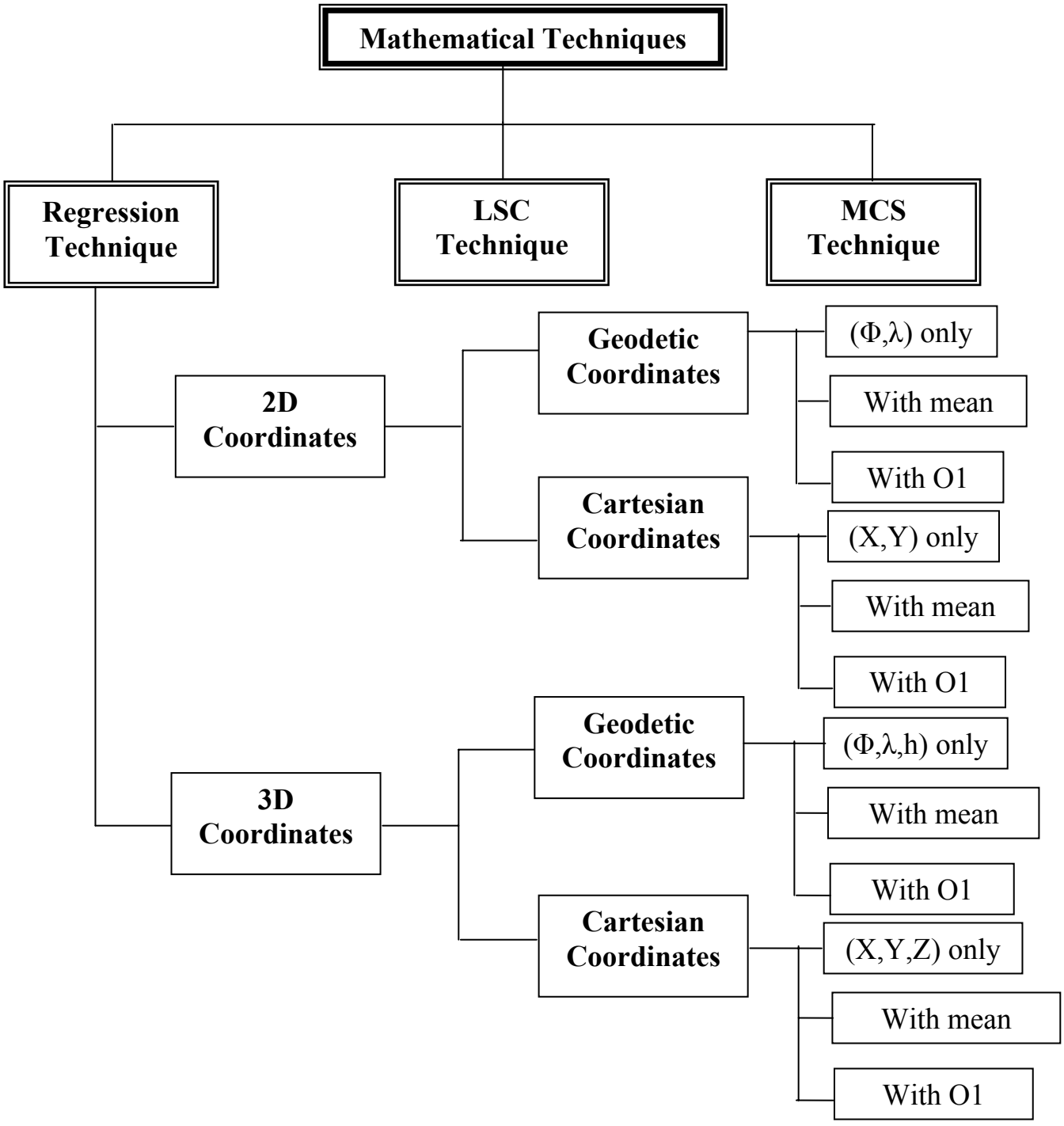

Figure (5.1): The used mathematical techniques

5.2 Results of regression models

The regression model is considered as the most common method which are used to determine the geoid undulation. The next part is devoted to illustrate the applicable regression models which estimate the geoid undulation parameters for the studying area (Egypt). Regression models can be classified into two main parts: first regression model is in two dimensions and the second regression model is in three dimensions. In the first and second regression models, Cartesian and the Geodetic coordinates are applied. Using the mean value of the data available and, point O1 (Φ = 29.85936392, λ = 31.34369133, h = 135.2113) on the WGS84 datum, to be the mean value of observations for Egypt, which were applied in the two regressions models. The value of coefficients can be estimated by using four linear regressions models (first, second, third and fourth) using the common points at WGS84 datum.

The used common points and check points are extracted from HARN network which mentioned in the final report of the new adjusted national geodetic network [S.Powell, 1997] as shown in tables (5.1) and (5.3).

On the other hand, the geoid undulation extracted from the report of (S.Powell, 1997), the common points shown in table (5.2), and check points shown in table (5.4).

Table (5.1) The coordinates of the used common points

The GPS ST.= OED-30	Geodetic coordinate							Cartesian coordinate		
	LATITUDE			LONGITUDE			Ellips.	X	Y	Z
	DEG	MIN	SEC	DEG	MIN	SEC	Height			
OZ2=O5	22	25	19.94361	31	33	45.26781	284.817	5026419.368	3087749.752	2417804.549
OZ7=A5	24	2	28.8962	32	49	58.0757	207.162	4897242.393	3160026.557	2582552.079
OZ8=B19	23	56	26.73463	35	23	50.53294	84.248	4754542.731	3378549.223	2572322.154

OZ9=B20	26	1	2.76559	34	19	16.33949	23.977	4736887.785	3233855.35	2780808.426
OZ10=M3	25	57	20.06853	32	9	24.25427	323.067	4858414.656	3054386.166	2774778.836
OZ11=I15	25	32	37.05482	29	24	10.53256	569.843	5017018.378	2827282.105	2733777.627
OZ12=NEW	28	30	26.01266	29	5	48.59469	284.916	4901454.426	2727759.562	3026156.542
OZ13=T2	27	16	3.09019	30	46	46.61555	223.345	4874398.459	2903374.688	2904698.744
OZ14=B11	27	52	48.6669	33	21	42.36244	63.896	4712281.068	3102667.275	2964805.144
OZ15=NEW	29	21	0.09509	34	46	20.60622	61.948	4570387.221	3173236.76	3107806.047
OZ16=B10ecc	31	7	9.786	34	10	55.44349	123.81	4521178.351	3070521.502	3277296.095
OZ17=A6	30	7	9.51771	32	36	22.44138	55.917	4651428.937	2975426.008	3181848.934
OZ18=NEW	31	35	45.40286	31	4	49.12642	32.061	4657082.606	2807149.786	3322369.803
OZ19=E7	29	50	2.97004	30	36	4.07107	230.875	4766411.552	2818974.913	3154554.543
OZ20=D8	30	50	32.5935	28	56	7.10237	42.806	4796794.204	2651830.557	3250924.75
OZ21=X8	31	19	39.01417	27	4	19.02623	138.281	4855829.779	2481854.818	3297036.49
OZ22=Z9	31	26	16.24367	25	23	55.08191	47.549	4920405.862	2336236.709	3307433.859

Table (5.2) The geoid undulation of the used common points

POINT	N
OZ2	9.779
OZ7	11.049
OZ8	10.668
OZ9	12.741
OZ10	12.158
OZ11	13.172
OZ12	14.219
OZ13	12.751
OZ14	14.644
OZ15	17
OZ16	17.026
OZ17	16.206
OZ18	17.826
OZ19	14.945
OZ20	15.067
OZ21	17.242
OZ22	19.33

Table (5.3) The coordinate of the used check points

	Geodetic coordinate							Cartesian coordinate		
The GPS ST.=	**LATITUDE**			**LONITUDE**			**ELLIPS.**	**X**	**Y**	**Z**
OED-30	**DEG**	**MIN**	**SEC**	**DEG**	**MIN**	**SEC**	**height(m)**			
OY27=N7	30	13	55.83453	29	50	25.27295	175.148	4784223.394	2744427.104	3192725.343
OY35=L5	22	45	7.89148	31	50	55.47227	406.916	4999107.594	3105468.866	2451592.35

OY36=R5	22	6	28.09885	31	33	7.9739	347.744	5038268.669	3093774.252	2385607.703
OY41=Y5	22	12	21.6148	31	33	17.57785	199.982	5034513.233	3091791.019	2395623.225
OZ32=P4	24	9	18.43374	32	58	5.39005	250.727	4885479.958	3168809.756	2594072.206
OZ44=A4	25	38	53.34491	32	41	36.07212	114.34	4841913.266	3107659.942	2744024.506
OZ52=E5	23	25	45.99662	32	49	36.22685	288.768	4920563.856	3174336.931	2520542.932
OZ66=B3	27	19	30.83725	31	11	18.94993	89.172	4850939.254	2936513.888	2910319.771
OZ68=S2	27	24	42.98709	30	32	36.21647	275.318	4880037.043	2879542.056	2918938.221
OZ70=A2	29	1	5.12772	31	9	34.73588	110.696	4776646.582	2888244.114	3075708.475
OZ74=L2	28	11	4.59862	30	48	16.62154	209.738	4832508.896	2881281.294	2994652.825
OZ97=F1	30	1	43.45961	31	16	39.63006	219.776	4723587.068	2869465.636	3173242.278

Table (5.4) The geoid undulation of the used check points

POINT	N
OY27=N7	15.088
OY35=L5	11.156
OY36=R5	9.974
OY41=Y5	10.092
OZ32=P4	11.397
OZ44=A4	12.02
OZ52=E5	10.098
OZ66=B3	12.842
OZ68=S2	13.488
OZ70=A2	15.216
OZ74=L2	13.738
OZ97=F1	15.268

The model was accomplished using 30 points of HARN and 33 points of OED-30 in total without any inconsistent point, because probable inconsistent points have been removed during the modeling studies as shown in figure (5.2). seventeen of these points were taken as modeling pins (common points) with known geoid undulation these points are distributed as shown in figure (5.3), and the rest 12 points were chosen for testing the model (check points) as shown in figure (5.4). While choosing these test points, the homogenous distribution and topogragraphic properties were considered and the availability of the data.

The geographic coordinates including heights (h) are identified in WGS84 datum and the practical heights (H) are identified from geometric leveling in the datum of Egypt, OED-30 datum.

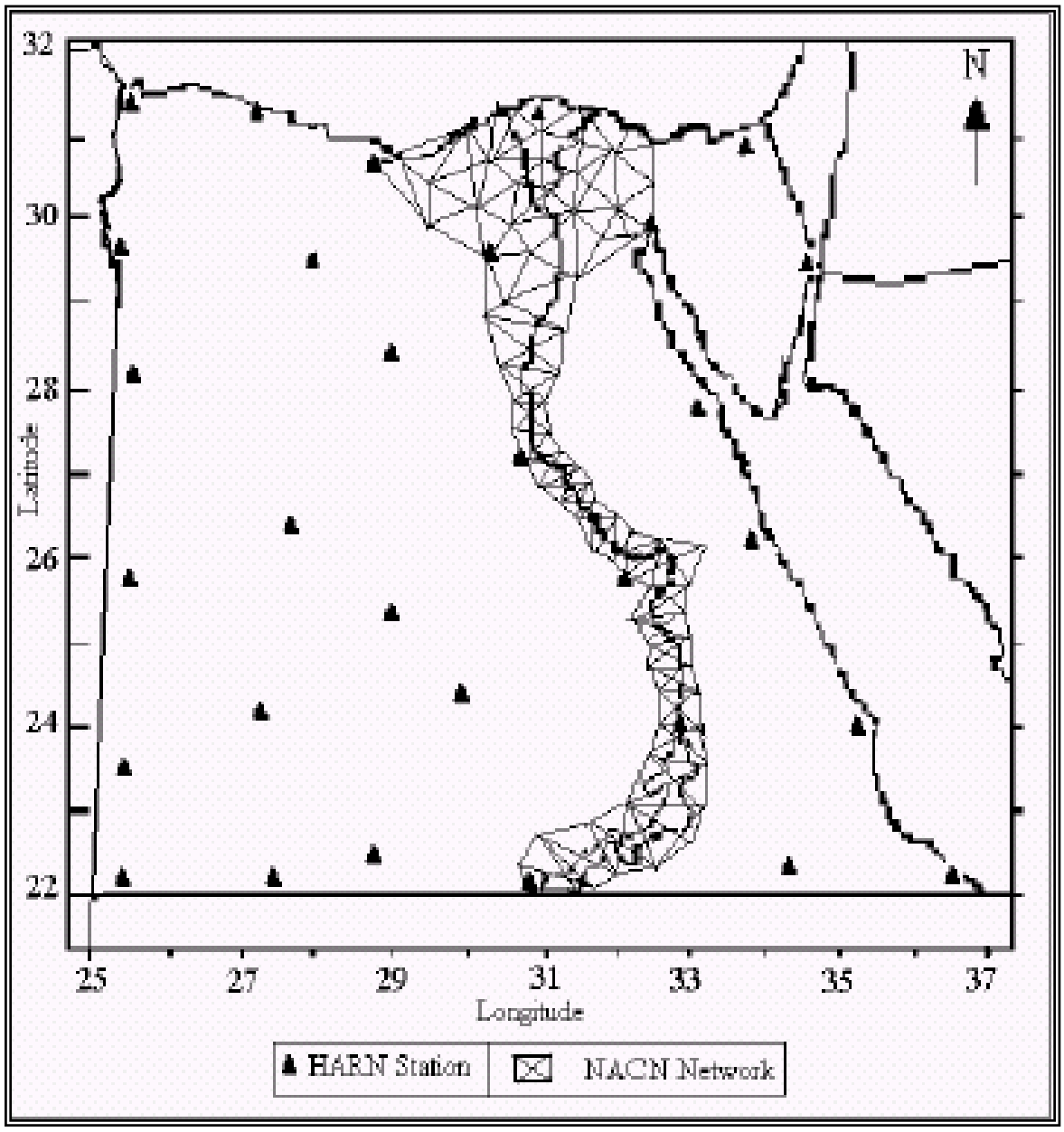

Figure (5.2): Recent precise GPS geodetic control networks in Egypt (G.M.Dawod, 2005)

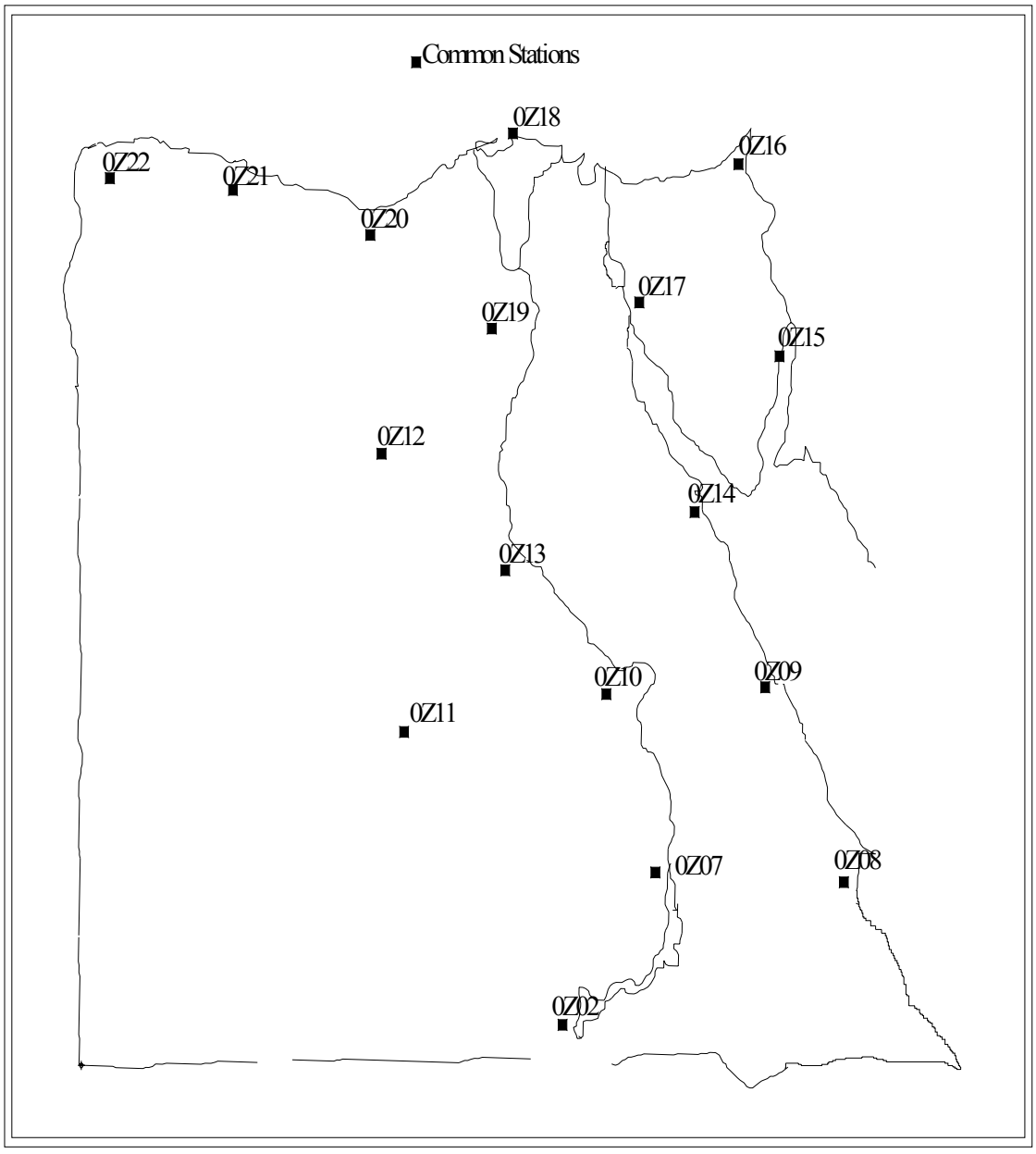

Figure (5.3) The used common points

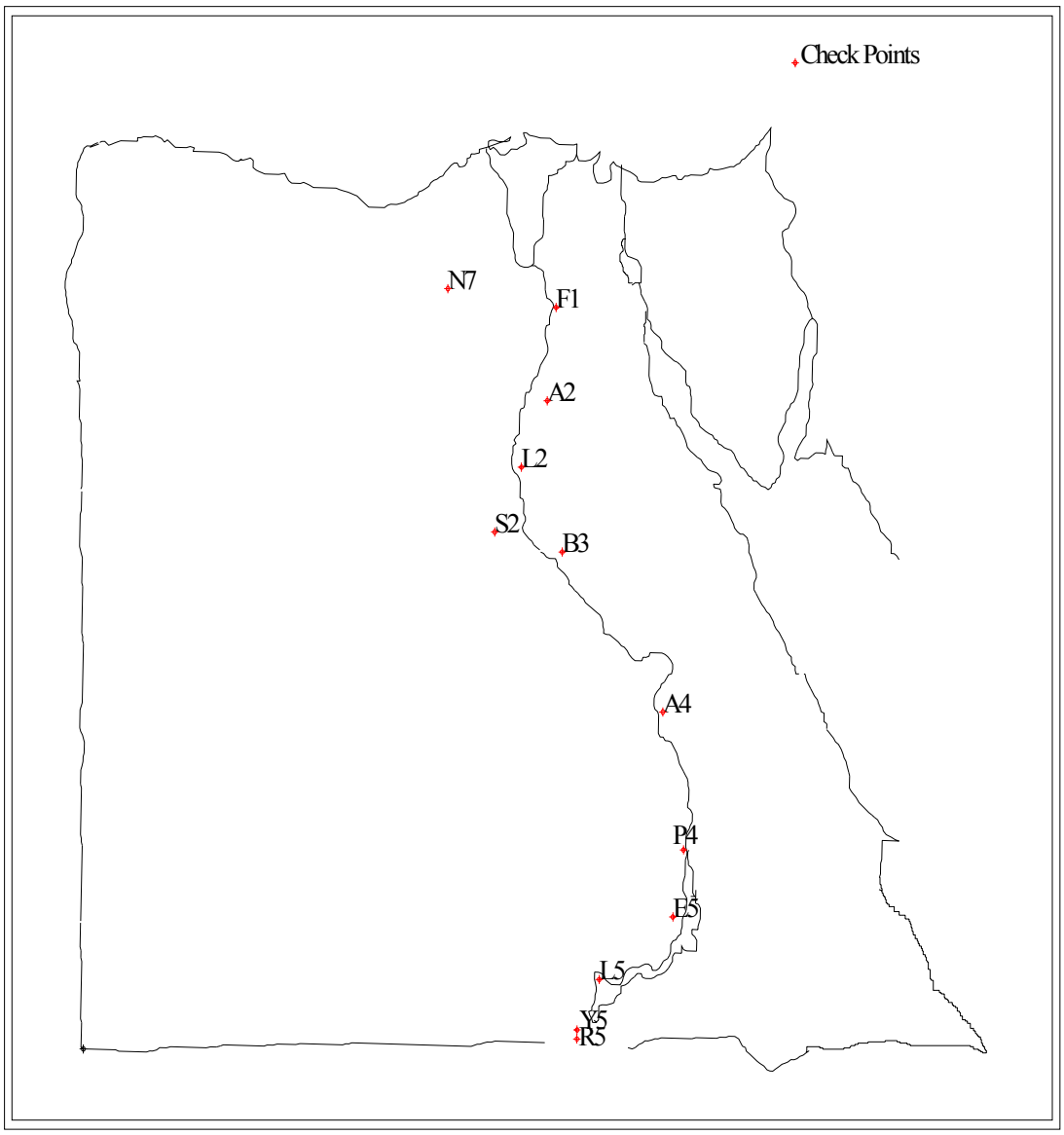

Figure (5.4) The used check points

In general the solution divided into two trials, the first trial used a technique to determine the geoid undulation by a linear multiple regression model in two dimensions for the geodetic coordinates of the points, and the second is to

determine it by Cartesian coordinates. To obtain the Cartesian coordinates we should convert the geodetic coordinates of points to the Cartesian coordinates because all available data are geodetic coordinates. The second trials use the mean value of known data and point (O1) as an average point of Egypt.

5.2.1 Tow Dimensional polynomial technique

5.2.1.1 Tow Dimensional polynomial technique with plane geodetic coordinates

The used polynomial model in the regression solution is as follow:

$$N = \sum_{i=0}^{n} \sum_{j=0}^{i} A_{ij} * \lambda^{i-j} * \phi^{j} \qquad \text{.....(5.1)}$$

Trial uses the geodetic coordinate in two dimensions (Φ,λ) only and uses it in the polynomial model (first, second, third and fourth) degree. In the second trial, it uses the mean value of longitude and latitude in the same equation of polynomial as follow;

$$N = \sum_{i=0}^{n} \sum_{j=0}^{i} A_{ij} * (\lambda - \lambda_o)^{i-j} * (\phi - \phi_o)^{j} \qquad \text{.....(5.2)}$$

Then, uses the point O1 equally the mean value of above equation as follow

$$N = \sum_{i=0}^{n} \sum_{j=0}^{i} A_{ij} * (\lambda - 31.34369133)^{i-j} * (\phi - 29.85936392)^{j} \qquad \text{.....(5.3)}$$

The results of the used polynomial model with least square method are shown in table (5.5).

Table (5.5) Comparison of various polynomial degrees (Φ,λ). Unit (m)

Degree	Test	Max.dist.	Min.dist.	S.D.dist.	Average dist.
First Degree	**Φ,λ only**	1.265862723	0.067587077	0.356054367	0.620689001
	With mean	1.265862723	0.067587077	0.356054367	0.620689001

	With O1	1.265862723	0.067587077	0.356054367	0.620689001
Sec. Degree	**Φ,λ only**	0.706943399	0.058985627	0.232491278	0.303259486
	With mean	0.850853984	0.066258689	0.266230491	0.300319663
	With O1	0.850853984	0.066258689	0.266230491	0.300319663
Third Degree	**Φ,λ only**	0.788438563	0.066823542	0.249446916	0.328392631
	With mean	0.784895727	0.071875784	0.247107709	0.327490099
	With O1	0.784895727	0.071875784	0.247107709	0.327490099
Fourth Degree	**Φ,λ only**	261.9146256	5.591150034	95.85310137	136.1270782
	With mean	1.076674039	0.058514803	0.345641922	0.393025862
	With O1	1.076674039	0.058514803	0.345641922	0.393025862

From table (5.5), it is obvious that:-

- The first degree: all trials (Φ,λ only, With mean and With O1) have the same maximum, minimum, average distortion and standard deviation of distortion.
- The second degree of solution: the (Φ,λ only) is the best solution because , it is less than distortion and standard deviation for other.
- In the third degree the method of using (with mean, with O1) showed the best solution in comparison with first and second and the same results were obtained for fourth degree.
- The results clearly show that by using the points O1, for the mean of Egypt, gave the same values of distortion when using the mean value of data point.

The comparison between the distortions values of the test point obtained at the best solution of the different degrees is illustrated in figure (5.5). The average of distortions of the best models is illustrated in figure (5.6) and the standard deviation of the best model is illustrated figure (5.7).

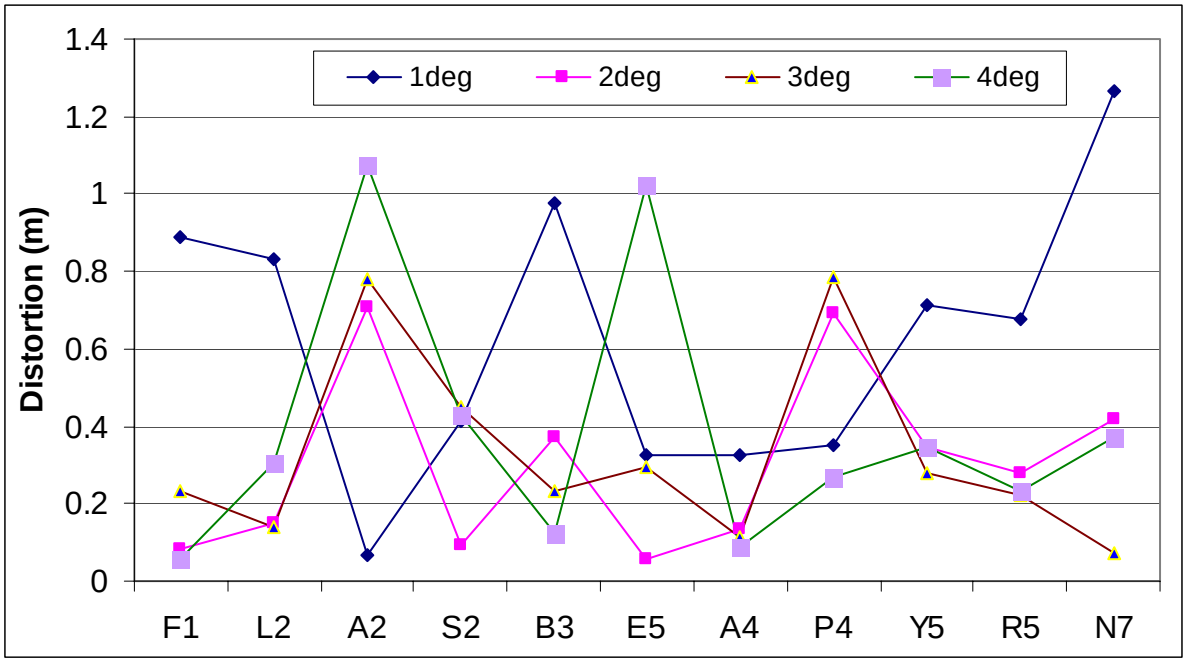

Figure (5.5) The distortion at check points by (Φ,λ) polynomial technique

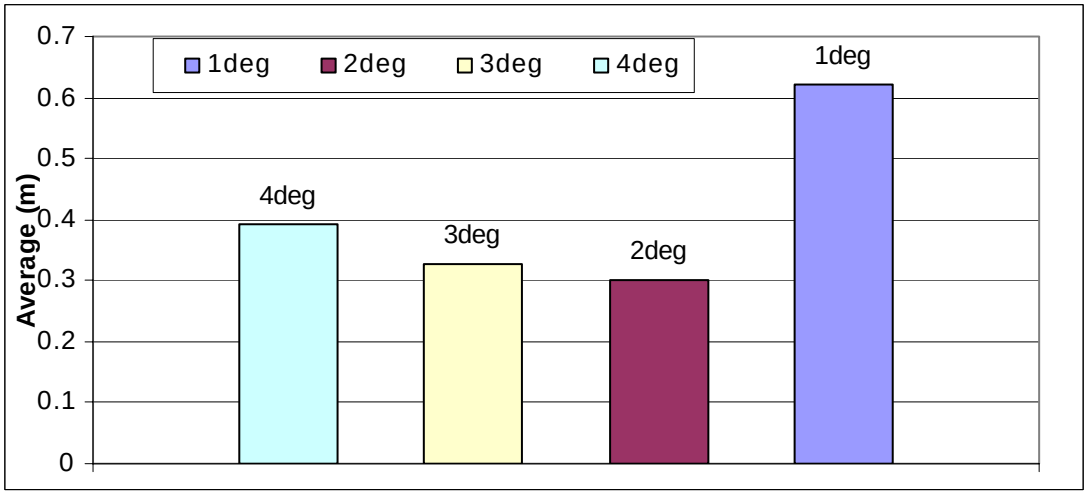

Figure (5.6) The average distortion at check points by(Φ,λ) polynomial technique

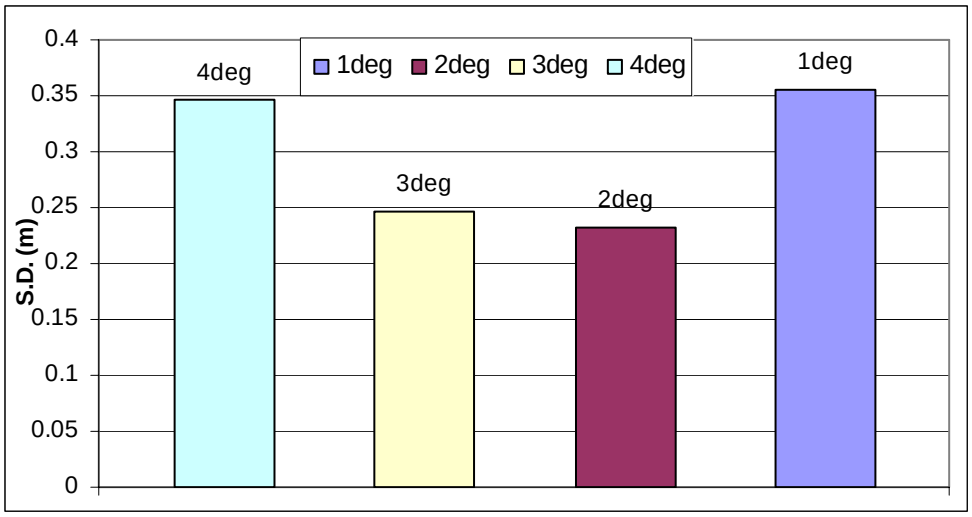

Figure (5.7) The standard deviation at check points by(Φ,λ) polynomial technique

From the obtained figures, the second degree (Φ,λ only) of polynomial method is the best solution, because it c gives the minimum distortion and high accuracy as compared with the other degrees of solutions, and gives the best value of geoid undulation in Egypt.

5.2.1.2 Tow Dimensional polynomial technique with plane Cartesian coordinates

As the same in section (5.2.1.1), but using Cartesian coordinates with applying (X,Y) coordinate of common and check points.

Using the polynomial regression model as follow:

$$N = \sum_{i=0}^{n} \sum_{j=0}^{i} A_{ij} * X^{i-j} * Y^{j} \quad \text{.....(5.4)}$$

The Cartesian coordinate in two dimensions ((X,Y) only) are used in the polynomial model (first, second, third and fourth) degree as a first trial. In the second trial, the mean value of X and Y were used in the same equation of polynomial method.

$$N = \sum_{i=0}^{n} \sum_{j=0}^{i} A_{ij} * (X - X_o)^{i-j} * (Y - Y_o)^{j} \quad \text{.....(5.5)}$$

Also using the point O1 equally the mean value of above trial in this equation

$$N = \sum_{i=0}^{n} \sum_{j=0}^{i} A_{ij} * (X - 4728311.34465516)^{i-j} * (Y - 2377486.19313806)^{j}$$

……..…(5.6)

The results of the used polynomial model with least square method are shown in table (5.6).

Table (5.6) Comparison of various polynomial degrees (X,Y). Unit (m)

Degree	Test	Max.dist.	Min.dist.	S.D.dist.	Average dist.
First Degree	X,Y only	1.14455652	0.131294442	0.304268744	0.501109626
	With mean	1.144558887	0.13129207	0.304269444	0.501110257
	With O1	1.144558885	0.131292072	0.304269444	0.501110257
Sec. Degree	X,Y only	62779.25117	61131.77078	607.4655653	61851.74435
	With mean	0.730779035	0.04860083	0.241029352	0.314165262
	With O1	0.727119393	0.051335838	0.239679409	0.313903869
Third Degree	X,Y only	3.10474E+14	2.41321E+14	2.82861E+13	2.79302E+14
	With mean	324.8422101	7.748025958	116.1481204	199.1617382
	With O1	229636.0693	28105.22274	62383.28222	98816.53039
Fourth Degree	X,Y only	9.50612E+26	8.73293E+26	2.449E+25	9.08179E+26
	With mean	25425688403	78284568.22	9544919304	7327853892
	With O1	3.4132E+14	9.25973E+12	1.42421E+14	1.37026E+14

From table (5.6), it is obvious that:

- The first degree in (X,Y only) trial is the best solution than the other trials.
- The second degree in(X,Y with mean and with O1)are best solution.

The comparison between the distortions values of the test points by using the best solution of the results obtained is illustrated in figure (5.8). The average of distortions of the best models is illustrated in figure (5.9) and the standard deviation of the best models is illustrated figure (5.10). In these figures, the

third and fourth degrees are neglected, because the distortion of it is greater than other method.

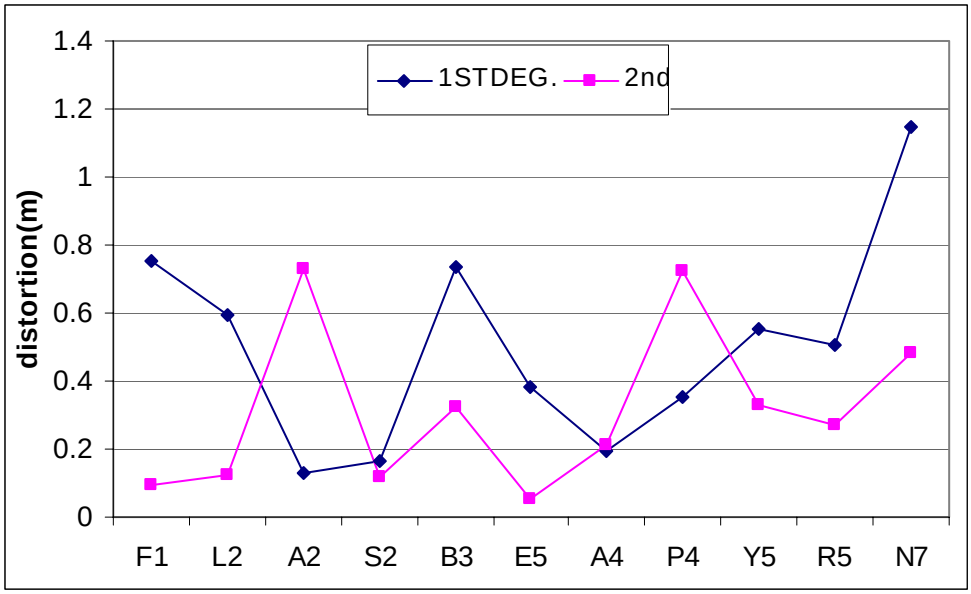

Figure (5.8) The distortion at check points by (X,Y)polynomial technique

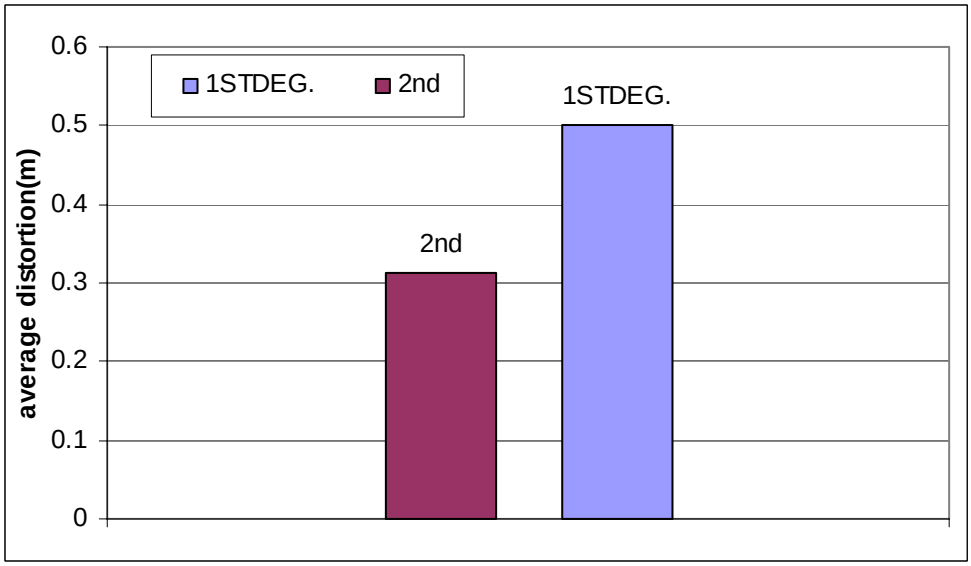

Figure (5.9) The average distortion at check points by(X,Y) polynomial technique

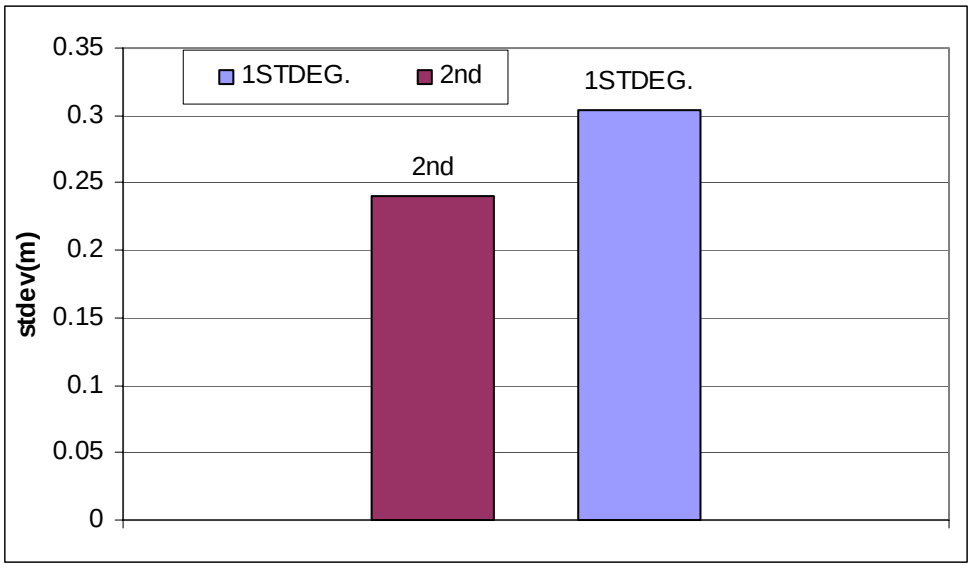

Figure (5.10) The standard deviation at check points by(X,Y) polynomial technique

From the obtained figures, the second degree with mean point O1 is the best solution of this method, because it can give the minimum distortion and high accuracy than the other degrees.

5.2.2 The three dimensions polynomial technique

The second trial uses the three dimensions with polynomial and least square technique. The geodetic and Cartesian coordinates are used to compute the geoid undulation by regression methods (first, second and third degree). This trial used the coordinates directly, the coordinates with mean values and the coordinates with the mean of O1 point.

5.2.2.1 The three dimensions polynomial with geodetic coordinates

Firstly, this trial uses the geodetic coordinate (longitude, latitude and height (Φ,λ,h)), the trial in three dimension is shown in table (5.7)

Table (5.7) Comparison of various polynomial degrees (Φ,λ,h). Unit (m)

Degree	Test	Max.dist.	Min.dist.	S.D.dist.	Average dist.
First Degree	Φ,λ,h	1.239877476	0.085553861	0.347158068	0.609358325
	With mean	1.239877476	0.085553861	0.347158068	0.609358325
	With O1	1.239877476	0.085553861	0.347158068	0.609358325
Sec. Degree	Φ,λ,h	1.57578104	0.006143095	0.4572741	0.583250581
	With mean	13.34195755	4.01786462	3.140453117	9.030476256
	With O1	20.48246684	0.037137874	6.283818387	9.565787764
Third Degree	Φ,λ,h	3.743712393	0.091645784	1.074923142	1.376493093
	With mean	35.68848576	5.49819287	8.232383758	18.52844301
	With O1	106.7974514	6.010384086	30.64462477	30.2072299

From table (5.5), it is obvious that:

- The first degree in all trials is the same.
- The second trial in case of (Φ,λ,h) is the best solution.
- The third trial in case of (Φ,λ,h) is the best solution.

The comparison between the best solutions obtained from the three degrees, the distortion at the check points is shown in figure (5.11). The average of this distortion is shown in figure (5.12) and the standard deviation of distortion is shown in figure (5.13).

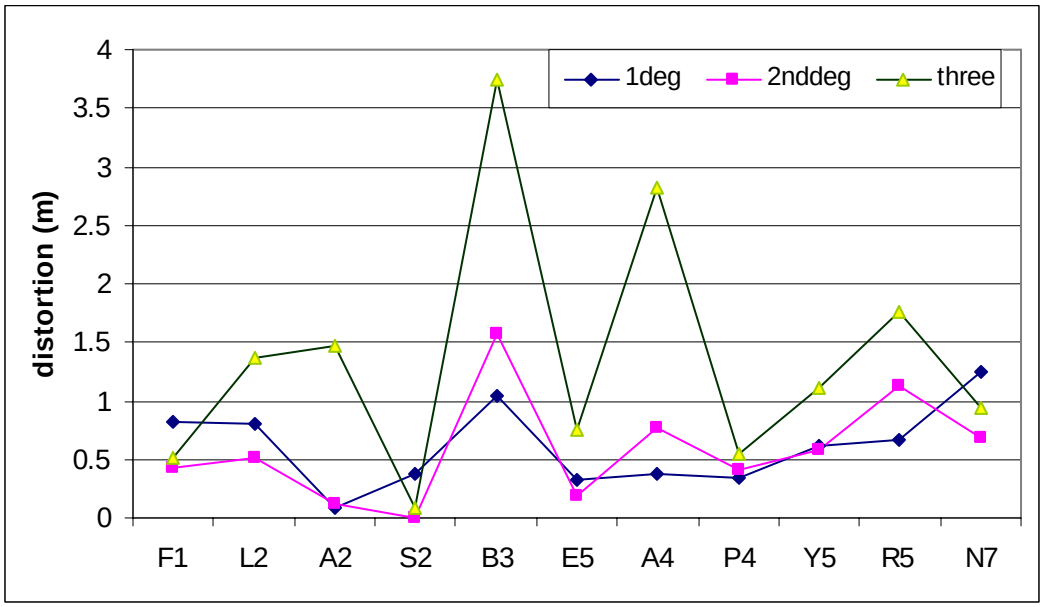

Figure (5.11) The distortion at check points by(Φ,λ,h) polynomial technique

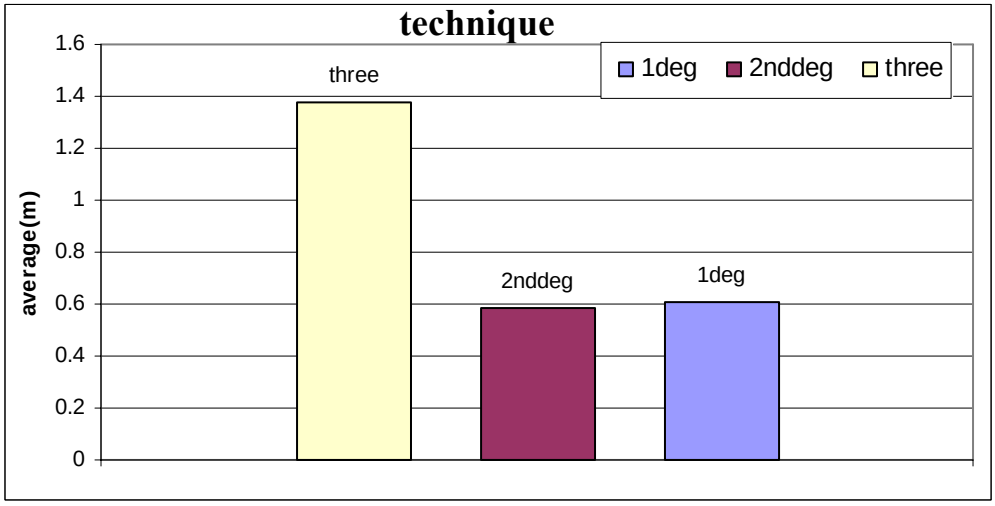

Figure (5.12) The average distortion at check points by(Φ,λ,h) polynomial technique

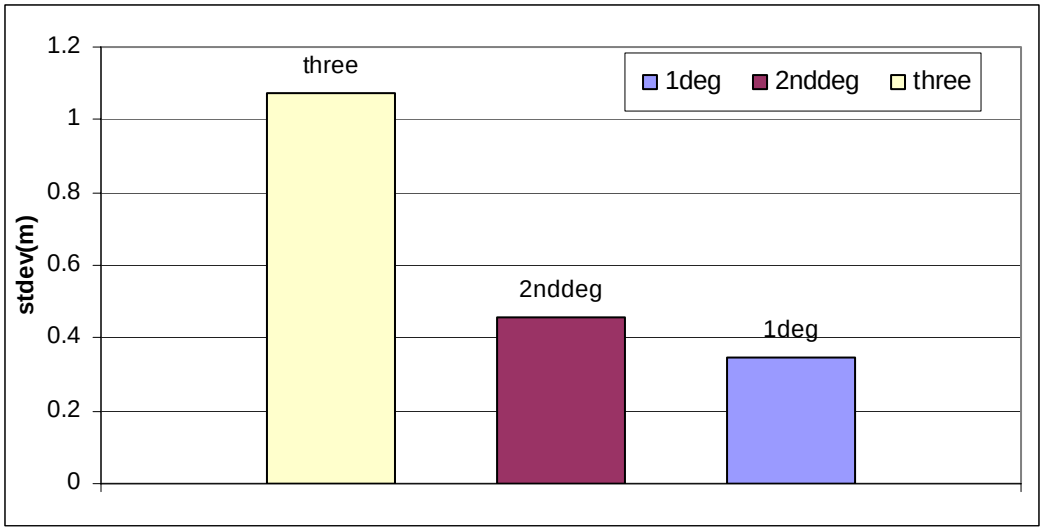

Figure (5.13) The standard deviation at check points(Φ,λ,h) by polynomial technique

Table (5.5) and figures (5.11), (5.12) and (5.13) clearly show that:

- The second degree with three dimensions is the best solution.
- In general the ellipsoidal height (h) in this models, gives high distortion due to the errors in the vertical coordinate high.

5.2.1.2 The three dimensions polynomial with Cartesian coordinates

As the same trial uses the Cartesian coordinates (X,Y,Z) that converted from known geodetic coordinate by MATLABE program as shown in Appendix (D). This trial applied the Cartesian coordinates directly, the coordinates with the mean values and the coordinates with the mean of O1 point.

The distortion of the check points and comparison between all trials is shown in table (5.8).

Table (5.8) Comparison of various polynomial degrees (X,Y,Z). Unit (m)

Degree	Test	Max.dist.	Min.dist.	S.D.dist.	Average dist.
First Degree	X,Y,Z	0.964349712	0.041007874	0.265122123	0.359561363
	With	0.964349712	0.041007873	0.265122123	0.359561363

	mean				
	With O1	0.964349712	0.041007873	0.265122123	0.359561363
Sec. Degree	**X,Y,Z**	1.69799E+44	1.60377E+43	5.68184E+43	8.66883E+43
	With mean	3.78035E+13	6.89996E+12	9.96675E+12	1.70061E+13
	With O1	97031.41213	1505.989477	36306.81223	34248.84386
Third Degree	**X,Y,Z**	5.77194E+12	3.21063E+12	9.35712E+11	4.52942E+12
	With mean	70.50620623	2.707902668	24.98034281	32.98028722
	With O1	686889546.5	180944882.8	174690271.2	422151401.2

The results in the above table show that;

- The first degrees in three cases are the same and give the best solution as compared with the other.

From tables (5.5 to 5.8) and figures (5.5 to 5.13) it is concluded that:

Comparing the best solutions obtained from the all degrees, the distortion at the check points is shown in figure (5.14). The average of distortion is shown in figure (5.15) and the standard deviation of distortion is shown in figure (5.16).

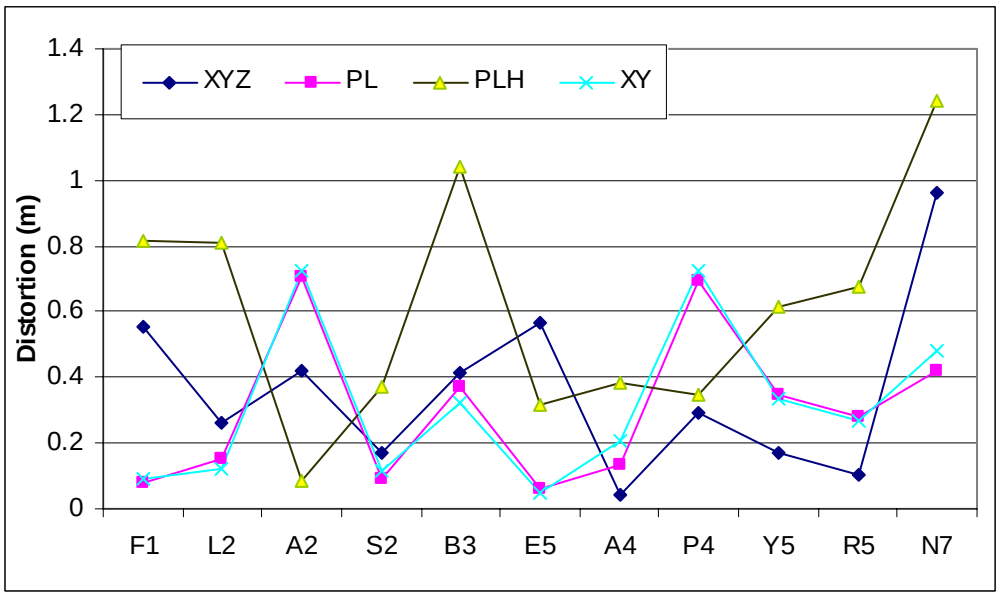

Figure (5.14) The distortion at check points by polynomial techniques

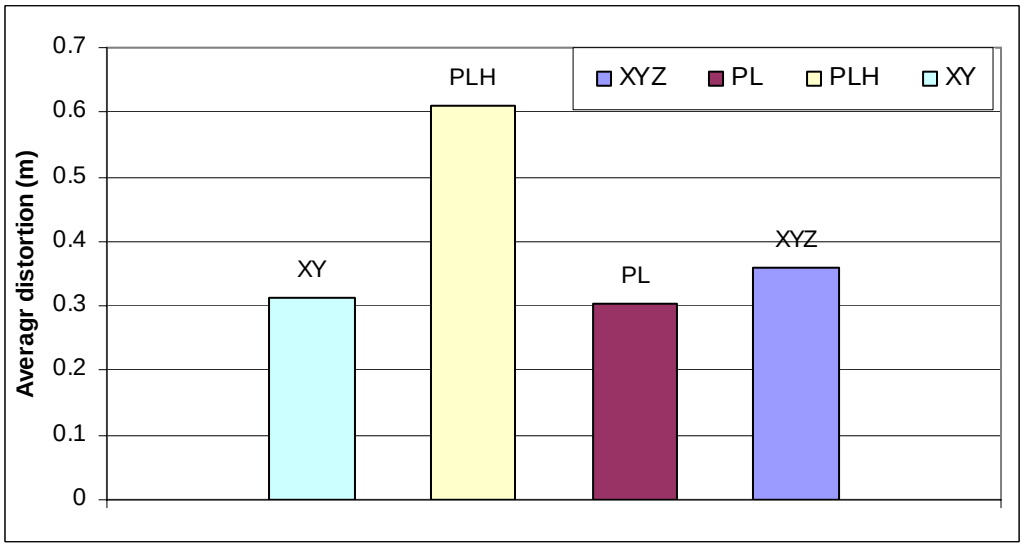

Figure (5.15) The average distortion at check points by polynomial technique

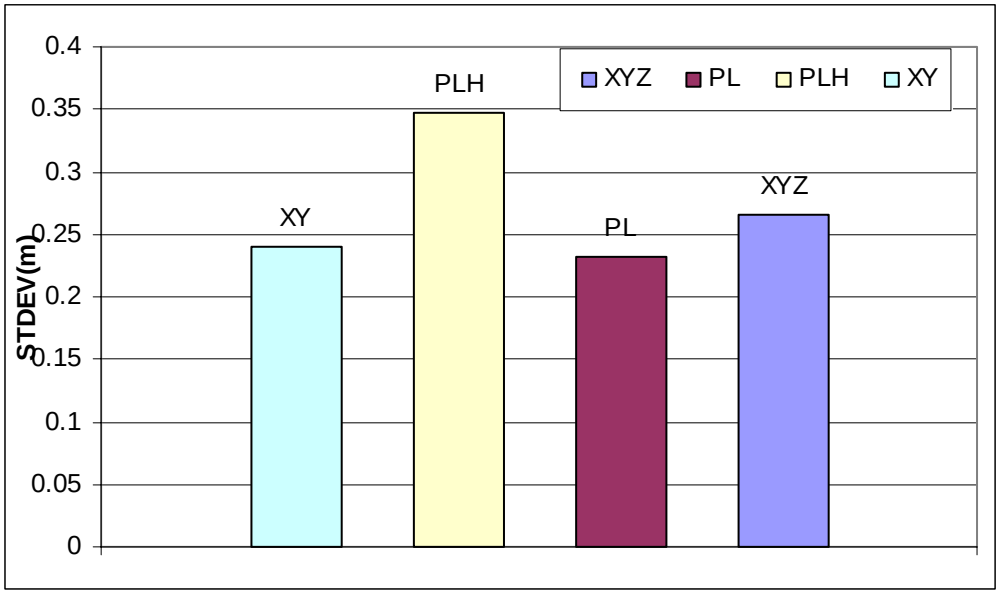

Figure (5.16) The standard deviation at check points by polynomial technique

The best solution in this cases, is the second degree in the plane coordinate with geodetic coordinate with (Φ,λ only).

This best model is represented by the equation (5.7)

$$N = A_{00} + A_{10}\lambda + A_{11}\Phi + A_{20}\lambda^2 + A_{21}\lambda\Phi + A_{22}\Phi^2 \quad \text{.....(5.7)}$$

And the parameters of this equation is illustrated in table (5.9)

Table (5.9) the parameter of two dimension equation (5.7)

parameter	A00	A10	A11	A20	A21	A22
value	**205.3798832**	**-9.98915691**	**-3.26361544**	**0.116691334**	**0.094886366**	**0.018998481**

The geoid undulation of Egypt by using the best model with HARN points is represented in figure (5.17). Is show that the results are different in the western part of Egypt because the available data in this region are smaller and less than that for other regions. The geoid undulation at the Egyptian grids given in the Appendix (B).

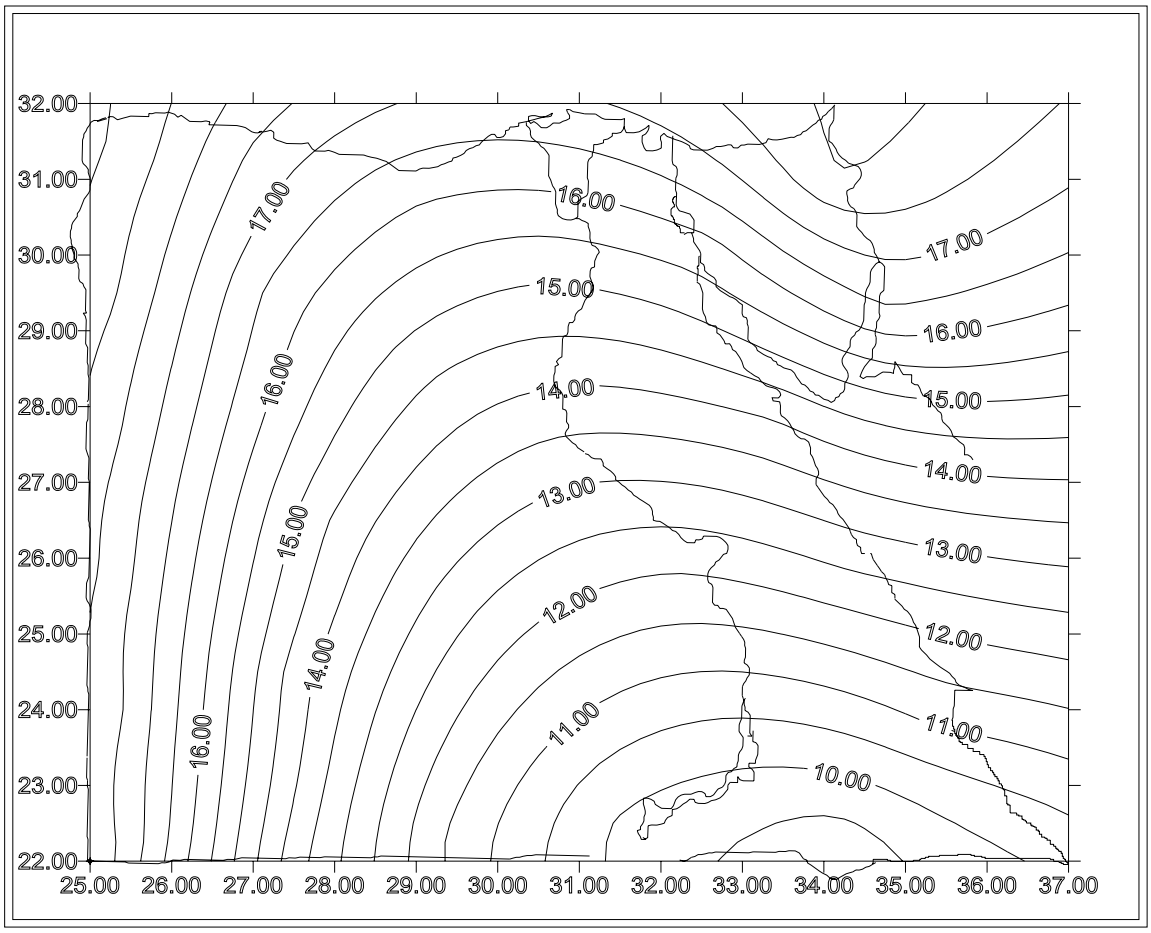

Figure (5.17) The geoid undulation by using second degree polynomial model in two direction (geodetic coordinates) in the HARN data

5.2.3 The polynomial technique with complex numbers

A Polynomial technique with complex numbers, as shown in equation (5.8), was used in first and second degrees.

$$N= (A_1+iA_2) (\Phi+i\lambda) + (A_3+iA_4) (\Phi+i\lambda)^2 \quad \ldots\ldots\ldots\ldots\ldots\ldots\ldots\ldots\ldots\ldots (5.8)$$

The result of the distortion of the geoid undulation is shown in table (5.10).

Table (5.10) The distortion at check points using complex numbers of polynomial technique

Point	First degree	Sec. degree
N7	10.16827708	20.44608771
R5	0.959092248	61.99786122
Y5	0.051057533	248.6241365
P4	0.667322158	399.5121706
A4	1.305132623	541.8299258
E5	0.855130282	805.633836
B3	0.713632378	802.5323206
S2	3.126881101	872.2112358
A2	3.452463694	1049.579868
L2	5.017521293	1360.056544
F1	3.663683378	1433.622184
Max.distortion (m)	10.16827708	1433.622184
Min.distortion (m)	0.051057533	20.44608771
Average distortion (m)	2.725472161	690.5496518
STDEV.(m)	2.937521674	483.1479126

From table (5.10):

- The first degree solution is better than second degree but it is not better than solution of real polynomial method.

5.3 Results of Least Square Collocation (LSC) model

The least square collocation technique is a grid transformation technique. This technique need to divide the area of study to a grid as shown figure (4.1), shifts between geoid and ellipsoid models are calculated for common points.

The calculation of this technique can be summarized as the following:

☞ The difference between the geoid and ellipsoidal models are computed.

☞ The priory covariance matrix can be formed using the following relation $C_{ij} = \Sigma N_i N_j / 2$

☞ Solving the relation between distance and covariance of common points using least square theory to get the general equation $C_{ij} = ae^{-br_{ij}}$

☞ Calculating the covariance matrix between data points and the computation points.

☞ Rearranging the original equations of differences in the form $\boldsymbol{BS + N = b}$.

☞ Solving the system using least square theory with the following equations for collocation method.

$$\boldsymbol{S^{\backslash} = C_s B^T (C_n + C_{s11})^{-1} b}$$

$$\boldsymbol{C_{s\backslash} = C_s B^T (C_n + C_{s11})^{-1} B C_s}$$

$$\boldsymbol{n^{\backslash} = C_n (C_n + C_{s11})^{-1} b}$$

$$\boldsymbol{C_{n\backslash} = C_n (C_n + C_{s11})^{-1} C_n}$$

From the above steps, using the available data, shown in table (5.1), with the program (LSC) is shown in Appendix (D). Obtain the results shown bellow:

The difference at the common points is shown in table (5.11) and the distortion at the test points shown in table (5.12).

Table (5.11) The different at common points by the LSC program

Point	Distortion (m)
OZ02	-1.19757779484043
OZ07	-0.52094371371138
OZ08	-0.05660273646831
OZ09	0.47114006372585
OZ10	-0.48653752000845

OZ11	0.55086737344387
OZ12	0.34836684489816
OZ13	-0.61335214085733
OZ14	1.07652153037670
OZ15	3.51917899386560
OZ16	3.02252828789112
OZ17	1.71635483275438
OZ18	3.04842550261280
OZ19	0.50382540414394
OZ20	0.62011052129405
OZ21	2.90544378688164
OZ22	5.6497170775597

Table (5.12) The distortion at check points by the LSC program

Point	Distortion (m)
N7	**2.075872636**
R5	**1.463509299**
Y5	**1.419522602**
P4	**0.476191869**
A4	**0.176301473**
E5	**0.807534034**
B3	**0.847459177**
S2	**0.852855942**
A2	**1.60187933**
L2	**1.211368401**
F1	**2.05926112**
Max.distortion	**2.075872636**
Min.distortion	**0.176301473**
Average	**1.181068717**
S.D.	**0.61249361**
Range	**1.899571163**

The results of this method are given in Appendix (C).

The contour map of the geoid undulation for the Egyptian grids by using LSC model is shown in figure (5.18).

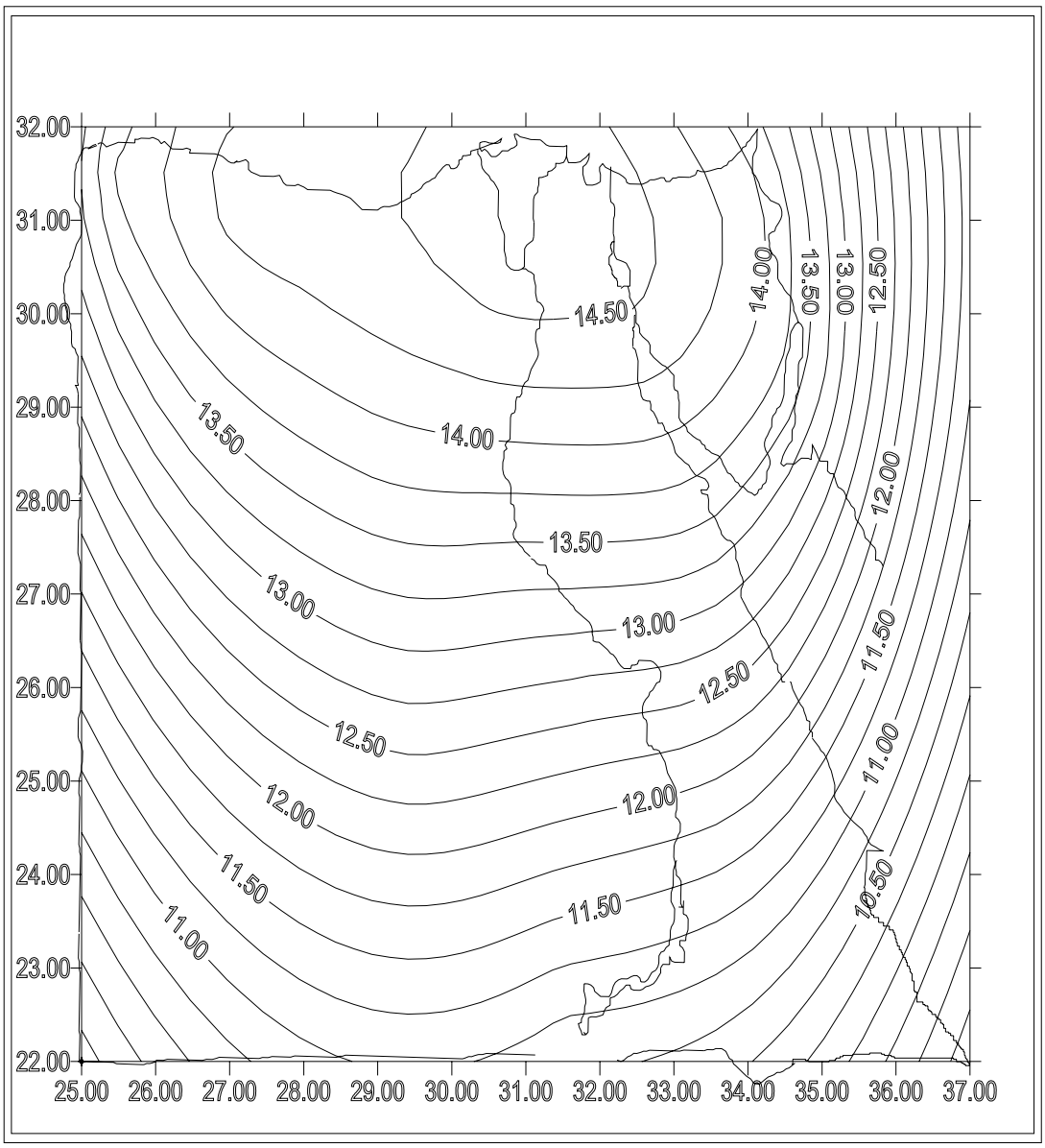

Figure (5.18) The geoid undulation by using LSC model in two direction (geodetic coordinates)

5.4 Results of minimum curvature surface (MCS) model

MCS technique was a grid transformation technique as LSC technique. But in this technique was not depended on a priori variance covariance matrix. After construction the grids above the area of study, as shown in figure (4.1), can be summarized the steps of solution as following:

- ☞ The differences between two models are computed.
- ☞ The observation equations can be formed according to laplace model

$$\frac{2\varphi_a}{k_1(k_1+k_2)}+\frac{2\varphi_c}{k_1(k_1+k_2)}+\frac{2\varphi_b}{l_1(l_1+l_2)}+\frac{2\varphi_4}{l_1(l_1+l_2)}-(\frac{2}{(l_1l_2)}+\frac{2}{(k_1k_2)})\phi_0=\begin{cases}0, Laplace\\ h^2 f_0, Poisson\end{cases}$$

- ☞ Forming the reduced condition equation of the laplace model and applying least square theory with unified technique give the posterior variance.
- ☞ The variance of used common points is obtained and trials are stooped according to covariance of variance.
- ☞ Computing the geoid undulation at unknown grids and drawing the contour map.

From above steps, using the available data shown in section (5.2), with the program (MCS) is shown in Appendix (D). Calculating the distortion at common points, and from that we neglected the points (OZ13, OZ15, OZ19, OZ20, and OZ22) as shown in table (5.13)

Table (5.13) The distortion at common points by the MCS program

Point	Distortion (m)
OZ02	0.07721684810177
OZ07	0.00347249793973
OZ08	-0.22918189336117
OZ09	0.05266968934737
OZ10	-0.60297546581746
OZ11	0.77287428229446
OZ12	-0.7017543695959443
OZ13	-1.0794388009004
OZ14	0.3525176513764
OZ15	1.49303195651246
OZ16	0.00570559336130
OZ17	-0.00291306256056
OZ18	0.32937727462008
OZ19	-1.06750166631848
OZ20	-1.83890599444540
OZ21	-0.11787994573827
OZ22	1.083846763956781

The distortion at check points is shown in table (5.14)

Table (5.14) The distortion at check points by the MCS program

Point	Distortion (m)
N7	0.030532957
R5	0.008740674
Y5	0.008160271
P4	0.009515733
A4	0.016913142
E5	0.004675824
B3	0.01980998
S2	0.017392122
A2	0.029476479
L2	0.023046078
F1	0.035859744
Max.distortion	0.035859744
Min.distortion	0.004675824
Average	0.018556637
STDEV	0.010328157
Range	0.03118392

The results of this method are given in Appendix (A).

The contour map of the geoid undulation for Egyptian grids by using MCS model is shown in figure (5.19).

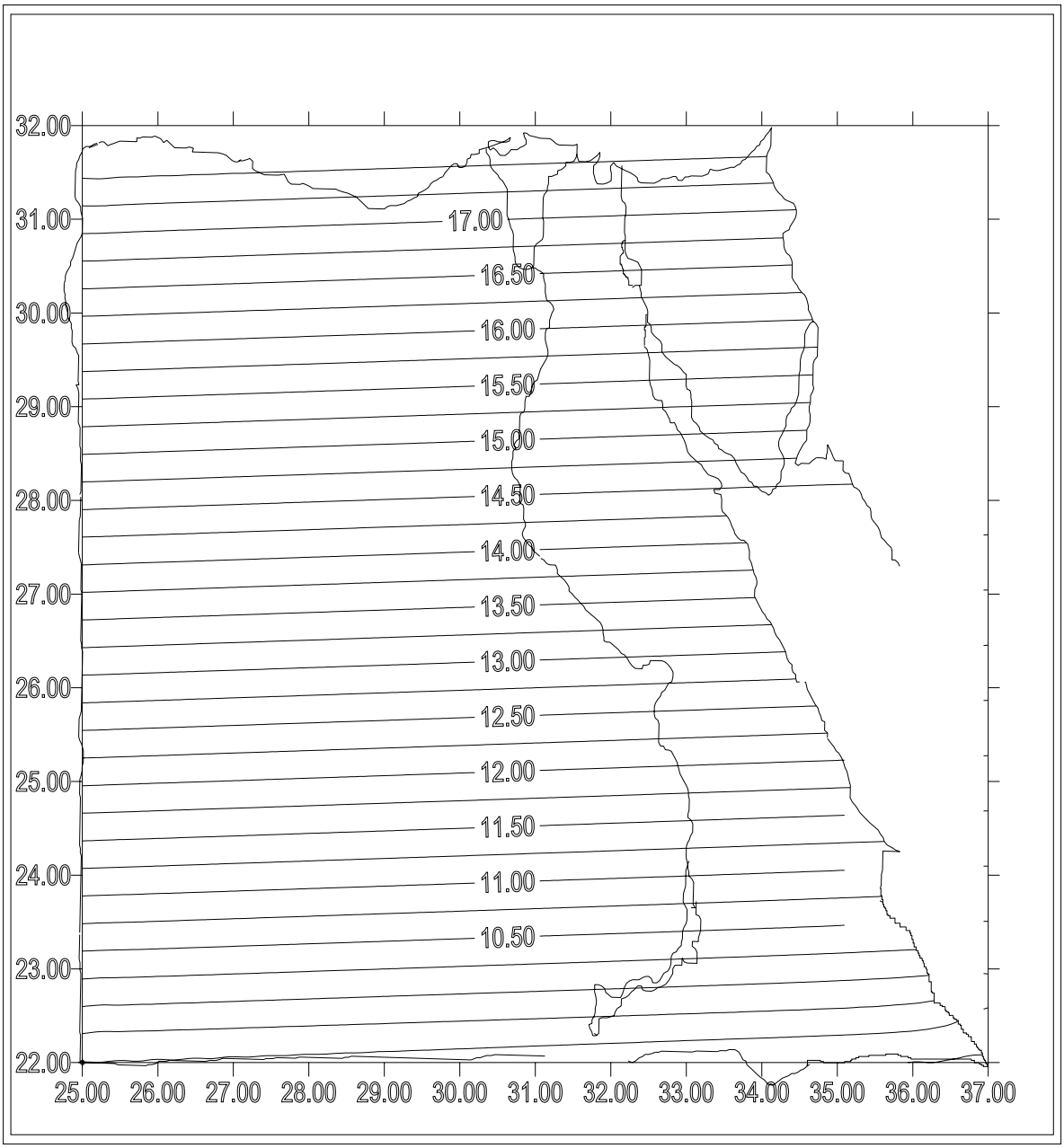

Figure (5.19) The geoid undulation by using MCS model in two direction (geodetic coordinates)

5.5 The comparison between the used mathematical models

In this section the comparison between the regression, LSC and MCS models, was done to choose the best technique that can be used in Egypt.

For comparing between those mathematical models, the distortion at check points, calculated in the previous sections, are used to obtain the following figures. Distortion at check points is shown in figure (5.20), average distortion

is shown in figure (5.21) and the standard deviation of the distortion is shown in figure (5.22). The value of distortion at check points by Regression is shown in table (5.6), LSC technique is shown in table (5.12) and by MCS technique is shown in table (5.14).

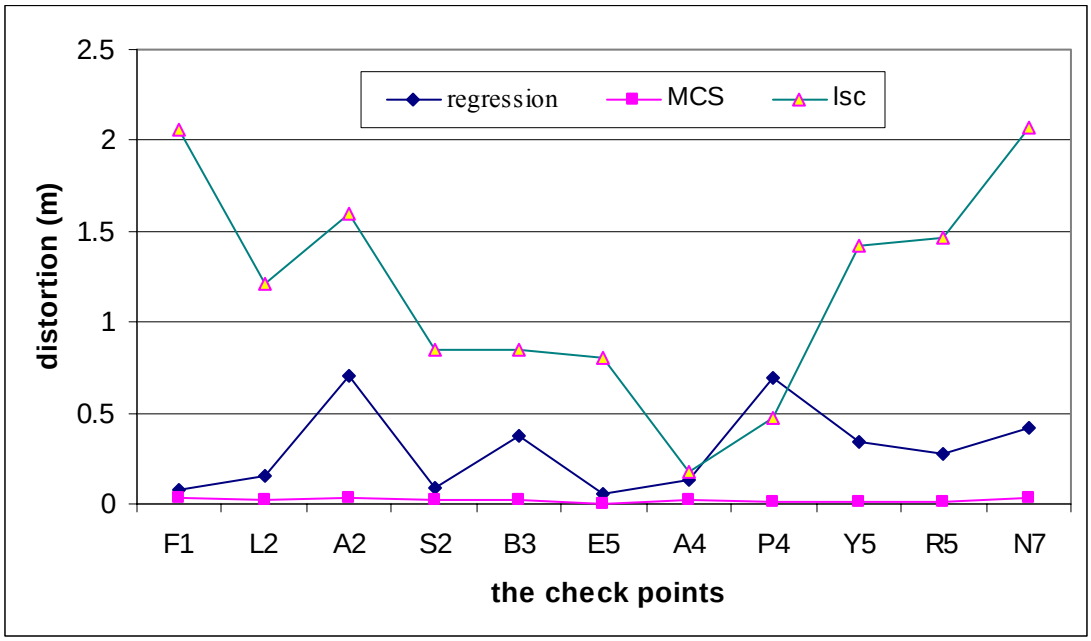

Figure (5.20) The distortion at check points by different mathematical models

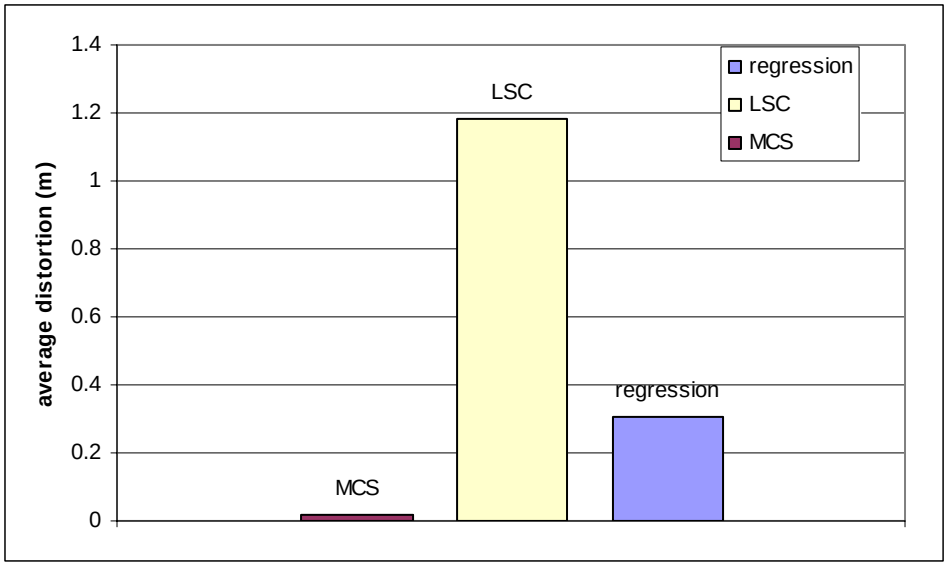

Figure (5.21) The average distortion by different mathematical models

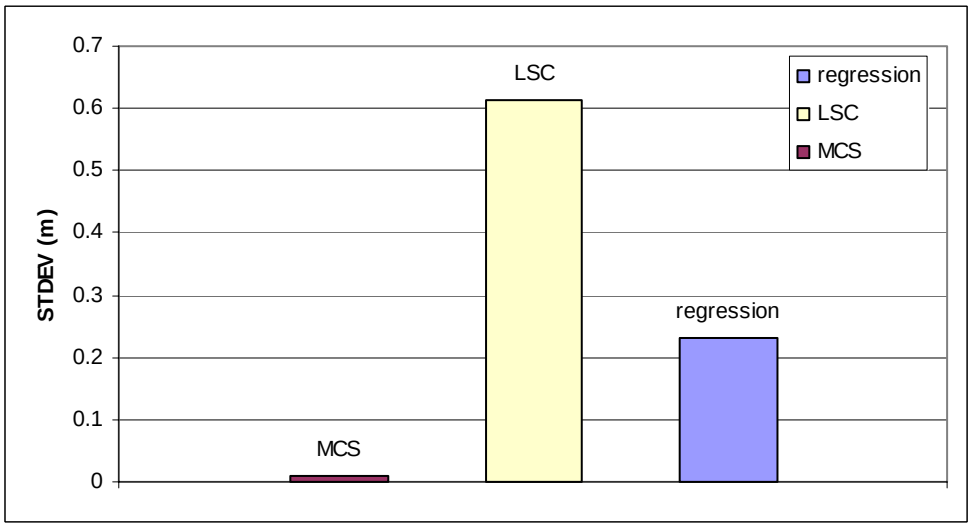

Figure (5.22) The standard deviation of the distortion by different mathematical models

From the previous tables and figures it is obvious that the MCS model has the minimum distortion with high accuracy. This means that the MCS is a best model to compute the geoid undulation in Egypt.

5.6 Comparisons between EGM96, OSU91A and MCS techniques in Egypt

The known best geoid models in the world are EGM96, as shown in figure (3.4), and OSU91A. In this section, comparison between these models and the MCS model was done:

The value of distortion at check points, maximum and minimum distortion, average distortion and the standard deviation of distortion by using different geoid models are shown in table (5.15).

Determination the value of distortions at check points as follow:

- The value of geoid undulation on OSU-91A and the distortion it from the actual geoid undulation is shown in (S.Powell, 1997).
- Calculated the value of the geoid undulation on the EGM96 at check points uses the Geomatics program, determining the distortion between it and the actual geoid undulation from S.Powell report.
- Calculated the distortion at check points uses the MCS program as shown in Appendix (D).

Table (5.15) The comparison between different geoid model at check points

point	OSU-91A	EGM-96	MCS
N7	2.21	0.827	0.030532957
R5	0.549	0.376	0.008740674
Y5	0.669	0.561	0.008160271
P4	0.708	0.928	0.009515733
A4	0.387	0.581	0.016913142
E5	0.701	0.149	0.004675824
B3	0.453	0.05	0.01980998
S2	0.226	0.322	0.017392122
A2	0.456	0.024	0.029476479
L2	0.835	0.278	0.023046078

F1	**1.068**	**0.163**	**0.035859744**
max	**2.21**	**0.928**	**0.035859744**
min	**0.226**	**0.024**	**0.004675824**
S.D.	**0.535915377**	**0.3037**	**0.010328157**
average	**0.751090909**	**0.3872**	**0.018556637**

The distortion at the check points as shown in figure (5.23), the average distortion as shown in figure (5.24) and the standard deviation of the distortion as shown in figure (5.25).

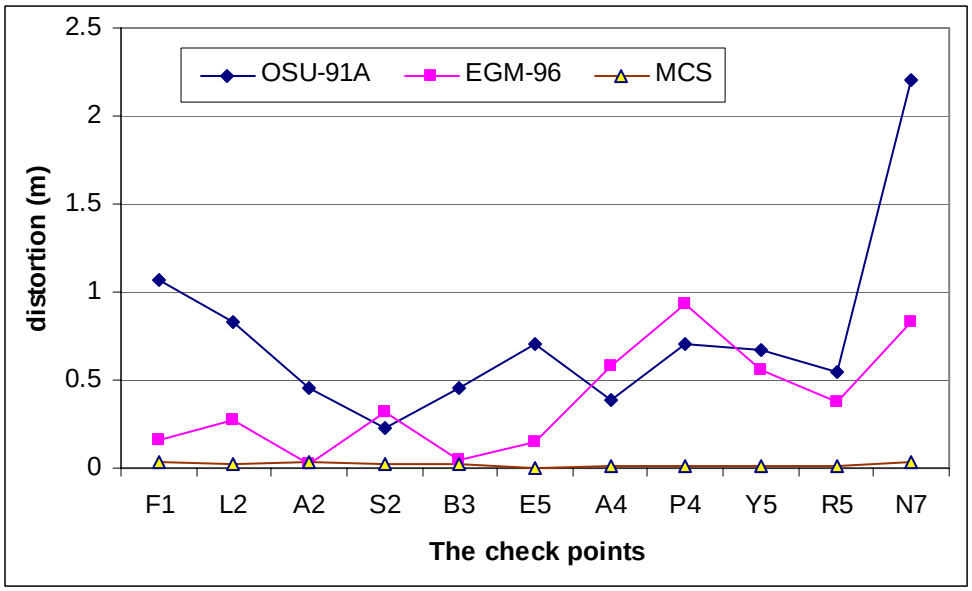

Figure (5.23) The distortion at check points by different geoid models

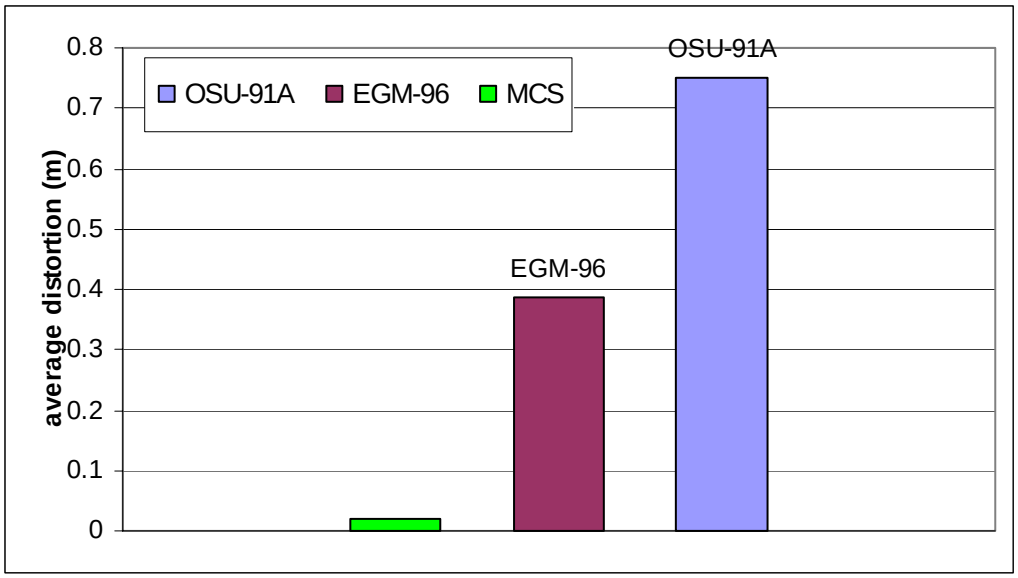

Figure (5.24) The average distortion by different geoid models

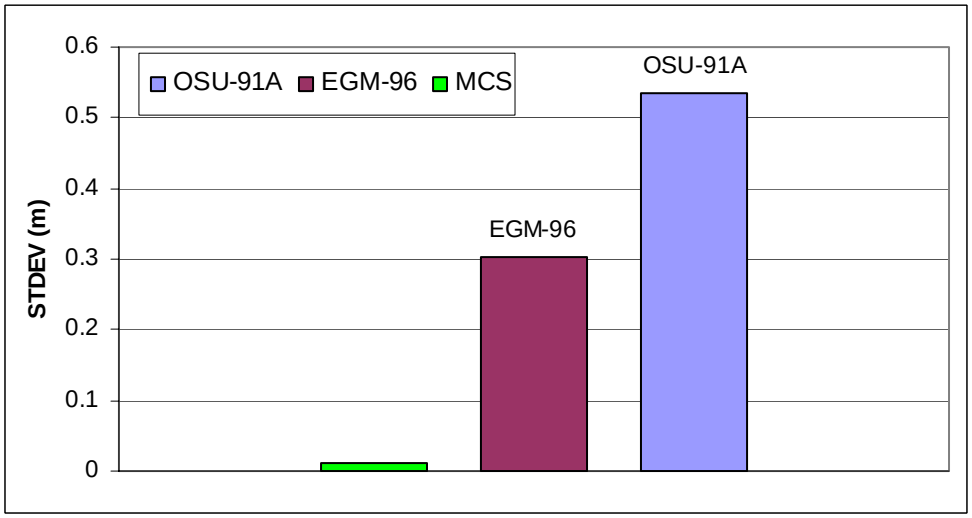

Figure (5.25) The standard deviation of the distortion by different geoid models

From table (5.15) and those figures, it is obvious that, the MCS technique is the best model for Egypt and gives the geoid undulation by high accurate and less time and costs.

5.7 Case study by using MCS model

A case study of" Naser lack". To verify the MCS model was chosen. The data of this region is shown in table (5.16), and available from the NRI, with a

comparison of the observed geoid undulation (N_{obs}) and calculated geoid undulation by the MCS technique (N_{MCS}).

Table (5.16) The comparison between the geoid undulation (N_{obs} and $N_{MCS.}$)

point	latitu.	longitu.	h	H	N_{obs} (m)	N_{MCS} (m)
dam13	24.032368	32.863689	131.84	121.2986	10.5414	10.54973253
dam12	24.030022	32.860706	153.51	142.9274	10.5826	10.59090545
dam11	24.025503	32.858181	151.8	141.204	10.596	10.60426787
dam10	24.018234	32.857872	178.13	167.5824	10.5476	10.5558244
dam09	24.014378	32.853733	184.23	173.6234	10.6066	10.61478336
dam08	24.004421	32.852749	186.38	175.8943	10.4857	10.49382128
dam07	23.994453	32.854034	192.19	181.6111	10.5789	10.5869694
dam06	23.989676	32.853607	196.69	186.1762	10.5138	10.52183982
dam04	23.981094	32.853863	200.32	189.8198	10.5002	10.50819131
dam03	23.978214	32.855679	196.4	185.91	10.49	10.49798286
dam02	23.977167	32.860516	197.81	187.2999	10.5101	10.51809869
dam01	23.976591	32.864426	202.73	191.9123	10.8177	10.82571305
dam00	23.970802	32.868248	200.76	190.209	10.551	10.55899684

As shown table (5.17) the different in the geoid undulation at this zone varied between maximum different (0.833 cm) and minimum different (0.798 cm). The contour maps of the observed value and calculated value by MCS for the geoid undulation and the different between two geoid values are shown in figure (5.26). These are drawing by SURFER program with kriging gridding method.

Table (5.17) The different at points of case study

point	Distortion (m)
dam13	0.008332526
dam12	0.00830545
dam11	0.00826787
dam10	0.008224402

dam09	0.008183355
dam08	0.008121276
dam07	0.0080694
dam06	0.008039821
dam04	0.007991311
dam03	0.00798286
dam02	0.007998689
dam01	0.008013049
dam00	0.007996841
Max. dist.	0.008332526
Min. dist.	0.00798286
average	0.00811745
S.D.	0.000129723

From figure (5.27), it is obvious that, there is a high correlation between geoid undulation (N_{obs}) and (N_{MCS}) where R^2=1.00.

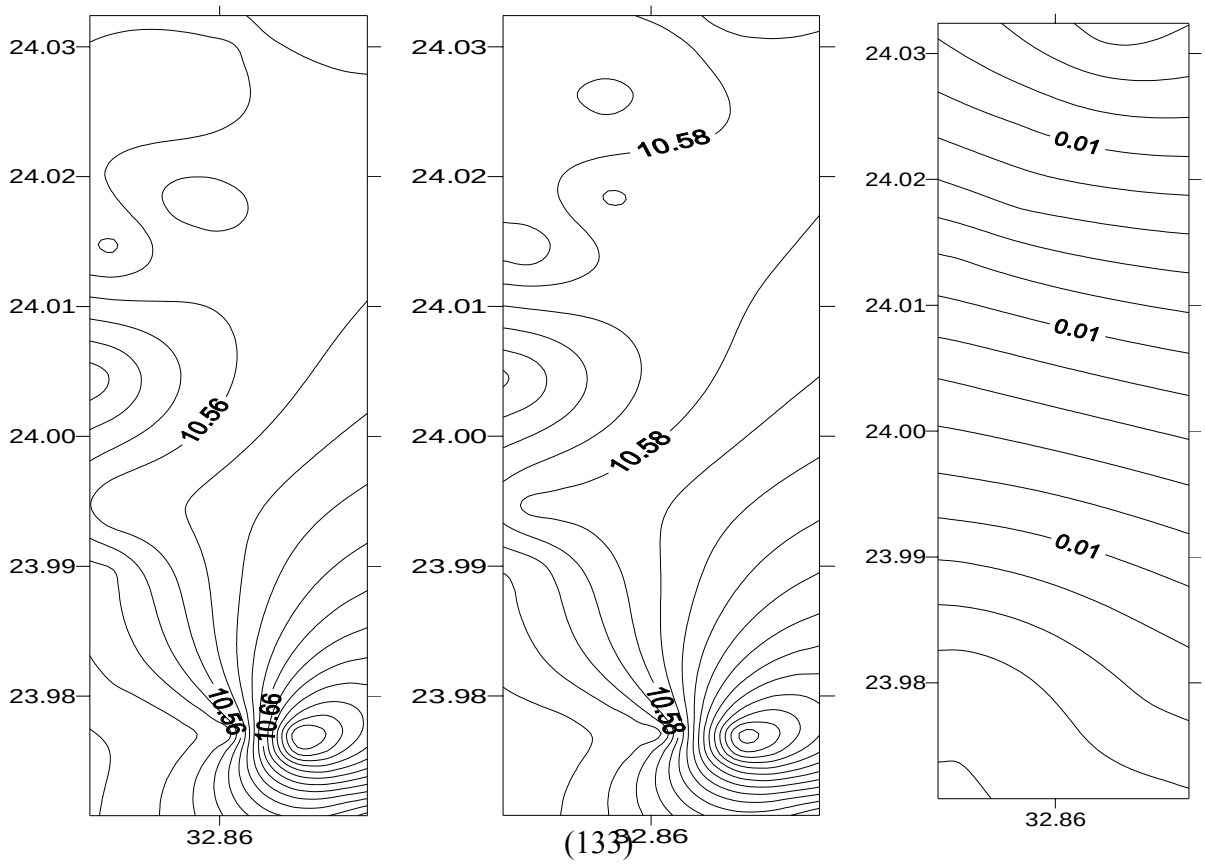

(A) (B) (C)

Figure (5.26) A) a contour map of observed geoid, B) a contour map of MCS geoid and C) the difference between A and B.

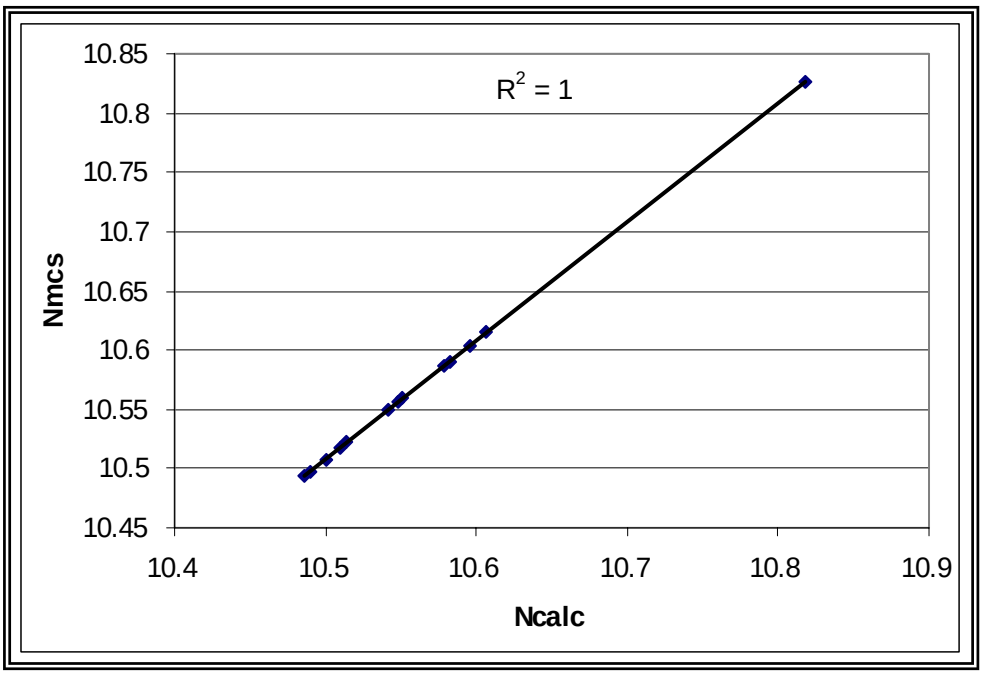

Figure (5.27) The correlation between the observed (N_{obs}) and the calculated (N_{MCS}) geoid undulation

Chapter (6)

CONCLUSIONS AND RECOMMENDATIONS

6.1 Conclusions

Based on the previous analysis and numerical results obtained in this research, the following conclusions can be summarized as follows:

1- The first degree polynomial technique is giving same solution with all trials in distortion and standard deviations.

2- The second degree polynomial with geodetic coordinate solution gives a best solution.

3- Distribution obtained using both O1 (predetermined control point in Egypt) and the average data points are similar. O1 might be used at the average control point for Egypt.

4- Due to higher errors in the vertical coordinates of the ellipsoidal, the distortion values were inconsistent. Three dimensions models proved higher distortion then two dimension model. So, the two dimension model may be more appropriate to be used in distortion evaluation.

5- Among available data and techniques, GPS/Leveling with MCS technique might be the most appropriate combination for geoid model precise outputs in Egypt.

6- Geoid undulation average distortion difference between engineering method and MCS technique was 1.86 cm (acceptable range: 0.50 – 3.60 cm) with 1.033 cm standard deviation.

7-The LSC technique gives less geoid accurate. Recommend to used MCS or polynomial techniques.

8-The MCS technique gives a best geoid undulation beside the EGM96 and OSU91 geoid models in Egypt. Recommend to use MCS technique to compute the geoid undulation in Egypt.

9-The value of geoid undulation ranges between 10 to 17 m from south to north of Egypt. The value of geoid undulation is increase from south to north.

6.2 Recommendations

Based on the previous conclusions, some recommendations may be suggested:-

1-The accuracy of the geoid determination in Egypt can be significantly improved by making addition geodetic measurements in void area, especially the south-west part of the western desert.

2- Other mathematical methods can be used to calculate the geoid.

3- It is highly recommended that the GPS/leveling networks being incorporated with gravimetric network and solved by MCS technique, that is give high accurate geoid in Egypt and over the world.

4- Modern GPS observations should cover all Egypt area. And new digital maps based on new geodetic stations observed by GPS must be achieved, to face the disadvantages of geoid determination.

5- To recommend to use the minimum curvature surface model when calculated the geoid at any region because it's giving minimum distortion beside other models.

REFERENCES

1-A.A.Saad, G.M.Dawood, 2002 " A precise integrated GPS/Gravity geoid model for Egypt" Shoubra Faculty of Engineering, Egypt.

2-A.H.EL-SHazly,2005 "GPS leveling without geoid in Egypt applied to Borg EL-Arab city" FIG working week 2005 and GSDI-8, Cairo, Egypt April 16-12, 2005.

3- A.Sedeek,1992 "Engineering mathematics literature notes" Faculty of Engineering. Mansoura University.

4-A.Ustun, 2002 " Determination of the geoid profile between the Mediterranean and the Black Sea by GPS/leveling " The Graduate School of Natural and Applied Sciences, Yildiz Technical University, Istanbul, Turkey

5-B.Hofmann-Wellenhof, 1995, fifth, revised edition. "Global positioning system theory and practice"

6-Bradford W. Parkinson, 1996, " Global Positioning system: Theory and Applications ", U.S.

7-ChenYong-qi, 2002 "Precise Determination of Hong Kong Geoid Using Heterogeneous Data", Hong Kong, China

8-C.Liu, 1993. "Precise GPS positioning in the Marine Environment" Calgary, Alberta, Canada

9- D.Sobhy, 1986 " Determination of the geoid in Egypt using heterogeneous geodetic data", Cairo University, Egypt.

10-Dr.M.El-Mewafi, Dr.A.Awad, 2002 "Topographic and Geodetic surveying" Faculty of Engineering, Mansoura UN., Egypt.

11-E.Farag, 2000. "Evaluation and Enhancement of Gravity Field for Egypt Based on Gravity Network ENGSN97 and Geopotential Model EGM96"
Faculty of Engineering at Cairo University, Egypt
12-EMR, 1995 " GPS positioning guid " the department of Energy, Mines, and Resources, Canada
13- EUG (Epicenter Usage Guide), 1998 "Geographic coordinate system transformations" Version 2.2.
14-Erol and Celik, 2004. "Precise local geoid determination to make GPS technique more effective in practical applications of geodesy" FIG Work 2004, 22-27 May, Athens, Greece.Turkey.
15-Featherstone, W. E., Denith, M. S. and Kirby J. F. (1998) “Strategies for the accurate determination of Orthometric Heights”, Survey Review, Vol 34, No 267, January 1998, pp.278-296
16-G.El-Fiky, 2003. "Error Contributors and Accuracy in GPS Measurements" The Permanent Scientific Committee for Public Works, Egypt.
17-G. Fotopoulos ,2003 "An analysis on the optimal combination of geoid, orthometric and ellipsoidal height data" Department of Geomatics Engineering , Calgary, Alberta, Canada.
18-G. Fotopoulos, C. Kotsakis, and M.G. Sideris,1999 "Evaluation of Geoid Models and Their Use in Combined GPS/Levelling/Geoid Height Network Adjustments " Department of Geomatics Engineering ,The University of Calgary, Calgary, Alberta, Canada
19-G.M.Dawod, 2005 "Enhancing the Integrity of the National Geodetic Data Bases in Egypt" FIG working week 2005 and GSDI-8, Cairo, Egypt April 16-12, 2005.

20-H.Lang,M.Merry and Ruther " Determination of an orthometric height profile in the Okavango Delta Using GPS leveling" Dep. Of Geomatics UV. OF Cape Town, Unvi. Of Bundeswehr Munich, Germany.

21- Hong-Sic Yun, 1999"Precision geoid determination by spherical FFT in and around the Korean peninsula" Department of Civil Engineering, Sungkyunkwan University, Korea

22-H.EL-Shmbaky, 2004 "Development and Improvement the transformation parameters for Egyptian coordinates", Public work Dep., Faculty of Engineering, EL-Mansoura UN. Egypt.

23- H.Abou-Halima, 2002. "Improvement in positioning accuracy using kinematic GPS", Public Works Department, Faculty of Engineering, Mansoura University, Egypt.

24-Jing Shi, 1994 "High Accuracy Airborne Differential GPS Positioning Using a Multi-Receiver Configuration " Department of Geomatics Engineering, Calgary, Alberta, Canada.

25- K.Prijatna, 1998 "A strategy for geoid determination in the Indonesian Archipelago", Faculty of Engineering and Geosciences, Delft University of Technology, Delft, Netherlands.

26-Lars Harrie, 1993 " Some specific problems in geoid determination" Department of Geodesy and Photogrammetry Royal Institute of Technology, Sweden

27-Leick, A., 1990," GPS satellite surveying" Wiley and Sons, New York. U.S.

28-M.Amin, 2005 "A Precise Geoidal Map of the Southern Part of Egypt by Collocation Toshka Geoid" FIG working week 2005 and GSDI-8, Cairo, Egypt April 16-12, 2005.

29- M.L.El Gizawy, 2003 " Development of an ionosphere monitoring technique using GPS measurements for high latitude GPS users" Department of Geomatics Engineering, Calgary, Alberta, Canada.

30-M.Rabah, 1998. "Enhancing Kinematic GPS-Ambiguity resolution for medium baselines using a regional ionosphere model in real-time"

31-Mark G. Petovello, 2003 " Real-Time Integration of a Tactical-Grade IMU and GPS for High-Accuracy Positioning and Navigation " Department of Geomatics Engineering ,Calgary, Alberta, Canada

32-M.M.Nassar, El-Tokhy, El-Maghraby, 2002 "Accuracy improvement of GPS-Geoid derived orthometric height differences in Egypt using the Latest Egyptian ASU-GEOID" Faculty of Engineering, Ain Shams University, Egypt.

33-M.EL-Tokhey, 1986 "Geoid determination in Egypt", Faculty of Engineering, Ain Shams University, Egypt.

34-M-El-mowafy, 1983 "Errors arising in precise leveling nets", Public work Dep., Faculty of Engineering, EL-Mansoura University, Egypt.

35-M.C.Olynik, 2002 "Temporal Characteristics of GPS Error Sources and their impact on Relative Positioning" Department of Geomatics Engineering , Calgary, Alberta, Canada.

36- Mikhail E.M., 1976 " Observations and least squares" Dun Donnelly New York.

37-Moritz, H. (1978): “Least-squares collocation”, Reviews of geophysics and space physics

38- Nikos Drakos, 1997 "Regularizing smooth data with splines in tension." Computer Based Learning Unit, University of Leads.

39-P.A.Cross, 1983 "Advanced least squares applied to position-fixing", Department of land surveying, London.

40-R.Pratar, 1999 New York "Getting started with MATLAB 5", oxford university press.

41-Robert L.Vanatwerp, 1994"Engineering and Design-Deformation Monitoring and Control Surveying ", U.S Army Corps of Engineering, U.S

42- S. A. Benahmed Daho, 2001 " A new quasi-geoid computation from gravity and GPS data in Algeria" National Centre of Space Techniques, Geodetic Laboratory - Algeria.

43-S.Powell, 1997 "Results of the final adjustment of the new national geodetic network", The Egyptian survey authority.

44-Smith and Milbert, 1997a "Evaluation of preliminary models of the geopotential in the United States" International Geoid Service Bulletin.

45- Smith and Milbert, 1997b"Evaluation of EGM96 model of the geopotential in the United States" International Geoid Service Bulletin.

46-"The GPS Tutor"

47-Trimble Geometrics office program

48-Van Sickle J., 1996," GPS for land surveyors" Ann Arbor Press, Chelsea, Michigan

49-V.Hoyle, 2005 "Data Assimilation for 4-D Wet Refractivity Modelling in a Regional GPS Network" Department of Geomatics Engineering ,The University of Calgary, Calgary, Alberta, Canada

50- X.Shen, 2002 " Improving ambiguity convergence in carrier phase-based precise point positioning" Department of Geomatics Engineering , Calgary, Alberta, Canada.

51-Y.Ahn, 2005 "Analysis of NGS CORS Network for GPS RTK Performance Using External NOAA Tropospheric Corrections Integrated with a Multiple Reference Station Approach" Department of Geomatics Engineering, the University of Calgary, Calgary, Alberta, Canada

52-Z.Liu, 2004 "Ionosphere tomographic modeling and applications using Global positioning system (GPS) measurements" Department of Geomatics Engineering, The University of Calgary, Calgary, Alberta, Canada.

Latitude	Longitude	Geoid Undulation	STDEV
31.5	27	1.75078800E+01	9.39723860E-25
31.5	27.5	1.74965200E+01	9.39723860E-25
31.5	28	1.74851610E+01	9.39723860E-25
31.5	28.5	1.74738040E+01	9.39723860E-25
31.5	29	1.74624470E+01	9.39723860E-25
31.5	29.5	1.74510910E+01	9.39723860E-25
31.5	30	1.74397360E+01	9.39723860E-25
31.5	30.5	1.74283820E+01	9.39723860E-25
31.5	31	1.74170300E+01	9.39723860E-25
31.5	31.5	1.74056780E+01	9.39723860E-25
31.5	32	1.73943280E+01	9.39723860E-25
31.5	32.5	1.73829790E+01	9.39723860E-25
31.5	33	1.73716320E+01	9.39723860E-25
31.5	33.5	1.73602890E+01	9.39723860E-25
31.5	34	1.73489490E+01	9.39723860E-25
31.5	34.5	1.73376110E+01	9.39723860E-25
31.5	35	1.73262770E+01	9.39723860E-25
31.5	35.5	1.73149460E+01	9.39723860E-25
31.5	36	1.73036180E+01	9.39723860E-25
31.5	36.5	1.72922940E+01	9.39723860E-25
31.5	37	1.72809740E+01	9.39723860E-25
31	25	1.71290720E+01	4.69862120E-28
31	25.5	1.71177120E+01	9.39723860E-25
31	26	1.71063490E+01	9.39723860E-25
31	26.5	1.70949860E+01	9.39723860E-25
31	27	1.70836230E+01	9.39723860E-25
31	27.5	1.70722610E+01	9.39723860E-25
31	28	1.70608990E+01	9.39723860E-25
31	28.5	1.70495380E+01	9.39723860E-25
31.5	29	1.70381770E+01	9.39723860E-25
31.5	29.5	1.70268170E+01	9.39723860E-25
31.5	30	1.70154570E+01	9.39723860E-25
31.5	30.5	1.70040980E+01	9.39723860E-25
31.5	31	1.69927400E+01	9.39723860E-25
31.5	31.5	1.69813830E+01	9.39723860E-25
31.5	32	1.69700270E+01	9.39723860E-25
31.5	32.5	1.69586720E+01	9.39723860E-25
31.5	33	1.69473180E+01	9.39723860E-25
31.5	33.5	1.69359650E+01	9.39723860E-25
31.5	34	1.69246130E+01	9.39723860E-25
31.5	34.5	1.69132620E+01	9.39723860E-25
31.5	35	1.69019120E+01	9.39723860E-25
31.5	35.5	1.68905630E+01	9.39723860E-25
31.5	36	1.68792150E+01	9.39723860E-25
31.5	36.5	1.68678680E+01	9.39723860E-25
31.5	37	1.68565220E+01	9.39723860E-25
32	25	1.70246470E+01	9.39723860E-25
32	25.5	1.70132870E+01	9.39723860E-25
32	26	1.70019280E+01	9.39723860E-25
32	26.5	1.69905690E+01	9.39723860E-25
32	27	1.69792110E+01	9.39723860E-25
32	27.5	1.69678540E+01	9.39723860E-25
32	28	1.69564980E+01	9.39723860E-25
32	28.5	1.69451430E+01	9.39723860E-25
32	29	1.69337890E+01	9.39723860E-25
32	29.5	1.69224360E+01	9.39723860E-25
32	30	1.69110840E+01	9.39723860E-25
32	30.5	1.68997330E+01	9.39723860E-25
32	31	1.68883830E+01	9.39723860E-25
32	31.5	1.68770340E+01	9.39723860E-25
32	32	1.68656860E+01	9.39723860E-25
32	32.5	1.68543400E+01	9.39723860E-25
32	33	1.68429940E+01	9.39723860E-25
32	33.5	1.68316490E+01	9.39723860E-25
32	34	1.68203050E+01	9.39723860E-25
32	34.5	1.68089620E+01	9.39723860E-25
32	35	1.67976200E+01	9.39723860E-25
32	35.5	1.67862790E+01	9.39723860E-25
32	36	1.67749390E+01	9.39723860E-25
32	36.5	1.67635990E+01	9.39723860E-25
32	37	1.67522610E+01	9.39723860E-25
32.5	25	1.69203220E+01	9.39723860E-25
32.5	25.5	1.69089630E+01	9.39723860E-25
32.5	26	1.68976050E+01	9.39723860E-25
32.5	26.5	1.68862480E+01	9.39723860E-25
32.5	27	1.68748920E+01	9.39723860E-25
32.5	27.5	1.68635370E+01	9.39723860E-25
32.5	28	1.68521830E+01	9.39723860E-25
32.5	28.5	1.68408300E+01	9.39723860E-25
32.5	29	1.68294780E+01	9.39723860E-25
32.5	29.5	1.68181270E+01	9.39723860E-25
32.5	30	1.68067770E+01	9.39723860E-25
32.5	30.5	1.67954280E+01	9.39723860E-25
32.5	31	1.67840800E+01	9.39723860E-25
32.5	31.5	1.67727330E+01	9.39723860E-25
32.5	32	1.67613870E+01	9.39723860E-25
32.5	32.5	1.67500420E+01	9.39723860E-25
32.5	33	1.67386980E+01	9.39723860E-25
32.5	33.5	1.67273550E+01	9.39723860E-25
32.5	34	1.67160130E+01	9.39723860E-25
32.5	34.5	1.67046720E+01	9.39723860E-25
32.5	35	1.66933320E+01	9.39723860E-25
32.5	35.5	1.66819930E+01	9.39723860E-25
32.5	36	1.66706550E+01	9.39723860E-25
32.5	36.5	1.66593180E+01	9.39723860E-25
32.5	37	1.66479820E+01	9.39723860E-25
33	25	1.67160220E+01	9.39723860E-25
33	25.5	1.67046870E+01	9.39723860E-25
33	26	1.66933530E+01	9.39723860E-25
33	26.5	1.66820200E+01	9.39723860E-25
33	27	1.66706880E+01	9.39723860E-25
33	27.5	1.66593570E+01	9.39723860E-25
33	28	1.66480270E+01	9.39723860E-25
33	28.5	1.66366980E+01	9.39723860E-25
33	29	1.66253700E+01	9.39723860E-25
33	29.5	1.66140430E+01	9.39723860E-25
33	30	1.66027170E+01	9.39723860E-25
33	30.5	1.65913920E+01	9.39723860E-25
33	31	1.65800680E+01	9.39723860E-25
33	31.5	1.65687450E+01	9.39723860E-25
33	32	1.65574230E+01	9.39723860E-25
33	32.5	1.65461020E+01	9.39723860E-25
33	33	1.65347820E+01	9.39723860E-25
33	33.5	1.65234630E+01	9.39723860E-25
33	34	1.65121450E+01	9.39723860E-25
33	34.5	1.65008280E+01	9.39723860E-25
33	35	1.64895120E+01	9.39723860E-25
33	35.5	1.64781970E+01	9.39723860E-25
33	36	1.64668830E+01	9.39723860E-25
33	36.5	1.64555700E+01	9.39723860E-25
33	37	1.64442580E+01	9.39723860E-25
33.5	25	1.65117220E+01	9.39723860E-25
33.5	25.5	1.65004130E+01	9.39723860E-25
33.5	26	1.64891050E+01	9.39723860E-25
33.5	26.5	1.64777980E+01	9.39723860E-25
33.5	27	1.64664920E+01	9.39723860E-25
33.5	27.5	1.64551870E+01	9.39723860E-25
33.5	28	1.64438830E+01	9.39723860E-25
33.5	28.5	1.64325800E+01	9.39723860E-25
33.5	29	1.64212780E+01	9.39723860E-25
33.5	29.5	1.64099770E+01	9.39723860E-25
33.5	30	1.63986770E+01	9.39723860E-25
33.5	30.5	1.63873780E+01	9.39723860E-25
33.5	31	1.63760800E+01	9.39723860E-25
33.5	31.5	1.63647830E+01	9.39723860E-25
33.5	32	1.63534870E+01	9.39723860E-25
33.5	32.5	1.63421920E+01	9.39723860E-25
33.5	33	1.63308980E+01	9.39723860E-25
33.5	33.5	1.63196050E+01	9.39723860E-25
33.5	34	1.63083130E+01	9.39723860E-25
33.5	34.5	1.62970220E+01	9.39723860E-25
33.5	35	1.62857320E+01	9.39723860E-25
33.5	35.5	1.62744430E+01	9.39723860E-25
33.5	36	1.62631550E+01	9.39723860E-25
33.5	36.5	1.62518680E+01	9.39723860E-25
33.5	37	1.62405820E+01	9.39723860E-25
34	25	1.63073720E+01	9.39723860E-25
34	25.5	1.62960880E+01	9.39723860E-25
34	26	1.62848050E+01	9.39723860E-25
34	26.5	1.62735230E+01	9.39723860E-25
34	27	1.62622420E+01	9.39723860E-25
34	27.5	1.62509620E+01	9.39723860E-25
34	28	1.62396830E+01	9.39723860E-25
34	28.5	1.62284050E+01	9.39723860E-25
34	29	1.62171280E+01	9.39723860E-25
34	29.5	1.62058520E+01	9.39723860E-25
34	30	1.61945770E+01	9.39723860E-25
34	30.5	1.61833030E+01	9.39723860E-25
34	31	1.61720300E+01	9.39723860E-25
34	31.5	1.61607580E+01	9.39723860E-25
34	32	1.61494870E+01	9.39723860E-25
34	32.5	1.61382170E+01	9.39723860E-25
34	33	1.61269480E+01	9.39723860E-25
34	33.5	1.61156800E+01	9.39723860E-25
34	34	1.61044130E+01	9.39723860E-25
34	34.5	1.60931470E+01	9.39723860E-25
34	35	1.60818820E+01	9.39723860E-25
34	35.5	1.60706180E+01	9.39723860E-25
34	36	1.60593550E+01	9.39723860E-25
34	36.5	1.60480930E+01	9.39723860E-25
34	37	1.60368320E+01	9.39723860E-25
34.5	25	1.61030220E+01	9.39723860E-25
34.5	25.5	1.60917630E+01	9.39723860E-25
34.5	26	1.60805050E+01	9.39723860E-25
34.5	26.5	1.60692480E+01	9.39723860E-25
34.5	27	1.60579920E+01	9.39723860E-25
34.5	27.5	1.60467370E+01	9.39723860E-25
34.5	28	1.60354830E+01	9.39723860E-25
34.5	28.5	1.60242300E+01	9.39723860E-25
34.5	29	1.60129780E+01	9.39723860E-25
34.5	29.5	1.60017270E+01	9.39723860E-25
34.5	30	1.59904770E+01	9.39723860E-25
34.5	30.5	1.59792280E+01	9.39723860E-25
34.5	31	1.59679800E+01	9.39723860E-25
34.5	31.5	1.59567330E+01	9.39723860E-25
34.5	32	1.59454870E+01	9.39723860E-25
34.5	32.5	1.59342420E+01	9.39723860E-25
34.5	33	1.59229980E+01	9.39723860E-25
34.5	33.5	1.59117550E+01	9.39723860E-25
34.5	34	1.59005130E+01	9.39723860E-25
34.5	34.5	1.58892720E+01	9.39723860E-25
34.5	35	1.58780320E+01	9.39723860E-25
34.5	35.5	1.58667930E+01	9.39723860E-25
34.5	36	1.58555550E+01	9.39723860E-25
34.5	36.5	1.58443180E+01	9.39723860E-25
34.5	37	1.58330820E+01	9.39723860E-25
35	25	1.59000220E+01	9.39723860E-25
35	25.5	1.58887880E+01	9.39723860E-25
35	26	1.58775550E+01	9.39723860E-25
35	26.5	1.58663230E+01	9.39723860E-25
35	27	1.58550920E+01	9.39723860E-25
35	27.5	1.58438620E+01	9.39723860E-25
35	28	1.58326330E+01	9.39723860E-25
35	28.5	1.58214050E+01	9.39723860E-25
35	29	1.58101780E+01	9.39723860E-25
35	29.5	1.57989520E+01	9.39723860E-25
35	30	1.57877270E+01	9.39723860E-25
35	30.5	1.57765030E+01	9.39723860E-25
35	31	1.57652800E+01	9.39723860E-25
35	31.5	1.57540580E+01	9.39723860E-25
35	32	1.57428370E+01	9.39723860E-25
35	32.5	1.57316170E+01	9.39723860E-25
35	33	1.57203980E+01	9.39723860E-25
35	33.5	1.57091800E+01	9.39723860E-25
35	34	1.56979630E+01	9.39723860E-25
35	34.5	1.56867470E+01	9.39723860E-25
35	35	1.56755320E+01	9.39723860E-25
35	35.5	1.56643180E+01	9.39723860E-25
35	36	1.56531050E+01	9.39723860E-25
35	36.5	1.56418930E+01	9.39723860E-25
35	37	1.56306820E+01	9.39723860E-25
35.5	25	1.56973220E+01	9.39723860E-25
35.5	25.5	1.56861130E+01	9.39723860E-25
35.5	26	1.56749050E+01	9.39723860E-25
35.5	26.5	1.56636980E+01	9.39723860E-25
35.5	27	1.56524920E+01	9.39723860E-25
35.5	27.5	1.56412870E+01	9.39723860E-25
35.5	28	1.56300830E+01	9.39723860E-25
35.5	28.5	1.56188800E+01	9.39723860E-25
35.5	29	1.56076780E+01	9.39723860E-25
35.5	29.5	1.55964770E+01	9.39723860E-25
35.5	30	1.55852770E+01	9.39723860E-25
35.5	30.5	1.55740780E+01	9.39723860E-25
35.5	31	1.55628800E+01	9.39723860E-25
35.5	31.5	1.55516830E+01	9.39723860E-25
35.5	32	1.55404870E+01	9.39723860E-25
35.5	32.5	1.55292920E+01	9.39723860E-25
35.5	33	1.55180980E+01	9.39723860E-25
35.5	33.5	1.55069050E+01	9.39723860E-25
35.5	34	1.54957130E+01	9.39723860E-25
35.5	34.5	1.54845220E+01	9.39723860E-25
35.5	35	1.54733320E+01	9.39723860E-25
35.5	35.5	1.54621430E+01	9.39723860E-25
35.5	36	1.54509550E+01	9.39723860E-25
35.5	36.5	1.54397680E+01	9.39723860E-25
35.5	37	1.54285820E+01	9.39723860E-25
36	25	1.54946220E+01	9.39723860E-25
36	25.5	1.54834380E+01	9.39723860E-25
36	26	1.54722550E+01	9.39723860E-25
36	26.5	1.54610730E+01	9.39723860E-25
36	27	1.54498920E+01	9.39723860E-25
36	27.5	1.54387120E+01	9.39723860E-25
36	28	1.54275330E+01	9.39723860E-25
36	28.5	1.54163550E+01	9.39723860E-25
36	29	1.54051780E+01	9.39723860E-25
36	29.5	1.53940020E+01	9.39723860E-25
36	30	1.53828270E+01	9.39723860E-25
36	30.5	1.53716530E+01	9.39723860E-25
36	31	1.53604800E+01	9.39723860E-25
36	31.5	1.53493080E+01	9.39723860E-25
36	32	1.53381370E+01	9.39723860E-25
36	32.5	1.53269670E+01	9.39723860E-25
36	33	1.53157980E+01	9.39723860E-25
36	33.5	1.53046300E+01	9.39723860E-25
36	34	1.52934630E+01	9.39723860E-25
36	34.5	1.52822970E+01	9.39723860E-25
36	35	1.52711320E+01	9.39723860E-25
36	35.5	1.52599680E+01	9.39723860E-25
36	36	1.52488050E+01	9.39723860E-25
36	36.5	1.52376430E+01	9.39723860E-25
36	37	1.52264820E+01	9.39723860E-25
36.5	25	1.52919220E+01	9.39723860E-25
36.5	25.5	1.52807630E+01	9.39723860E-25
36.5	26	1.52696050E+01	9.39723860E-25
36.5	26.5	1.52584480E+01	9.39723860E-25
36.5	27	1.52472920E+01	9.39723860E-25
36.5	27.5	1.52361370E+01	9.39723860E-25
36.5	28	1.52249830E+01	9.39723860E-25
36.5	28.5	1.52138300E+01	9.39723860E-25
36.5	29	1.52026780E+01	9.39723860E-25
36.5	29.5	1.51915270E+01	9.39723860E-25
36.5	30	1.51803770E+01	9.39723860E-25
36.5	30.5	1.51692280E+01	9.39723860E-25
36.5	31	1.51580800E+01	9.39723860E-25
36.5	31.5	1.51469330E+01	9.39723860E-25
36.5	32	1.51357870E+01	9.39723860E-25
36.5	32.5	1.51246420E+01	9.39723860E-25
36.5	33	1.51134980E+01	9.39723860E-25
36.5	33.5	1.51023550E+01	9.39723860E-25
36.5	34	1.50912130E+01	9.39723860E-25
36.5	34.5	1.50800720E+01	9.39723860E-25
36.5	35	1.50689320E+01	9.39723860E-25
36.5	35.5	1.50577930E+01	9.39723860E-25
36.5	36	1.50466550E+01	9.39723860E-25
36.5	36.5	1.50355180E+01	9.39723860E-25
36.5	37	1.50243820E+01	9.39723860E-25
37	25	1.50892220E+01	9.39723860E-25
37	25.5	1.50780880E+01	9.39723860E-25
37	26	1.50669550E+01	9.39723860E-25
37	26.5	1.50558230E+01	9.39723860E-25
37	27	1.50446920E+01	9.39723860E-25
37	27.5	1.50335620E+01	9.39723860E-25
37	28	1.50224330E+01	9.39723860E-25
37	28.5	1.50113050E+01	9.39723860E-25
37	29	1.50001780E+01	9.39723860E-25
37	29.5	1.49890520E+01	9.39723860E-25
37	30	1.49779270E+01	9.39723860E-25
37	30.5	1.49668030E+01	9.39723860E-25
37	31	1.49556800E+01	9.39723860E-25
37	31.5	1.49445580E+01	9.39723860E-25
37	32	1.49334370E+01	9.39723860E-25
37	32.5	1.49223170E+01	9.39723860E-25
37	33	1.49111980E+01	9.39723860E-25
37	33.5	1.49000800E+01	9.39723860E-25
37	34	1.48889630E+01	9.39723860E-25
37	34.5	1.48778470E+01	9.39723860E-25
37	35	1.48667320E+01	9.39723860E-25
37	35.5	1.48556180E+01	9.39723860E-25
37	36	1.48445050E+01	9.39723860E-25
37	36.5	1.48333930E+01	9.39723860E-25
37	37	1.48222820E+01	9.39723860E-25

3015	30	1.76134380E+01	9.39723890E-25
3015	30.5	1.76046890E+01	9.39723890E-25
3015	31	1.75960420E+01	9.39723890E-25
3015	31.5	1.75874980E+01	9.39723890E-25
3015	32	1.75790590E+01	9.39723890E-25
3015	32.5	1.75707230E+01	9.39723890E-25
3015	33	1.75624930E+01	9.39723890E-25
3015	33.5	1.75543670E+01	9.39723890E-25
3015	34	1.75463470E+01	4.69862890E-25
30	3455	1.75384330E+01	4.69862890E-25
30	3555	1.75306250E+01	9.39723890E-25
30	3565	1.75229230E+01	9.39723890E-25
30	3665	1.75153270E+01	9.39723890E-25
30	3675	1.75078370E+01	9.39723890E-25
30	3775	1.75004530E+01	4.69862910E-25
3005	28	1.74931750E+01	4.69862960E-25
3005	28.5	1.74860030E+01	9.39723960E-25
3005	29	1.74789370E+01	9.39723890E-25
3005	29.5	1.74719770E+01	9.39723900E-25
3005	30	1.74651230E+01	9.39723900E-25
3005	30.5	1.74583750E+01	9.39723900E-25
3005	31	1.74517330E+01	9.39723900E-25
3005	31.5	1.74451970E+01	9.39723900E-25
3005	32	1.74387670E+01	9.39723900E-25
3005	32.5	1.74324430E+01	9.39723900E-25
3005	33	1.74262250E+01	9.39723900E-25
3005	33.5	1.74201130E+01	9.39723900E-25
3005	34	1.74141070E+01	9.39723900E-25
3005	34.5	1.74082070E+01	9.39723900E-25
3005	35	1.74024130E+01	9.39723900E-25
3005	35.5	1.73967250E+01	9.39723900E-25

30	26.5	1.60979730E+01	9.39723890E-25
30	27	1.60896000E+01	9.39723860E-25
30	27.5	1.60782070E+01	9.39723890E-25
29.5	28	1.58668320E+01	9.39723910E-25
29.5	28.5	1.58549780E+01	9.39723860E-25
29.5	29	1.58436970E+01	9.39723890E-25
29.5	29.5	1.58322140E+01	9.39723900E-25
29.5	30	1.58198360E+01	9.39723910E-25
29.5	30.5	1.58069840E+01	9.39723910E-25
29.5	31	1.57951740E+01	9.39723910E-25
29.5	31.5	1.57847960E+01	9.39723910E-25
29.5	32	1.57738600E+01	9.39723910E-25
29.5	32.5	1.57619480E+01	9.39723910E-25
29.5	33	1.57506870E+01	9.39723910E-25
29.5	33.5	1.57382430E+01	9.39723910E-25
29.5	34	1.57278690E+01	9.39723910E-25
29.5	34.5	1.57160970E+01	9.39723910E-25
29.5	35	1.57047290E+01	9.39723910E-25
29.5	35.5	1.56934060E+01	9.39723900E-25
29.5	36	1.56822200E+01	9.39723890E-25
29.5	36.5	1.56709660E+01	9.39723860E-25
29.5	37	1.56597250E+01	4.69862210E-28
29.5	37.5	1.56478040E+01	4.69862240E-28
29.5	38	1.56366540E+01	9.39723860E-25
29.5	38.5	1.56253650E+01	9.39723890E-25
29.5	39	1.56143120E+01	9.39723890E-25
29.5	39.5	1.56032340E+01	9.39723860E-25
29.5	40	1.55919760E+01	4.69862210E-28
29.5	40.5	1.55807220E+01	4.69862230E-28
29.5	41	1.55696730E+01	4.69862230E-28
29.5	41.5	1.55587110E+01	9.39723860E-25
29.5	42	1.55468220E+01	9.39723890E-25

2885	29.5	1.49027870E+01	9.39723910E-25
2885	30	1.48940670E+01	9.39723910E-25
2885	30.5	1.48853470E+01	9.39723910E-25
2885	31	1.48766270E+01	9.39723910E-25
2885	31.5	1.48679080E+01	9.39723910E-25
2885	32	1.48591870E+01	9.39723910E-25
2885	32.5	1.48504680E+01	9.39723900E-25
2885	33	1.48417490E+01	9.39723890E-25
2885	33.5	1.48330290E+01	9.39723860E-25
2885	34	1.48243100E+01	4.69862240E-28
2785	34.5	1.48155910E+01	4.69862250E-28
2785	35	1.48068720E+01	9.39723860E-25
2785	35.5	1.47981530E+01	9.39723890E-25
2785	36	1.47894340E+01	9.39723890E-25
2785	36.5	1.47807150E+01	9.39723860E-25
2785	37	1.47719960E+01	4.69862240E-28
2785	37.5	1.47632780E+01	4.69862240E-28
2785	38	1.47545590E+01	4.69862240E-28
2785	38.5	1.47458400E+01	9.39723860E-25
2785	39	1.47371210E+01	9.39723890E-25
2785	39.5	1.47284030E+01	9.39723900E-25
2785	40	1.47196840E+01	9.39723910E-25
2785	40.5	1.47109650E+01	9.39723910E-25
2785	41	1.47022460E+01	9.39723910E-25
2785	41.5	1.46935280E+01	9.39723910E-25
2785	42	1.46848090E+01	9.39723910E-25
2785	42.5	1.46760900E+01	9.39723910E-25
2785	43	1.46673710E+01	9.39723910E-25
2785	43.5	1.46586530E+01	9.39723910E-25
2785	44	1.46499340E+01	9.39723910E-25
2785	44.5	1.46412150E+01	9.39723910E-25
2785	45	1.46324960E+01	9.39723910E-25

26.5	32.5	1.32804360E+01	9.39723990E-25
26.5	33	1.32702540E+01	9.39723990E-25
26.5	33.5	1.32603690E+01	9.39723960E-25
26.5	34	1.32508970E+01	4.69862250E-28
26.75	28	1.32451870E+01	4.69862250E-28
26.75	28.5	1.32317920E+01	9.39723960E-25
26.75	29	1.32193600E+01	9.39723990E-25
26.75	29.5	1.32089850E+01	9.39723900E-25
26.75	30	1.31990640E+01	9.39723910E-25
26.75	30.5	1.31882370E+01	9.39723910E-25
26.75	31	1.31768920E+01	9.39723910E-25
26.75	31.5	1.31654590E+01	9.39723910E-25
26.75	32	1.31544960E+01	9.39723910E-25
26.75	32.5	1.31439340E+01	9.39723910E-25
26.75	33	1.31328280E+01	9.39723910E-25
26.75	33.5	1.31221270E+01	9.39723910E-25
26.75	34	1.31119380E+01	9.39723910E-25
26.75	34.5	1.31019680E+01	9.39723910E-25
26.75	35	1.30923050E+01	9.39723910E-25
26.75	35.5	1.30830940E+01	9.39723900E-25
26.75	36	1.30742640E+01	9.39723890E-25
26.75	36.5	1.30657240E+01	9.39723960E-25
26.75	37	1.30575120E+01	4.69862250E-28
27	32.5	1.32886380E+01	4.69862240E-28
27	33	1.32787230E+01	9.39723960E-25
27	33.5	1.32690860E+01	9.39723990E-25
27	34	1.32598670E+01	9.39723990E-25
27	34.5	1.32511860E+01	9.39723960E-25
27	35	1.32427360E+01	4.69862250E-28
27	35.5	1.32345470E+01	4.69862250E-28
27.25	28	1.32108730E+01	4.69862250E-28
27.25	28.5	1.31976500E+01	9.39723960E-25

2365	32	1.23025460E+01	9.39723910E-25
2365	32.5	1.22940320E+01	9.39723910E-25
2365	33	1.22854080E+01	9.39723910E-25
2365	33.5	1.22767880E+01	9.39723910E-25
2365	34	1.22680270E+01	9.39723910E-25
2365	34.5	1.22593660E+01	9.39723910E-25
2365	35	1.22506740E+01	9.39723910E-25
2365	35.5	1.22419570E+01	9.39723900E-25
2365	36	1.22332040E+01	9.39723890E-25
2365	36.5	1.22244620E+01	9.39723860E-25
2365	37	1.22156700E+01	4.69861240E-25
26	3255	1.22068470E+01	4.69862230E-25
26	3355	1.21980040E+01	9.39723860E-25
26	3365	1.21891670E+01	9.39723890E-25
26	3465	1.21803470E+01	9.39723890E-25
26	3565	1.21715000E+01	9.39723860E-25
26	3575	1.21626760E+01	4.69862240E-25
2355	28	1.21538230E+01	4.69862240E-25
2355	28.5	1.21449870E+01	9.39723860E-25
2355	29	1.21361310E+01	9.39723890E-25
2355	29.5	1.21272670E+01	9.39723900E-25
2355	30	1.21184060E+01	9.39723910E-25
2355	30.5	1.21095780E+01	9.39723910E-25
2355	31	1.21007180E+01	9.39723910E-25
2355	31.5	1.20918760E+01	9.39723910E-25
2355	32	1.20830090E+01	9.39723910E-25
2355	32.5	1.20741900E+01	9.39723910E-25
2355	33	1.20653630E+01	9.39723910E-25
2355	33.5	1.20565210E+01	9.39723910E-25
2355	34	1.20476590E+01	9.39723910E-25
2355	34.5	1.20387960E+01	9.39723910E-25

24	25.5	1.18708680E+01	9.39723960E-25
24	26	1.17969680E+01	9.39723990E-25
24	26.5	1.17236980E+01	9.39723990E-25
24	26.75	1.17452390E+01	9.39723960E-25
24	27.75	1.17638940E+01	4.69862210E-28
24.5	28	1.16213540E+01	4.69862210E-28
24.5	28.5	1.16006610E+01	9.39723960E-25
24.5	29	1.15986690E+01	9.39723990E-25
24.5	29.5	1.15978530E+01	9.39723900E-25
24.5	30	1.15784350E+01	9.39723910E-25
24.5	30.5	1.15670920E+01	9.39723910E-25
24.5	31	1.15436660E+01	9.39723910E-25
24.5	31.5	1.15442210E+01	9.39723910E-25
24.5	32	1.15228660E+01	9.39723910E-25
24.5	32.5	1.15182540E+01	9.39723910E-25
24.5	33	1.15066160E+01	9.39723910E-25
24.5	33.5	1.04986780E+01	9.39723910E-25
24.5	34	1.04875850E+01	9.39723910E-25
24.5	34.5	1.04765980E+01	9.39723910E-25
24.5	35	1.04574050E+01	9.39723900E-25
24.5	35.5	1.04434370E+01	9.39723900E-25
24.5	36	1.04307840E+01	9.39723990E-25
24.5	36.5	1.04187280E+01	9.39723960E-25
24.5	37	1.04073090E+01	4.69862190E-28
24.5	37.25	1.03954780E+01	4.69862190E-28
24.5	37.5	1.03841940E+01	9.39723960E-25
24.5	37.75	1.03727460E+01	9.39723990E-25
24.5	38	1.03603660E+01	9.39723990E-25
24.5	38.25	1.03509900E+01	9.39723960E-25
24.5	38.75	1.03486200E+01	4.69862200E-28
24.5	39	1.03397010E+01	4.69862190E-28

2235	28.5	1.06932690E+01	9.39723990E-25
2235	29	1.06847260E+01	9.39723990E-25
2235	29.5	1.06760630E+01	9.39723990E-25
2235	30	1.06673680E+01	9.39723990E-25
2235	30.5	1.06586360E+01	9.39723990E-25
2235	31	1.06498640E+01	9.39723990E-25
2235	31.5	1.06410470E+01	9.39723990E-25
2235	32	1.06321810E+01	9.39723990E-25
2235	32.5	1.06232620E+01	9.39723990E-25
2235	33	1.06142860E+01	9.39723990E-25
2235	33.5	1.06052490E+01	9.39723990E-25
2235	34	1.05961470E+01	4.69862190E-28
23.5	3455	9.95766520E+00	4.69862960E-28
23.5	3555	9.96564190E+00	9.39723960E-25
23.5	3655	9.97288870E+00	9.39723960E-25
23.5	3755	9.97942950E+00	9.39723860E-25
23.5	3855	9.98527320E+00	9.39723860E-25
23.5	3955	9.99043080E+00	4.69862860E-28
2235	28	9.94882820E+00	4.69862820E-28
2235	28.5	9.93249470E+00	9.39723860E-25
2235	29	9.91568880E+00	9.39723860E-25
2235	29.5	9.89840430E+00	9.39723860E-25
2235	30	9.88063780E+00	9.39723860E-25
2235	30.5	9.86238790E+00	9.39723860E-25
2235	31	9.84365370E+00	9.39723860E-25
2235	31.5	9.82443240E+00	9.39723860E-25
2235	32	9.80472870E+00	9.39723860E-25
2235	32.5	9.78453900E+00	9.39723860E-25
2235	33	9.76385900E+00	9.39723860E-25
2235	33.5	9.74269020E+00	9.39723860E-25
2235	34	9.72104270E+00	9.39723860E-25

22.5	34.5	9.69874480E+00	9.39723860E-25
22.5	35	9.68504650E+00	9.39723860E-25
22.5	35.5	9.66796680E+00	9.39723860E-25
22.5	36	9.64068350E+00	9.39723860E-25
22.5	36.5	9.57903200E+00	9.39723850E-25
22.5	37	9.39010850E+00	4.69862060E-28
22	25	9.49279330E+00	4.69861960E-28
22	25.5	9.48142660E+00	4.69862060E-28
22	26	9.47006450E+00	4.69862120E-28
22	26.5	9.45870540E+00	4.69862160E-28
22	27	9.44734830E+00	4.69862190E-28
22	27.5	9.43599280E+00	4.69862210E-28
22	28	9.42463870E+00	4.69862230E-28
22	28.5	9.41328580E+00	4.69862240E-28
22	29	9.40193380E+00	4.69862250E-28
22	29.5	9.39058270E+00	4.69862250E-28
22	30	9.37923250E+00	4.69862260E-28
22	30.5	9.36788300E+00	4.69862260E-28
22	31	9.35653420E+00	4.69862260E-28
22	31.5	9.34518620E+00	4.69862260E-28
22	32	9.33383890E+00	4.69862260E-28
22	32.5	9.32249230E+00	4.69862250E-28
22	33	9.31114660E+00	4.69862250E-28
22	33.5	9.29980170E+00	4.69862240E-28
22	34	9.28845780E+00	4.69862230E-28
22	34.5	9.27711510E+00	4.69862210E-28
22	35	9.26577360E+00	4.69862190E-28
22	35.5	9.25443370E+00	4.69862160E-28
22	36	9.24309590E+00	4.69862120E-28
22	36.5	9.23176090E+00	4.69862060E-28
22	37	9.22043030E+00	4.69861960E-28

Latitude	Longitude	Geoid Undulation
32	25	19.51088754
32	25.5	18.98094712
32	26	18.50935236
32	26.5	18.09610327
32	27	17.74119984
32	27.5	17.44464209
32	28	17.20643
32	28.5	17.02656357
32	29	16.90504282
32	29.5	16.84186773
32	30	16.8370383
32	30.5	16.89055455
32	31	17.00241646
32	31.5	17.17262403
32	32	17.40117728
32	32.5	17.68807619
32	33	18.03332077
32	33.5	18.43691101
32	34	18.89884692
32	34.5	19.4191285
32	35	19.99775575
32	35.5	20.63472866
32	36	21.33004724
32	36.5	22.08371148
32	37	22.89572139
31.5	25	19.3534139
31.5	25.5	18.79975189
31.5	26	18.30443554
31.5	26.5	17.86746486

31.5	27	17.48883984
31.5	27.5	17.16856049
31.5	28	16.90662681
31.5	28.5	16.70303879
31.5	29	16.55779645
31.5	29.5	16.47089976
31.5	30	16.44234875
31.5	30.5	16.4721434
31.5	31	16.56028372
31.5	31.5	16.70676971
31.5	32	16.91160136
31.5	32.5	17.17477868
31.5	33	17.49630166
31.5	33.5	17.87617032
31.5	34	18.31438464
31.5	34.5	18.81094462
31.5	35	19.36585028
31.5	35.5	19.9791016
31.5	36	20.65069858
31.5	36.5	21.38064124
31.5	37	22.16892956
31	25	19.20543951
31	25.5	18.6280559
31	26	18.10901796
31	26.5	17.64832568
31	27	17.24597908
31	27.5	16.90197814
31	28	16.61632286
31	28.5	16.38901326
31	29	16.22004932
31	29.5	16.10943104

31	30	16.05715844
31	30.5	16.0632315
31	31	16.12765022
31	31.5	16.25041462
31	32	16.43152468
31	32.5	16.67098041
31	33	16.9687818
31	33.5	17.32492886
31	34	17.73942159
31	34.5	18.21225999
31	35	18.74344405
31	35.5	19.33297378
31	36	19.98084917
31	36.5	20.68707024
31	37	21.45163697
30.5	25	19.06696435
30.5	25.5	18.46585915
30.5	26	17.92309962
30.5	26.5	17.43868575
30.5	27	17.01261755
30.5	27.5	16.64489502
30.5	28	16.33551816
30.5	28.5	16.08448696
30.5	29	15.89180143
30.5	29.5	15.75746156
30.5	30	15.68146736
30.5	30.5	15.66381883
30.5	31	15.70451597
30.5	31.5	15.80355877
30.5	32	15.96094724
30.5	32.5	16.17668138

30.5	33	16.45076118
30.5	33.5	16.78318665
30.5	34	17.17395779
30.5	34.5	17.62307459
30.5	35	18.13053706
30.5	35.5	18.6963452
30.5	36	19.320499
30.5	36.5	20.00299847
30.5	37	20.74384361
30	25	18.93798843
30	25.5	18.31316164
30	26	17.74668052
30	26.5	17.23854506
30	27	16.78875527
30	27.5	16.39731115
30	28	16.06421269
30	28.5	15.7894599
30	29	15.57305278
30	29.5	15.41499132
30	30	15.31527553
30	30.5	15.27390541
30	31	15.29088095
30	31.5	15.36620217
30	32	15.49986904
30	32.5	15.69188159
30	33	15.9422398
30	33.5	16.25094368
30	34	16.61799322
30	34.5	17.04338844
30	35	17.52712931
30	35.5	18.06921586

30	36	18.66964807
30	36.5	19.32842595
30	37	20.0455495
29.5	25	18.81851176
29.5	25.5	18.16996338
29.5	26	17.57976066
29.5	26.5	17.04790361
29.5	27	16.57439223
29.5	27.5	16.15922651
29.5	28	15.80240647
29.5	28.5	15.50393208
29.5	29	15.26380337
29.5	29.5	15.08202032
29.5	30	14.95858294
29.5	30.5	14.89349123
29.5	31	14.88674518
29.5	31.5	14.9383448
29.5	32	15.04829009
29.5	32.5	15.21658104
29.5	33	15.44321766
29.5	33.5	15.72819995
29.5	34	16.0715279
29.5	34.5	16.47320152
29.5	35	16.93322081
29.5	35.5	17.45158576
29.5	36	18.02829638
29.5	36.5	18.66335267
29.5	37	19.35675463
29	25	18.70853432
29	25.5	18.03626435
29	26	17.42234004

29	26.5	16.8667614
29	27	16.36952843
29	27.5	15.93064112
29	28	15.55009948
29	28.5	15.22790351
29	29	14.9640532
29	29.5	14.75854856
29	30	14.61138959
29	30.5	14.52257629
29	31	14.49210865
29	31.5	14.51998668
29	32	14.60621037
29	32.5	14.75077973
29	33	14.95369476
29	33.5	15.21495546
29	34	15.53456182
29	34.5	15.91251385
29	35	16.34881154
29	35.5	16.84345491
29	36	17.39644394
29	36.5	18.00777863
29	37	18.67745899
28.5	25	18.60805613
28.5	25.5	17.91206456
28.5	26	17.27441866
28.5	26.5	16.69511843
28.5	27	16.17416387
28.5	27.5	15.71155497
28.5	28	15.30729174
28.5	28.5	14.96137417
28.5	29	14.67380228

28.5	29.5	14.44457605
28.5	30	14.27369548
28.5	30.5	14.16116058
28.5	31	14.10697135
28.5	31.5	14.11112779
28.5	32	14.17362989
28.5	32.5	14.29447766
28.5	33	14.4736711
28.5	33.5	14.71121021
28.5	34	15.00709498
28.5	34.5	15.36132541
28.5	35	15.77390152
28.5	35.5	16.24482329
28.5	36	16.77409073
28.5	36.5	17.36170383
28.5	37	18.0076626
28	25	18.51707717
28	25.5	17.79736402
28	26	17.13599653
28	26.5	16.5329747
28	27	15.98829855
28	27.5	15.50196806
28	28	15.07398324
28	28.5	14.70434408
28	29	14.39305059
28	29.5	14.14010277
28	30	13.94550061
28	30.5	13.80924412
28	31	13.7313333
28	31.5	13.71176815
28	32	13.75054866

28	32.5	13.84767484
28	33	14.00314668
28	33.5	14.2169642
28	34	14.48912738
28	34.5	14.81963622
28	35	15.20849073
28	35.5	15.65569091
28	36	16.16123676
28	36.5	16.72512827
28	37	17.34736545
27.5	25	18.43559746
27.5	25.5	17.69216271
27.5	26	17.00707363
27.5	26.5	16.38033022
27.5	27	15.81193247
27.5	27.5	15.30188039
27.5	28	14.85017397
27.5	28.5	14.45681323
27.5	29	14.12179815
27.5	29.5	13.84512873
27.5	30	13.62680498
27.5	30.5	13.4668269
27.5	31	13.36519449
27.5	31.5	13.32190774
27.5	32	13.33696667
27.5	32.5	13.41037125
27.5	33	13.54212151
27.5	33.5	13.73221743
27.5	34	13.98065902
27.5	34.5	14.28744627
27.5	35	14.65257919

27.5	35.5	15.07605778
27.5	36	15.55788203
27.5	36.5	16.09805196
27.5	37	16.69656754
27	25	18.36361699
27	25.5	17.59646065
27	26	16.88764998
27	26.5	16.23718497
27	27	15.64506563
27	27.5	15.11129196
27	28	14.63586395
27	28.5	14.21878161
27	29	13.86004494
27	29.5	13.55965394
27	30	13.3176086
27	30.5	13.13390893
27	31	13.00855492
27	31.5	12.94154658
27	32	12.93288391
27	32.5	12.98256691
27	33	13.09059557
27	33.5	13.2569699
27	34	13.4816899
27	34.5	13.76475556
27	35	14.10616689
27	35.5	14.50592388
27	36	14.96402655
27	36.5	15.48047488
27	37	16.05526888
26.5	25	18.30113576
26.5	25.5	17.51025783

26.5	26	16.77772556
26.5	26.5	16.10353896
26.5	27	15.48769803
26.5	27.5	14.93020277
26.5	28	14.43105317
26.5	28.5	13.99024924
26.5	29	13.60779098
26.5	29.5	13.28367838
26.5	30	13.01791145
26.5	30.5	12.81049019
26.5	31	12.66141459
26.5	31.5	12.57068466
26.5	32	12.5383004
26.5	32.5	12.5642618
26.5	33	12.64856887
26.5	33.5	12.79122161
26.5	34	12.99222002
26.5	34.5	13.25156409
26.5	35	13.56925383
26.5	35.5	13.94528923
26.5	36	14.3796703
26.5	36.5	14.87239704
26.5	37	15.42346945
26	25	18.24815377
26	25.5	17.43355424
26	26	16.67730039
26	26.5	15.9793922
26	27	15.33982968
26	27.5	14.75861282
26	28	14.23574163
26	28.5	13.77121611

26	29	13.36503625
26	29.5	13.01720207
26	30	12.72771354
26	30.5	12.49657069
26	31	12.3237735
26	31.5	12.20932198
26	32	12.15321613
26	32.5	12.15545594
26	33	12.21604142
26	33.5	12.33497256
26	34	12.51224938
26	34.5	12.74787186
26	35	13.04184
26	35.5	13.39415382
26	36	13.8048133
26	36.5	14.27381845
26	37	14.80116926
25.5	25	18.20467102
25.5	25.5	17.3663499
25.5	26	16.58637445
25.5	26.5	15.86474467
25.5	27	15.20146056
25.5	27.5	14.59652211
25.5	28	14.04992933
25.5	28.5	13.56168222
25.5	29	13.13178077
25.5	29.5	12.76022499
25.5	30	12.44701488
25.5	30.5	12.19215043
25.5	31	11.99563165
25.5	31.5	11.85745854

25.5	32	11.77763109
25.5	32.5	11.75614932
25.5	33	11.7930132
25.5	33.5	11.88822276
25.5	34	12.04177798
25.5	34.5	12.25367887
25.5	35	12.52392542
25.5	35.5	12.85251765
25.5	36	13.23945553
25.5	36.5	13.68473909
25.5	37	14.18836831
25	25	18.17068751
25	25.5	17.3086448
25	26	16.50494776
25	26.5	15.75959639
25	27	15.07259068
25	27.5	14.44393064
25	28	13.87361627
25	28.5	13.36164757
25	29	12.90802453
25	29.5	12.51274716
25	30	12.17581545
25	30.5	11.89722942
25	31	11.67698905
25	31.5	11.51509434
25	32	11.4115453
25	32.5	11.36634193
25	33	11.37948423
25	33.5	11.45097219
25	34	11.58080582
25	34.5	11.76898512

25	35	12.01551008
25	35.5	12.32038071
25	36	12.68359701
25	36.5	13.10515898
25	37	13.58506661
24.5	25	18.14620324
24.5	25.5	17.26043894
24.5	26	16.43302031
24.5	26.5	15.66394735
24.5	27	14.95322005
24.5	27.5	14.30083842
24.5	28	13.70680245
24.5	28.5	13.17111216
24.5	29	12.69376753
24.5	29.5	12.27476857
24.5	30	11.91411527
24.5	30.5	11.61180764
24.5	31	11.36784568
24.5	31.5	11.18222938
24.5	32	11.05495875
24.5	32.5	10.98603379
24.5	33	10.9754545
24.5	33.5	11.02322087
24.5	34	11.12933291
24.5	34.5	11.29379061
24.5	35	11.51659398
24.5	35.5	11.79774302
24.5	36	12.13723773
24.5	36.5	12.5350781
24.5	37	12.99126414
24	25	18.13121821

24	25.5	17.22173232
24	26	16.3705921
24	26.5	15.57779754
24	27	14.84334865
24	27.5	14.16724543
24	28	13.54948788
24	28.5	12.99007599
24	29	12.48900977
24	29.5	12.04628921
24	30	11.66191433
24	30.5	11.33588511
24	31	11.06820155
24	31.5	10.85886366
24	32	10.70787144
24	32.5	10.61522489
24	33	10.580924
24	33.5	10.60496878
24	34	10.68735923
24	34.5	10.82809534
24	35	11.02717713
24	35.5	11.28460457
24	36	11.60037769
24	36.5	11.97449647
24	37	12.40696092
23.5	25	18.12573242
23.5	25.5	17.19252494
23.5	26	16.31766313
23.5	26.5	15.50114698
23.5	27	14.7429765
23.5	27.5	14.04315169
23.5	28	13.40167254

23.5	28.5	12.81853906
23.5	29	12.29375125
23.5	29.5	11.8273091
23.5	30	11.41921262
23.5	30.5	11.06946181
23.5	31	10.77805667
23.5	31.5	10.54499719
23.5	32	10.37028338
23.5	32.5	10.25391523
23.5	33	10.19589275
23.5	33.5	10.19621594
23.5	34	10.2548848
23.5	34.5	10.37189932
23.5	35	10.54725951
23.5	35.5	10.78096536
23.5	36	11.07301689
23.5	36.5	11.42341408
23.5	37	11.83215693
23	25	18.12974587
23	25.5	17.1728168
23	26	16.2742334
23	26.5	15.43399566
23	27	14.65210359
23	27.5	13.92855718
23	28	13.26335644
23	28.5	12.65650137
23	29	12.10799197
23	29.5	11.61782823
23	30	11.18601016
23	30.5	10.81253776
23	31	10.49741102

23	31.5	10.24062995
23	32	10.04219455
23	32.5	9.90210481
23	33	9.820360741
23	33.5	9.796962338
23	34	9.831909602
23	34.5	9.925202532
23	35	10.07684113
23	35.5	10.28682539
23	36	10.55515533
23	36.5	10.88183092
23	37	11.26685219
22.5	25	18.14325857
22.5	25.5	17.1626079
22.5	26	16.24030291
22.5	26.5	15.37634358
22.5	27	14.57072991
22.5	27.5	13.82346192
22.5	28	13.13453959
22.5	28.5	12.50396293
22.5	29	11.93173193
22.5	29.5	11.4178466
22.5	30	10.96230694
22.5	30.5	10.56511294
22.5	31	10.22626462
22.5	31.5	9.945761954
22.5	32	9.723604959
22.5	32.5	9.559793631
22.5	33	9.45432797
22.5	33.5	9.407207976
22.5	34	9.418433648

22.5	34.5	9.488004987
22.5	35	9.615921993
22.5	35.5	9.802184666
22.5	36	10.04679301
22.5	36.5	10.34974701
22.5	37	10.71104669
22	25	18.1662705
22	25.5	17.16189825
22	26	16.21587166
22	26.5	15.32819074
22	27	14.49885548
22	27.5	13.7278659
22	28	13.01522197
22	28.5	12.36092372
22	29	11.76497113
22	29.5	11.22736421
22	30	10.74810296
22	30.5	10.32718737
22	31	9.964617452
22	31.5	9.660393199
22	32	9.414514612
22	32.5	9.226981693
22	33	9.09779444
22	33.5	9.026952854
22	34	9.014456935
22	34.5	9.060306683
22	35	9.164502097
22	35.5	9.327043179
22	36	9.547929927
22	36.5	9.827162342
22	37	10.16474042

Latitude	Longitude	Geoid Undulation	STDEV
32	25	1.3199939E+01	7.8055652E-01
32	25.5	1.3666757E+01	8.0531750E-01
32	26	1.3898240E+01	8.1527293E-01
32	26.5	1.4084669E+01	8.2580443E-01
32	27	1.4247314E+01	8.3698441E-01
32	27.5	1.4311905E+01	8.4018870E-01
32	28	1.4337421E+01	8.4205864E-01
32	28.5	1.4373659E+01	8.4682529E-01
32	29	1.4421748E+01	8.5149594E-01
32	29.5	1.4477806E+01	8.5358743E-01
32	30	1.4549147E+01	8.5625593E-01
32	30.5	1.4638276E+01	8.6136390E-01
32	31	1.4719068E+01	8.6705118E-01
32	31.5	1.4651825E+01	8.6180161E-01
32	32	1.4532241E+01	8.5466471E-01
32	32.5	1.4407741E+01	8.4989604E-01
32	33	1.4267207E+01	8.4631099E-01
32	33.5	1.4101544E+01	8.4346779E-01
32	34	1.3886068E+01	8.3963449E-01
32	34.5	1.3552048E+01	8.2775364E-01
32	35	1.3109157E+01	8.0750674E-01
32	35.5	1.2616411E+01	7.8355343E-01

32	36	1.2102845E+01	7.5765157E-01
32	36.5	1.1586236E+01	7.3076507E-01
32	37	1.1077491E+01	7.0353454E-01
31.5	25	1.3268494E+01	7.8732478E-01
31.5	25.5	1.3806384E+01	8.1712077E-01
31.5	26	1.3960810E+01	8.2185896E-01
31.5	26.5	1.4143310E+01	8.3312698E-01
31.5	27	1.4346011E+01	8.4957259E-01
31.5	27.5	1.4372724E+01	8.4965181E-01
31.5	28	1.4381318E+01	8.5130989E-01
31.5	28.5	1.4416631E+01	8.5830008E-01
31.5	29	1.4467617E+01	8.6513958E-01
31.5	29.5	1.4520353E+01	8.6576924E-01
31.5	30	1.4592989E+01	8.6779465E-01
31.5	30.5	1.4691204E+01	8.7315578E-01
31.5	31	1.4810140E+01	8.8101553E-01
31.5	31.5	1.4724598E+01	8.7353565E-01
31.5	32	1.4611654E+01	8.6663546E-01
31.5	32.5	1.4503244E+01	8.6298841E-01
31.5	33	1.4375947E+01	8.5987525E-01
31.5	33.5	1.4228243E+01	8.5777401E-01
31.5	34	1.4052948E+01	8.5721279E-01
31.5	34.5	1.3710859E+01	8.4479586E-01
31.5	35	1.3233926E+01	8.2200654E-01
31.5	35.5	1.2714285E+01	7.9636312E-01
31.5	36	1.2177206E+01	7.6892915E-01
31.5	36.5	1.1641698E+01	7.4069754E-01
31.5	37	1.1118437E+01	7.1231519E-01
31	25	1.3216613E+01	7.8557784E-01
31	25.5	1.3704196E+01	8.1214746E-01
31	26	1.3921503E+01	8.2189507E-01

31	26.5	1.4114494E+01	8.3430173E-01
31	27	1.4307748E+01	8.5007615E-01
31	27.5	1.4352192E+01	8.5299495E-01
31	28	1.4368755E+01	8.5683090E-01
31	28.5	1.4411190E+01	8.6667248E-01
31	29	1.4472278E+01	8.7791026E-01
31	29.5	1.4515604E+01	8.7530534E-01
31	30	1.4584451E+01	8.7697058E-01
31	30.5	1.4674778E+01	8.8191230E-01
31	31	1.4749780E+01	8.8516403E-01
31	31.5	1.4712078E+01	8.8062892E-01
31	32	1.4633453E+01	8.7615265E-01
31	32.5	1.4553500E+01	8.7479111E-01
31	33	1.4437017E+01	8.7167448E-01
31	33.5	1.4297482E+01	8.6904714E-01
31	34	1.4150855E+01	8.7008178E-01
31	34.5	1.3810559E+01	8.5772054E-01
31	35	1.3319937E+01	8.3434562E-01
31	35.5	1.2779845E+01	8.0760491E-01
31	36	1.2222565E+01	7.7883750E-01
31	36.5	1.1671632E+01	7.4942763E-01
31	37	1.1137236E+01	7.2004516E-01
30.5	25	1.3082981E+01	7.7831151E-01
30.5	25.5	1.3525999E+01	8.0241045E-01
30.5	26	1.3799858E+01	8.1676629E-01
30.5	26.5	1.4008701E+01	8.3026617E-01
30.5	27	1.4179181E+01	8.4369399E-01
30.5	27.5	1.4260435E+01	8.5128082E-01
30.5	28	1.4302649E+01	8.5870923E-01
30.5	28.5	1.4355136E+01	8.7036251E-01
30.5	29	1.4416764E+01	8.8147398E-01

30.5	29.5	1.4462981E+01	8.8138364E-01
30.5	30	1.4526739E+01	8.8385403E-01
30.5	30.5	1.4604083E+01	8.8922639E-01
30.5	31	1.4652544E+01	8.8931885E-01
30.5	31.5	1.4638249E+01	8.8522203E-01
30.5	32	1.4597573E+01	8.8323686E-01
30.5	32.5	1.4558716E+01	8.8556744E-01
30.5	33	1.4444352E+01	8.8134335E-01
30.5	33.5	1.4301037E+01	8.7703466E-01
30.5	34	1.4135944E+01	8.7514819E-01
30.5	34.5	1.3831787E+01	8.6541873E-01
30.5	35	1.3364895E+01	8.4467278E-01
30.5	35.5	1.2809577E+01	8.1717994E-01
30.5	36	1.2236267E+01	7.8725458E-01
30.5	36.5	1.1674659E+01	7.5688592E-01
30.5	37	1.1133341E+01	7.2669150E-01
30	25	1.2915850E+01	7.6913191E-01
30	25.5	1.3332870E+01	7.9216898E-01
30	26	1.3630525E+01	8.0882921E-01
30	26.5	1.3853040E+01	8.2335111E-01
30	27	1.4021702E+01	8.3667078E-01
30	27.5	1.4125818E+01	8.4722805E-01
30	28	1.4192619E+01	8.5783575E-01
30	28.5	1.4255336E+01	8.7064728E-01
30	29	1.4316441E+01	8.8126065E-01
30	29.5	1.4367678E+01	8.8478334E-01
30	30	1.4425430E+01	8.8842750E-01
30	30.5	1.4493608E+01	8.9604565E-01
30	31	1.4523286E+01	8.9292574E-01
30	31.5	1.4519406E+01	8.8832907E-01
30	32	1.4504472E+01	8.8767295E-01

30	32.5	1.4498993E+01	8.9267052E-01
30	33	1.4387582E+01	8.8768966E-01
30	33.5	1.4244275E+01	8.8255723E-01
30	34	1.4072783E+01	8.7899915E-01
30	34.5	1.3810102E+01	8.7184101E-01
30	35	1.3373125E+01	8.5373849E-01
30	35.5	1.2799580E+01	8.2494456E-01
30	36	1.2216190E+01	7.9408216E-01
30	36.5	1.1650132E+01	7.6304566E-01
30	37	1.1106799E+01	7.3225471E-01
29.5	25	1.2732923E+01	7.5927839E-01
29.5	25.5	1.3130360E+01	7.8171716E-01
29.5	26	1.3435710E+01	7.9957971E-01
29.5	26.5	1.3667847E+01	8.1507972E-01
29.5	27	1.3842371E+01	8.2920863E-01
29.5	27.5	1.3963255E+01	8.4201997E-01
29.5	28	1.4049270E+01	8.5520699E-01
29.5	28.5	1.4122512E+01	8.6970822E-01
29.5	29	1.4187243E+01	8.8192571E-01
29.5	29.5	1.4237961E+01	8.8692079E-01
29.5	30	1.4286353E+01	8.9060002E-01
29.5	30.5	1.4337866E+01	8.9689231E-01
29.5	31	1.4359765E+01	8.9430650E-01
29.5	31.5	1.4362113E+01	8.9016655E-01
29.5	32	1.4359108E+01	8.8975829E-01
29.5	32.5	1.4346816E+01	8.9250043E-01
29.5	33	1.4266520E+01	8.9068772E-01
29.5	33.5	1.4136758E+01	8.8664285E-01
29.5	34	1.3968058E+01	8.8234671E-01
29.5	34.5	1.3745747E+01	8.7733719E-01
29.5	35	1.3336475E+01	8.6111816E-01

29.5	35.5	1.2744048E+01	8.3052504E-01
29.5	36	1.2161316E+01	7.9927602E-01
29.5	36.5	1.1598409E+01	7.6793770E-01
29.5	37	1.1058336E+01	7.3677131E-01
29	25	1.2541117E+01	7.4917574E-01
29	25.5	1.2921745E+01	7.7120694E-01
29	26	1.3227143E+01	7.8977540E-01
29	26.5	1.3465123E+01	8.0618969E-01
29	27	1.3646836E+01	8.2141264E-01
29	27.5	1.3780613E+01	8.3607914E-01
29	28	1.3881069E+01	8.5140822E-01
29	28.5	1.3964052E+01	8.6805921E-01
29	29	1.4034639E+01	8.8360832E-01
29	29.5	1.4080755E+01	8.8830231E-01
29	30	1.4116708E+01	8.9095480E-01
29	30.5	1.4148847E+01	8.9497874E-01
29	31	1.4166043E+01	8.9418558E-01
29	31.5	1.4172463E+01	8.9116819E-01
29	32	1.4173787E+01	8.9066072E-01
29	32.5	1.4160497E+01	8.9239996E-01
29	33	1.4102040E+01	8.9275459E-01
29	33.5	1.3988448E+01	8.9024168E-01
29	34	1.3818975E+01	8.8488306E-01
29	34.5	1.3596579E+01	8.7874818E-01
29	35	1.3203437E+01	8.6277203E-01
29	35.5	1.2639808E+01	8.3369160E-01
29	36	1.2072868E+01	8.0293382E-01
29	36.5	1.1521064E+01	7.7166243E-01
29	37	1.0989373E+01	7.4031095E-01
28.5	25	1.2344094E+01	7.3901199E-01
28.5	25.5	1.2709525E+01	7.6074107E-01

28.5	26	1.3011215E+01	7.7978407E-01
28.5	26.5	1.3251983E+01	7.9702569E-01
28.5	27	1.3439752E+01	8.1335689E-01
28.5	27.5	1.3583238E+01	8.2957500E-01
28.5	28	1.3694254E+01	8.4663759E-01
28.5	28.5	1.3784760E+01	8.6512180E-01
28.5	29	1.3861637E+01	8.8489052E-01
28.5	29.5	1.3900583E+01	8.8808915E-01
28.5	30	1.3924179E+01	8.9028245E-01
28.5	30.5	1.3939640E+01	8.9403746E-01
28.5	31	1.3949557E+01	8.9431959E-01
28.5	31.5	1.3957359E+01	8.9188490E-01
28.5	32	1.3959806E+01	8.9130934E-01
28.5	32.5	1.3948902E+01	8.9284143E-01
28.5	33	1.3907906E+01	8.9501244E-01
28.5	33.5	1.3809111E+01	8.9406656E-01
28.5	34	1.3630527E+01	8.8664375E-01
28.5	34.5	1.3386038E+01	8.7768692E-01
28.5	35	1.3005058E+01	8.6119571E-01
28.5	35.5	1.2494264E+01	8.3502116E-01
28.5	36	1.1954913E+01	8.0534079E-01
28.5	36.5	1.1420842E+01	7.7438106E-01
28.5	37	1.0901935E+01	7.4296557E-01
28	25	1.2144229E+01	7.2888645E-01
28	25.5	1.2495626E+01	7.5038279E-01
28	26	1.2791678E+01	7.6977929E-01
28	26.5	1.3032871E+01	7.8774709E-01
28	27	1.3224817E+01	8.0508886E-01
28	27.5	1.3375230E+01	8.2259024E-01
28	28	1.3493625E+01	8.4097970E-01
28	28.5	1.3588775E+01	8.6042441E-01

28	29	1.3662839E+01	8.7865123E-01
28	29.5	1.3701451E+01	8.8534573E-01
28	30	1.3715467E+01	8.8888817E-01
28	30.5	1.3714999E+01	8.9396913E-01
28	31	1.3715946E+01	8.9525127E-01
28	31.5	1.3723601E+01	8.9255391E-01
28	32	1.3724748E+01	8.9208979E-01
28	32.5	1.3715483E+01	8.9355890E-01
28	33	1.3687138E+01	8.9681664E-01
28	33.5	1.3603955E+01	8.9780191E-01
28	34	1.3412273E+01	8.8771050E-01
28	34.5	1.3155547E+01	8.7691183E-01
28	35	1.2788896E+01	8.5993781E-01
28	35.5	1.2321005E+01	8.3549617E-01
28	36	1.1813403E+01	8.0688016E-01
28	36.5	1.1301281E+01	7.7628019E-01
28	37	1.0798457E+01	7.4483160E-01
27.5	25	1.1943228E+01	7.1885540E-01
27.5	25.5	1.2281529E+01	7.4016565E-01
27.5	26	1.2570910E+01	7.5983815E-01
27.5	26.5	1.2810732E+01	7.7842464E-01
27.5	27	1.3004933E+01	7.9663768E-01
27.5	27.5	1.3159873E+01	8.1518491E-01
27.5	28	1.3283113E+01	8.3458240E-01
27.5	28.5	1.3380872E+01	8.5452572E-01
27.5	29	1.3452829E+01	8.7202003E-01
27.5	29.5	1.3490256E+01	8.8145212E-01
27.5	30	1.3496572E+01	8.8677676E-01
27.5	30.5	1.3480867E+01	8.9386868E-01
27.5	31	1.3471423E+01	8.9635664E-01
27.5	31.5	1.3477567E+01	8.9294932E-01

27.5	32	1.3474121E+01	8.9312339E-01
27.5	32.5	1.3463673E+01	8.9433344E-01
27.5	33	1.3437727E+01	8.9662690E-01
27.5	33.5	1.3355807E+01	8.9668922E-01
27.5	34	1.3172735E+01	8.8807185E-01
27.5	34.5	1.2916594E+01	8.7694295E-01
27.5	35	1.2565333E+01	8.5945165E-01
27.5	35.5	1.2131026E+01	8.3577224E-01
27.5	36	1.1654464E+01	8.0788856E-01
27.5	36.5	1.1166182E+01	7.7752583E-01
27.5	37	1.0681564E+01	7.4599027E-01
27	25	1.1742384E+01	7.0895063E-01
27	25.5	1.2068383E+01	7.3010360E-01
27	26	1.2350529E+01	7.4999038E-01
27	26.5	1.2587623E+01	7.6908683E-01
27	27	1.2782375E+01	7.8802119E-01
27	27.5	1.2939829E+01	8.0741000E-01
27	28	1.3065948E+01	8.2761972E-01
27	28.5	1.3165298E+01	8.4815968E-01
27	29	1.3236996E+01	8.6636257E-01
27	29.5	1.3272930E+01	8.7776941E-01
27	30	1.3272349E+01	8.8387190E-01
27	30.5	1.3246993E+01	8.9121460E-01
27	31	1.3228034E+01	8.9450788E-01
27	31.5	1.3224823E+01	8.9262089E-01
27	32	1.3212466E+01	8.9448140E-01
27	32.5	1.3198236E+01	8.9517625E-01
27	33	1.3169026E+01	8.9509033E-01
27	33.5	1.3086046E+01	8.9362931E-01
27	34	1.2920414E+01	8.8805852E-01
27	34.5	1.2673786E+01	8.7782989E-01

27	35	1.2337792E+01	8.5953469E-01
27	35.5	1.1931137E+01	8.3608704E-01
27	36	1.1483309E+01	8.0857807E-01
27	36.5	1.1019167E+01	7.7822784E-01
27	37	1.0553857E+01	7.4649155E-01
26.5	25	1.1542703E+01	6.9918933E-01
26.5	25.5	1.1857090E+01	7.2019916E-01
26.5	26	1.2131704E+01	7.4024347E-01
26.5	26.5	1.2365059E+01	7.5974299E-01
26.5	27	1.2558939E+01	7.7925029E-01
26.5	27.5	1.2717246E+01	7.9930069E-01
26.5	28	1.2844685E+01	8.2019098E-01
26.5	28.5	1.2944930E+01	8.4154166E-01
26.5	29	1.3017693E+01	8.6145968E-01
26.5	29.5	1.3053085E+01	8.7480082E-01
26.5	30	1.3045435E+01	8.8016558E-01
26.5	30.5	1.3015332E+01	8.8590645E-01
26.5	31	1.2988057E+01	8.8966351E-01
26.5	31.5	1.2969344E+01	8.9129304E-01
26.5	32	1.2943887E+01	8.9617149E-01
26.5	32.5	1.2925077E+01	8.9602384E-01
26.5	33	1.2893256E+01	8.9335619E-01
26.5	33.5	1.2812542E+01	8.9083880E-01
26.5	34	1.2662504E+01	8.8780671E-01
26.5	34.5	1.2430018E+01	8.7934185E-01
26.5	35	1.2107966E+01	8.5968560E-01
26.5	35.5	1.1725471E+01	8.3644016E-01
26.5	36	1.1304013E+01	8.0903604E-01
26.5	36.5	1.0863438E+01	7.7842199E-01
26.5	37	1.0417770E+01	7.4634501E-01
26	25	1.1344981E+01	6.8958004E-01

26	25.5	1.1648369E+01	7.1044929E-01
26	26	1.1915319E+01	7.3059578E-01
26	26.5	1.2144189E+01	7.5039520E-01
26	27	1.2336058E+01	7.7033250E-01
26	27.5	1.2493864E+01	7.9087454E-01
26	28	1.2621309E+01	8.1229841E-01
26	28.5	1.2721561E+01	8.3446333E-01
26	29	1.2795766E+01	8.5656817E-01
26	29.5	1.2832812E+01	8.7264250E-01
26	30	1.2816331E+01	8.7554670E-01
26	30.5	1.2781599E+01	8.7988925E-01
26	31	1.2746060E+01	8.8437285E-01
26	31.5	1.2713810E+01	8.8885647E-01
26	32	1.2674372E+01	8.9710519E-01
26	32.5	1.2651185E+01	8.9600221E-01
26	33	1.2616913E+01	8.9153877E-01
26	33.5	1.2539368E+01	8.8792242E-01
26	34	1.2401708E+01	8.8605897E-01
26	34.5	1.2184408E+01	8.7945897E-01
26	35	1.1876854E+01	8.5924755E-01
26	35.5	1.1516780E+01	8.3677147E-01
26	36	1.1119700E+01	8.0924927E-01
26	36.5	1.0701711E+01	7.7806350E-01
26	37	1.0275489E+01	7.4551889E-01
25.5	25	1.1149854E+01	6.8012657E-01
25.5	25.5	1.1442797E+01	7.0084919E-01
25.5	26	1.1702062E+01	7.2104344E-01
25.5	26.5	1.1925915E+01	7.4104483E-01
25.5	27	1.2114885E+01	7.6127625E-01
25.5	27.5	1.2271101E+01	7.8214179E-01
25.5	28	1.2397411E+01	8.0390069E-01

25.5	28.5	1.2496453E+01	8.2657133E-01
25.5	29	1.2570130E+01	8.5006114E-01
25.5	29.5	1.2609575E+01	8.6927553E-01
25.5	30	1.2584663E+01	8.6956587E-01
25.5	30.5	1.2545685E+01	8.7357861E-01
25.5	31	1.2502548E+01	8.7904008E-01
25.5	31.5	1.2460058E+01	8.8534118E-01
25.5	32	1.2415306E+01	8.9344346E-01
25.5	32.5	1.2382858E+01	8.9393936E-01
25.5	33	1.2343530E+01	8.8953026E-01
25.5	33.5	1.2269186E+01	8.8443657E-01
25.5	34	1.2138979E+01	8.8130514E-01
25.5	34.5	1.1932748E+01	8.7443634E-01
25.5	35	1.1645737E+01	8.5784049E-01
25.5	35.5	1.1307175E+01	8.3708743E-01
25.5	36	1.0932812E+01	8.0910112E-01
25.5	36.5	1.0536249E+01	7.7702531E-01
25.5	37	1.0128924E+01	7.4394738E-01
25	25	1.0957835E+01	6.7083047E-01
25	25.5	1.1240842E+01	6.9139450E-01
25	26	1.1492479E+01	7.1158387E-01
25	26.5	1.1710955E+01	7.3169605E-01
25	27	1.1896358E+01	7.5209495E-01
25	27.5	1.2050133E+01	7.7312001E-01
25	28	1.2174352E+01	7.9498238E-01
25	28.5	1.2270909E+01	8.1767333E-01
25	29	1.2340477E+01	8.4072519E-01
25	29.5	1.2372184E+01	8.5797336E-01
25	30	1.2351017E+01	8.6193624E-01
25	30.5	1.2309075E+01	8.6692659E-01
25	31	1.2259127E+01	8.7366777E-01

25	31.5	1.2208837E+01	8.8113110E-01
25	32	1.2161666E+01	8.8829241E-01
25	32.5	1.2120565E+01	8.9074940E-01
25	33	1.2075170E+01	8.8739097E-01
25	33.5	1.2004649E+01	8.8014924E-01
25	34	1.1879799E+01	8.7479432E-01
25	34.5	1.1683968E+01	8.6773949E-01
25	35	1.1416696E+01	8.5554941E-01
25	35.5	1.1098451E+01	8.3748739E-01
25	36	1.0745318E+01	8.0830631E-01
25	36.5	1.0368920E+01	7.7510583E-01
25	37	9.9797099E+00	7.4154701E-01
24.5	25	1.0769336E+01	6.6169258E-01
24.5	25.5	1.1042884E+01	6.8208256E-01
24.5	26	1.1287010E+01	7.0221736E-01
24.5	26.5	1.1499886E+01	7.2235742E-01
24.5	27	1.1681242E+01	7.4280941E-01
24.5	27.5	1.1831942E+01	7.6384359E-01
24.5	28	1.1953348E+01	7.8559022E-01
24.5	28.5	1.2046497E+01	8.0788096E-01
24.5	29	1.2110451E+01	8.2961099E-01
24.5	29.5	1.2136177E+01	8.4566090E-01
24.5	30	1.2117737E+01	8.5305426E-01
24.5	30.5	1.2073716E+01	8.5989353E-01
24.5	31	1.2017433E+01	8.6825647E-01
24.5	31.5	1.1960411E+01	8.7674035E-01
24.5	32	1.1911513E+01	8.8326120E-01
24.5	32.5	1.1864604E+01	8.8715669E-01
24.5	33	1.1813637E+01	8.8509396E-01
24.5	33.5	1.1748417E+01	8.7483897E-01
24.5	34	1.1628382E+01	8.6752263E-01

24.5	34.5	1.1442415E+01	8.6059299E-01
24.5	35	1.1191918E+01	8.5227242E-01
24.5	35.5	1.0892156E+01	8.3802698E-01
24.5	36	1.0558847E+01	8.0629479E-01
24.5	36.5	1.0201259E+01	7.7206498E-01
24.5	37	9.8292253E+00	7.3824154E-01
24	25	1.0584688E+01	6.5271388E-01
24	25.5	1.0849228E+01	6.7291279E-01
24	26	1.1086007E+01	6.9294742E-01
24	26.5	1.1293172E+01	7.1304208E-01
24	27	1.1470162E+01	7.3344794E-01
24	27.5	1.1617351E+01	7.5436402E-01
24	28	1.1735475E+01	7.7582480E-01
24	28.5	1.1824801E+01	7.9748590E-01
24	29	1.1883514E+01	8.1796090E-01
24	29.5	1.1905206E+01	8.3366042E-01
24	30	1.1887524E+01	8.4351124E-01
24	30.5	1.1841677E+01	8.5247561E-01
24	31	1.1779175E+01	8.6278106E-01
24	31.5	1.1715215E+01	8.7252883E-01
24	32	1.1666606E+01	8.7819471E-01
24	32.5	1.1618788E+01	8.8211921E-01
24	33	1.1564215E+01	8.8086528E-01
24	33.5	1.1502708E+01	8.6817324E-01
24	34	1.1386462E+01	8.5957883E-01
24	34.5	1.1209275E+01	8.5274890E-01
24	35	1.0973124E+01	8.4696929E-01
24	35.5	1.0689771E+01	8.3734871E-01
24	36	1.0374743E+01	8.0224623E-01
24	36.5	1.0034500E+01	7.6770493E-01
24	37	9.6786147E+00	7.3398995E-01

23.5	25	1.0404158E+01	6.4389597E-01
23.5	25.5	1.0660119E+01	6.6388671E-01
23.5	26	1.0889751E+01	6.8378059E-01
23.5	26.5	1.1091184E+01	7.0376695E-01
23.5	27	1.1263623E+01	7.2404441E-01
23.5	27.5	1.1407036E+01	7.4474357E-01
23.5	28	1.1521642E+01	7.6580924E-01
23.5	28.5	1.1607132E+01	7.8677717E-01
23.5	29	1.1661449E+01	8.0629530E-01
23.5	29.5	1.1680195E+01	8.2199614E-01
23.5	30	1.1662388E+01	8.3365432E-01
23.5	30.5	1.1614932E+01	8.4463937E-01
23.5	31	1.1546378E+01	8.5708911E-01
23.5	31.5	1.1473840E+01	8.6870717E-01
23.5	32	1.1428968E+01	8.7277122E-01
23.5	32.5	1.1386557E+01	8.7446428E-01
23.5	33	1.1334182E+01	8.7157128E-01
23.5	33.5	1.1268567E+01	8.5998764E-01
23.5	34	1.1154643E+01	8.5087748E-01
23.5	34.5	1.0984999E+01	8.4394352E-01
23.5	35	1.0761401E+01	8.3847623E-01
23.5	35.5	1.0493513E+01	8.2746783E-01
23.5	36	1.0194018E+01	7.9566051E-01
23.5	36.5	9.8696164E+00	7.6196833E-01
23.5	37	9.5288139E+00	7.2880752E-01
23	25	1.0227953E+01	6.3524109E-01
23	25.5	1.0475747E+01	6.5500763E-01
23	26	1.0698459E+01	6.7472570E-01
23	26.5	1.0894212E+01	6.9455151E-01
23	27	1.1062023E+01	7.1463539E-01
23	27.5	1.1201537E+01	7.3504707E-01

23	28	1.1312568E+01	7.5566107E-01
23	28.5	1.1394437E+01	7.7596359E-01
23	29	1.1445174E+01	7.9478599E-01
23	29.5	1.1461729E+01	8.1060951E-01
23	30	1.1443646E+01	8.2360970E-01
23	30.5	1.1395189E+01	8.3629426E-01
23	31	1.1321677E+01	8.5078382E-01
23	31.5	1.1236981E+01	8.6539013E-01
23	32	1.1201059E+01	8.6657090E-01
23	32.5	1.1166382E+01	8.6507069E-01
23	33	1.1116005E+01	8.6055606E-01
23	33.5	1.1045662E+01	8.5051814E-01
23	34	1.0932926E+01	8.4141279E-01
23	34.5	1.0769659E+01	8.3416707E-01
23	35	1.0557047E+01	8.2758235E-01
23	35.5	1.0302925E+01	8.1458793E-01
23	36	1.0017311E+01	7.8693207E-01
23	36.5	9.7073482E+00	7.5497944E-01
23	37	9.3805769E+00	7.2277003E-01
22.5	25	1.0056235E+01	6.2675218E-01
22.5	25.5	1.0296260E+01	6.4628026E-01
22.5	26	1.0512299E+01	6.6579315E-01
22.5	26.5	1.0702478E+01	6.8541636E-01
22.5	27	1.0865670E+01	7.0525738E-01
22.5	27.5	1.1001270E+01	7.2533536E-01
22.5	28	1.1108794E+01	7.4547800E-01
22.5	28.5	1.1187359E+01	7.6517610E-01
22.5	29	1.1235208E+01	7.8348141E-01
22.5	29.5	1.1250190E+01	7.9943714E-01
22.5	30	1.1232098E+01	8.1340101E-01
22.5	30.5	1.1183688E+01	8.2733248E-01

22.5	31	1.1108121E+01	8.4322714E-01
22.5	31.5	1.1007819E+01	8.6201623E-01
22.5	32	1.0986500E+01	8.5882658E-01
22.5	32.5	1.0956780E+01	8.5477720E-01
22.5	33	1.0906783E+01	8.4920925E-01
22.5	33.5	1.0833069E+01	8.4017861E-01
22.5	34	1.0720976E+01	8.3128459E-01
22.5	34.5	1.0563092E+01	8.2361883E-01
22.5	35	1.0360006E+01	8.1568462E-01
22.5	35.5	1.0117918E+01	8.0171475E-01
22.5	36	9.8450089E+00	7.7690263E-01
22.5	36.5	9.5482481E+00	7.4699167E-01
22.5	37	9.2345034E+00	7.1600034E-01
22	25	9.8891248E+00	6.1843265E-01
22	25.5	1.0121762E+01	6.3771024E-01
22	26	1.0331390E+01	6.5699412E-01
22	26.5	1.0516143E+01	6.7638202E-01
22	27	1.0674790E+01	6.9594463E-01
22	27.5	1.0806538E+01	7.1566165E-01
22	28	1.0910701E+01	7.3533499E-01
22	28.5	1.0986305E+01	7.5449208E-01
22	29	1.1031843E+01	7.7238828E-01
22	29.5	1.1045791E+01	7.8842882E-01
22	30	1.1028146E+01	8.0302770E-01
22	30.5	1.0981028E+01	8.1770306E-01
22	31	1.0907485E+01	8.3395783E-01
22	31.5	1.0817972E+01	8.5051692E-01
22	32	1.0787855E+01	8.4885012E-01
22	32.5	1.0757317E+01	8.4381312E-01
22	33	1.0706163E+01	8.3770335E-01
22	33.5	1.0629941E+01	8.2930850E-01

22	34	1.0518310E+01	8.2065038E-01
22	34.5	1.0365016E+01	8.1256015E-01
22	35	1.0170187E+01	8.0350687E-01
22	35.5	9.9387012E+00	7.8908654E-01
22	36	9.6773784E+00	7.6624318E-01
22	36.5	9.3927247E+00	7.3829433E-01
22	37	9.0910651E+00	7.0864534E-01

The 2nd degree Regression program

```
data=[
22.42220656    31.56257439    9.779
24.04136006    32.83279881    11.049
23.94075962    35.39737026    10.668
26.01743489    34.32120541    12.741
25.95557459    32.1567373  12.158
25.54362634    29.40292571    13.172
28.50722574    29.09683186    14.219
27.26752505    30.77961543    12.751
27.88018525    33.36176734    14.644
29.35002641    34.77239062    17
31.119385   34.18206764    17.026
30.11931048    32.60623372    16.206
31.59594524    31.08031289    17.826
29.83415834    30.60113085    14.945
30.84238708    28.93530621    15.067
31.32750394    27.07195173    17.242
31.43784546    25.39863386    19.33
];
%=======================================================
%          initial parameters
%          ==================
par=[1;1;1;1;1;1];
%=======================================================
%      getting the size of data
%      ========================
```

```
[n,m]=size(data);
%=====================================================
%        Deree of fredom
%        ===============
r=n-6;
%=====================================================
%        least squre solution
%        ====================
%==============coef.matrix============================
A=-eye(n);
%==============matrix of parameter====================
for i=1:n
  B(i,1)=1;
  B(i,2)=data(i,2);
  B(i,3)=data(i,1);
  B(i,4)=(data(i,2))^2;
  B(i,5)=data(i,1)*data(i,2);
  B(i,6)=(data(i,1))^2;
end
%=========== vector of constant=====================
for i=1:n
  F(i,1)=data(i,3)-par(1,1)-par(2,1)*data(i,2)-par(3,1)*data(i,1)-
par(4,1)*(data(i,2))^2-par(5,1)*data(i,1)*data(i,2)-par(6,1)*(data(i,1))^2;
end
%=====================================================
%            THE ITTERATION
%            ==============
for k=1:3
  itteration=k
%=====================================================
%       constructing the F matrix
%       =========================
for i=1:n
  F(i,1)=data(i,3)-par(1,1)-par(2,1)*data(i,2)-par(3,1)*data(i,1)-
par(4,1)*(data(i,2))^2-par(5,1)*data(i,1)*data(i,2)-par(6,1)*(data(i,1))^2;
end
%=====================================================
```

```
covar=eye(n);
%=================================================
%          ==weight matrix==
W=inv(covar);
WE=inv(A*covar*A');
%======THE STEPS OF SOLUTION=====
N=B'*WE*B;
T=B'*WE*F;
delta=inv(N)*T;
par=par+delta
covp=inv(N);
STP=sqrt(diag(covp))
V=covar*A'*WE*(-B*delta+F)
VV=covar*A'*WE*A*covar-covar*A'*WE*B*covp*B'*WE*A*covar;
covar=covar+VV;
standobs=sqrt(diag(covar));
%=========================================================
%      calculate of the adjusted undulation
%=========================================================
%     ======================================
for i=1:n
  data(i,3)=data(i,3)+V(i,1);
end
%=========================================================
%             the posterir covariance
%             ========================
S=(V'*W*V/r)^0.50
S^2
%=========================================================%
% RUNING THE FISHER TEST AT 98% CONF.INTERVAL
% ==========================================
if S>1
  if S^2>2.25
     covar=(S^2)*covar;
     standobs=sqrt(diag(covar));
     STP=(S)*(sqrt(diag(covp)));
     VVV=(S^2)*VV;
```

```
    'TRUE1'
  end
end
if S<1
  if 1/S^2>3.6
    covar=(S^2)*covar;
    standobs=sqrt(diag(covar));
    STP=(S)*(sqrt(diag(covp)));
    VVV=(S^2)*VV;
    'TRUE2'
  end
end
%=========================================================
%         TESTING ON PARAMETER
%           BY T-DIST.
%  WITH CONFEEDENCE INTERVAL 99%
%  ======================================================
for m=1:6
  T(m,1)=par(m,1)/(S*STP(m,1));
  if T(m,1)>3.106|T(m,1)<-3.106
    m
    T(m,1)
    'a uesful prdiction'
  else
    m
    T(m,1)
    'a negligble prediction'
  end

end
par
end
%      THE DISTORTION
%      ==========================
olddata=[
30.23217626    29.8403536  15.088
22.75219208    31.8487423  11.156
```

```
22.10780524    31.55221497    9.974
22.20600411    31.55488274    10.092
24.15512048    32.9681639  11.397
25.64815136    32.69335337    12.02
23.42944351    32.82672968    10.098
27.32523257    31.1885972  12.842
27.41194086    30.54339346    13.488
29.01809103    31.15964886    15.216
28.18461073    30.80461709    13.738
30.02873878    31.27767502    15.268
];
[n,m]=size(olddata);
for i=1:n
newdata(i,1)=par(1,1)+par(2,1)*olddata(i,2)+par(3,1)*olddata(i,1)+par(4,1)*(ol
ddata(i,2))^2+par(5,1)*olddata(i,1)*olddata(i,2)+par(6,1)*(olddata(i,1))^2;
end
newdata
for i=1:n
  dist(i,1)=newdata(i,1)-olddata(i,3);
end
dist
end
```

The LSC program

```
data=[
22.42220656    31.56257439    284.817 09.779
24.04136006    32.83279881    207.162 11.049
23.94075962    35.39737026    084.248 10.668
26.01743489    34.32120541    023.977 12.741
25.95557459    32.15673730    323.067 12.158
25.54362634    29.40292571    569.843 13.172
28.50722574    29.09683186    284.916 14.219
27.26752505    30.77961543    223.345 12.751
27.88018525    33.36176734    063.896 14.644
29.35002641    34.77239062    061.948 17.000
31.11938500    34.18206764    123.810 17.026
30.11931048    32.60623372    055.917 16.206
31.59594524    31.08031289    032.061 17.826
```

```
29.83415834    30.60113085    230.875 14.945
30.84238708    28.93530621    042.806 15.067
31.32750394    27.07195173    138.281 17.242
31.43784546    25.39863386    047.549 19.330
];
%-------------------------------------------------
%Collecting the geographical cordinates of the grid
%-------------------------------------------------
gride=[
25.5   25 0
25.5   25.5   0
25.5   26 0
25.5   26.5   0
];
%-------------------------------------------------
% input the number of points
%-------------------------------------------------
[n,m]=size(data);
[n11,m11]=size(gride);
Dg =n^2-2;
%-------------------------------------------------
%converting the angles to radians
%-------------------------------------------------
  data(1:n,1)=data(1:n,1)*pi/180;
  data(1:n,2)=data(1:n,2)*pi/180;
  gride(1:n11,1)=gride(1:n11,1)*pi/180;
  gride(1:n11,2)=gride(1:n11,2)*pi/180;
%-------------------------------------------------
%collecting the ellipsoid constants
%-------------------------------------------------
wec=[6378137,0,0.00335281,0,0];
%-------------------------------------------------
%calculating the ellipse constants
%-------------------------------------------------
wec(1,2)=wec(1,1)-wec(1,1)*wec(1,3);
wec(1,4)=1/0.00335281;
wec(1,5)=2*wec(1,3)-(wec(1,3))^2;
```

```
%-----------------------------------------------------
%converting from geodetic to cartesian coordintes
%-----------------------------------------------------
%first  calculating the v vector
for m=1:n
wv(m,1)=(wec(1,1)/(sqrt(1-wec(1,5)*(sin(data(m,1)))^2)));
end

for m=1:n11
gv(m,1)=(wec(1,1)/(sqrt(1-wec(1,5)*(sin(gride(m,1)))^2)));
end
%Second  calculating the cartesian cooordinates
for m=1:n
   wca(1,m)=(wv(m,1)+data(m,3))*cos(data(m,1))*cos(data(m,2));
   wca(2,m)=(wv(m,1)+data(m,3))*cos(data(m,1))*sin(data(m,2));
   wca(3,m)=((1-wec(1,5))*wv(m,1)+data(m,3))*sin(data(m,1));
end
for m=1:n11
   gca(1,m)=(gv(m,1)+gride(m,3))*cos(gride(m,1))*cos(gride(m,2));
   gca(2,m)=(gv(m,1)+gride(m,3))*cos(gride(m,1))*sin(gride(m,2));
   gca(3,m)=((1-wec(1,5))*gv(m,1)+gride(m,3))*sin(gride(m,1));
 end
wca=wca';
gca=gca';
Owca=wca;
Ogca=gca;
Owca;
Ogca;
%-------------------------------------------------------------------------
for i=1:n
   def(i,1)=0;
   def(i,2)=0;
   def(i,3)=0.000001*data(i,4);
end
def;
%-----------------------------------------------------------------
k=1;
```

```
for i=1:n
  for j=i:n
  C(k,1)=0.000001*(sqrt((wca(i,1)-wca(j,1))^2+(wca(i,2)-wca(j,2))^2));
  C(k,2)=(def(i,1)*def(j,1))/2;
  C(k,3)=(def(i,2)*def(j,2))/2;
  C(k,4)=(def(i,3)*def(j,3))/2;
  C(k,5)=(def(i,1))^2+(def(j,1))^2;
  C(k,6)=(def(i,2))^2+(def(j,2))^2;
  C(k,7)=(def(i,3))^2+(def(j,3))^2;
  k=k+1;
  end
k=k;
end
k=1;
for i=1:n
  for j=1:n11
    C1(k,1)=0.000001*(sqrt((wca(i,1)-gca(j,1))^2+(wca(i,2)-gca(j,2))^2));
    k=k+1;
  end
  k=k;
end
k=1;
for i=1:n11
  for j=i:n11
    C2(k,1)=0.000001*(sqrt((gca(i,1)-gca(j,1))^2+(gca(i,2)-gca(j,2))^2));
    k=k+1;
  end
  k=k;
end
[n,m]=size(C);
%---------------------------------------------------------------------------
% Initial value of a & b in equation   c = a*e^-br
%---------------------------------------------------------------------------
factor=[
  1
  1
];
```

```
%--------------------------------------------------------------------------
for i=1:n
   COVA(i,i)=C(i,g+3);
end
%--------------------------------------------------------------------------
% apirior variance s
%--------------------------------------------------------------------------
s=1;
%--------------------------------------------------------------------
COVAR = s^2*COVA;
 %--------------------------------------------------------------------------
 for b= 1:1
   itteration=b
%--------------------------------------------------------------------------
for i=1:n
   B(i,1)=exp(-factor(2,1)*C(i,1));
   B(i,2)=-factor(1,1)*C(i,1)*exp(-factor(2,1)*C(i,1));
end
%-----------------------------------------------------------------------------------
for i=1:n
   F(i,1)=C(i,g);
end
%--------------------------------------------------------------------------
W=inv(COVAR);
COVA=(1/s^2)*COVAR;
%--------------------------------------------------------------------------
N=B'*W*B;
T=B'*W*F;
delta=inv(N)*T;
factor=factor+delta;
covp=inv(N);
stp=sqrt(diag(covp));
V=F-B*factor;
VV=COVA-B*covp*B';
COVA=COVA+VV;
%--------------------------------------------------------------------------
for i=1:n
```

```
  C(i,g)=C(i,g)-V(i,1);
end
%---------------------------------------------------------------------
s=(V'*W*V/Dg)^0.5
s^2
%---------------------------------------------------------------------
% Runing the Fisher Test at 99% confedance interval for posterior varaiance
%---------------------------------------------------------------------
if s > 1
  if s^2 > 1
    COVAR=(s^2)*COVA;
    stp=sqrt((s^2)*diag(covp));
    VVV=(s^2)*VV;
  end
        'true1';
end
if s < 1     if 1/s^2 > 1
    COVAR=(s^2)*COVA;
    stp=sqrt((s^2)*diag(covp));
    VVV=(s^2)*VV;
  end
    'true2';
end
stp;
factor
end
%---------------------------------------------------------------------
for i=1:n
  C(i,8)=factor(1,1)*exp(-factor(2,1)*C(i,1));
end
[n11,m11]=size(C1);

for i=1:n11
  C1(i,2)=factor(1,1)*exp(-factor(2,1)*C1(i,1));
end
[n11,m11]=size(C2);
```

```
for i=1:n11
  C2(i,2)=factor(1,1)*exp(-factor(2,1)*C2(i,1));
end
C3=[C(:,1) C(:,8)
  C1
  C2
  ];
%---------------------------------------------------------------------------
% graph and list the results
%---------------------------------------------------------------------------
plot(1000000*C3(:,1),C3(:,2),'+')
title('Distance-Variance Relationship')
xlabel('Distance (m)')
ylabel('Variance')
grid
%---------------------------------------------------------------------------
[n1,m1]=size(data);
k=1;
for i=1:n
  for j=i:n1
    Cs1(i,j)=C(k,8);
    Cs1(j,i)=Cs1(i,j);
    k=k+1;
  end
  k=k;
end
%---------------------------------------------------------------------------
[n11,m11]=size(gride);
[n,m]=size(C2);
k=1;
for i=1:n11
  for j=i:n11
    C22(i,j)=C2(k,2);
    C22(j,i)=C22(i,j);
    k=k+1;
  end
  k=k;
```

```
end
%-------------------------------------------------------------------------------
[n11,m11]=size(gride);
[n1,m1]=size(data);
k=1;
for i=1:n1
  for j=1:n11
    Cs12(i,j)= C1(k,2);
    k=k+1;
  end
  k=k;
end
Cs21=Cs12';
%-------------------------------------------------------------------------------
[n,m]=size(data);
Cn=eye(n,n);
%-------------------------------------------------------------------------------
Cs=[
  Cs1 Cs12
  Cs21 C22
  ];
%-------------------------------------------------------------------------------
D=[eye(n,n) zeros(n,n11)];
%-------------------------------------------------------------------------------
COL1=Cn+Cs1;
COL2=inv(COL1);
COL3=1000000*(Cs*D'*COL2*def(:,g-1));
[n,m]=size(COL3);
for i=1:n-15
  COL33(i,1)=COL3(15+i,1);
end
COL33;
COL4=Cs*D'*COL2*D*Cs;
[n,m]=size(COL4);
for i=1:n-15
    COL44(i,1)=sqrt(COL4(15+i,15+i));
end
```

```
COL44;
COL5=(Cn*COL2*def(:,g-1));
COL6=Cn*COL2*Cn;
COL66=sqrt(diag(COL6))
%-------------------------------------------------------------------------%
% saving data
%-------------------------------------------------------------------------
save c:\COL33.dat COL33 /ascii;
save c:\COL44.dat COL44 /ascii;
save c:\COL5.dat COL5 /ascii;
save c:\COL66.dat COL66 /ascii;
%-------------------------------------------------------------------------
%Calculation of posterior variance
%S=(COL33'*COL66*COL33)/437;
%s=sqrt(S);
%-------------------------------------------------------------------------
end
```

The MCS program

```
data=[
22.42220656    31.56257439    284.817 09.779
24.04136006    32.83279881    207.162 11.049
23.94075962    35.39737026    084.248 10.668
26.01743489    34.32120541    023.977 12.741
25.95557459    32.15673730    323.067 12.158
25.54362634    29.40292571    569.843 13.172
28.50722574    29.09683186    284.916 14.219
27.26752505    30.77961543    223.345 12.751
27.88018525    33.36176734    063.896 14.644
29.35002641    34.77239062    061.948 17.000
31.11938500    34.18206764    123.810 17.026
30.11931048    32.60623372    055.917 16.206
31.59594524    31.08031289    032.061 17.826
29.83415834    30.60113085    230.875 14.945
30.84238708    28.93530621    042.806 15.067
31.32750394    27.07195173    138.281 17.242
31.43784546    25.39863386    047.549 19.330
```

```
];
[n,m]=size(data);
%-------------------------------------------------------------------------
%calculating the degree of fredom
%-------------------------------------------------------------------------
dg=n-3;
%------------------------------Beging the regression step ---------------------
%entring the solutin number
%-------------------------------------------------------------------------
% getting the initial value of parameeters
%-------------------------------------------------------------------------
a=1; b=1; c=1;
%-------------------------------------------------------------------------
for i=1:n
Z(i,1)=data(i,4);
end
OZ=Z;
%-------------------------------------------------------------------------
A=eye(n);
%-------------------------------------------------------------------------
% initial value of matrix F
%-------------------------------------------------------------------------
F=eye(n,1);
%-------------------------------------------------------------------------
covar=eye(n);
%-------------------------------------------------------------------------
for i=1:n
  B(i,1)=data(i,1);
  B(i,2)=data(i,2);
  B(i,3)=1;
end
%-------------------------------------------------------------------------
%begining the itteration
%-------------------------------------------------------------------------
for k=1:2
  itteration=k
%-------------------------------------------------------------------------
```

```
for i=1:n
   F(i,1)=Z(i,1)-a*data(i,1)-b*data(i,2)-c;
end
F;
%-------------------------------------------------------------------------
W=inv(covar);
We=inv(A*covar*A');
%-------------------------------------------------------------------------
N=B'*We*B;
T=B'*We*F;
delta=inv(N)*T;
a=a+delta(1,1);
b=b+delta(2,1);
c=c+delta(3,1);
covp=inv(N);
stp=sqrt(diag(covp));
V=covar*A'*We*(-B*delta+F);
VV=covar*A'*We*A*covar-covar*A'*We*B*covp*B'*We*A*covar;
covar=covar+VV;
%-------------------------------------------------------------------------------
Z=Z(:,1)-V;
%-------------------------------------------------------------------------------------
s=(V'*W*V/dg)^0.5;
%-------------------------------------------------------------------------------
%-----------------------------------------------------------------------
% Runing the Fisher Test at 98% confedance interval
%-----------------------------------------------------------------------
if s > 1
  if s^2 > 2.08
     covar=(s^2)*covar;
      stand=sqrt(diag(covar));
      stp=(s)*(sqrt(diag(covp)));
      VVV=(s^2)*VV;
      'true1'
   end
end
if s < 1
```

```
  if 1/s^2 > 3.00
    covar=(s^2)*covar;
    stand=sqrt(diag(covar));
    stp=(s)*(sqrt(diag(covp)));
    VVV=(s^2)*VV;
    'true2'
  end
end
stp;
end
%-----------------------------------------------------------
for i=1:n
  dif(i,1)=OZ(i,1)-(a*data(i,1)+b*data(i,2)+c);
end
dif
%-----------------------------------------------------------
a1=1; b1=1; c1=1;
%-----------------------------------------------------------
A=eye(n);
%-------------------------------------------------------------
F=eye(n,1);
%-------------------------------------------------------------
covar=eye(n);
%-------------------------------------------------------------
for i=1:n
  B(i,1)=data(i,1);
  B(i,2)=data(i,2);
  B(i,3)=1;
end
%-------------------------------------------------------------------------------
%begining the itterartions
%-------------------------------------------------------------------------------
for k=1:2
  itteration=k
%-------------------------------------------------------------------
for i=1:n
  F(i,1)=dif(i,1)-a1*data(i,1)-b1*data(i,2)-c1;
```

```
end
F;
%----------------------------------------------------------------
W=inv(covar);
We=inv(A*covar*A');
%--------------------------------------------------------------------
N=B'*We*B;
T=B'*We*F;
delta=inv(N)*T;
a1=a1+delta(1,1);
b1=b1+delta(2,1);
c1=c1+delta(3,1);
covp=inv(N);
stp=sqrt(diag(covp));
V=covar*A'*We*(-B*delta+F);
VV=covar*A'*We*A*covar-covar*A'*We*B*covp*B'*We*A*covar;
covar=covar+VV;
%----------------------------------------------------------
dif=dif(:,1)-V;
%---------------------------------------------------------
s=(V'*W*V/dg)^0.5;
%------------------------------------------------------------------------------
%--------------------------------------------------------------------
% Runing the Fisher Test at 98% confedance interval
%--------------------------------------------------------------------
if s > 1
  if s^2 > 2.08
     covar=(s^2)*covar;
      stand=sqrt(diag(covar));
      stp=(s)*(sqrt(diag(covp)));
      VVV=(s^2)*VV;
      'true1'
   end
end
if s < 1
   if 1/s^2 > 3
      covar=(s^2)*covar;
```

```
      stand=sqrt(diag(covar));
      stp=(s)*(sqrt(diag(covp)));
      VVV=(s^2)*VV;
      'true2'
    end
end
stp;
end
%-------------------------------------------------------------------
Z=Z+dif
%------------------------ Begiging the MCS solution-------------------------------
Dg=353;
%-------------------------------------------------------------------------------
k=1; m=27;
for i=1:19
   for j=1:23
      U(k,m)=-4;
      U(k,m-1)=1;
      U(k,m-25)=1;
      U(k,m+1)=1;
      U(k,m+25)=1;
      k=k+1;
      m=m+1;
   end
   m=m+2;
end
U(437,525)=0;
%-------------------------------------------------------------------------------
for i=1:525
   X(i,1)=1;
   cova(i,i)=1000000;
end
%-------------------------------------------------------------------------
data1=[
32 25   22 25
32 25.5 22 25.5
32 34   22 34
```

```
];
data11=[
  22   25 22   37
  22.5 25 22.2 37
  28.5 25 28.5 37
];
[n1,m1]=size(data1);
[n2,m2]=size(data11);
k=1
for i=1:n1
  X(k,1)=a*data1(i,1)+b*data1(i,2)+c+a1*data1(i,1)+b1*data1(i,2)+c1;
  cova(k,k)=1;
  k=k+1;
end
k=501
for i=1:n1
  X(k,1)=a*data1(i,3)+b*data1(i,4)+c+a1*data1(i,3)+b1*data1(i,4)+c1;
  cova(k,k)=1;
  k=k+1;
end
k=501
for i=1:n2
  X(k,1)=a*data11(i,1)+b*data11(i,2)+c+a1*data11(i,1)+b1*data11(i,2)+c1;
  cova(k,k)=1;
  k=k-25;
end
k=525
for i=1:n2
  X(k,1)=a*data11(i,3)+b*data11(i,4)+c+a1*data11(i,3)+b1*data11(i,4)+c1;
  cova(k,k)=1;
  k=k-25;
end
%-----------------------------------
for i=1:2
  tteration = i
%--------------------------------------------------------------------------
w=inv(cova);
```

```
we=inv(U*cova*U');
%-------------------------------------------------------------------------
f=-U*X;
%-----------------------------------------------------------------
K=we*f;
v=cova*U'*K;
X=X+v;
vv=cova*U'*we*U*cova;
cova=cova+vv;
sta=sqrt(diag(cova));
%-------------------------------------------------------------------------
S=(v'*w*v/Dg)^0.5
S^2
%-----------------------------------------------------------------
% Runing the Fisher Test at 99% confedance interval for posterior varaiance
%-----------------------------------------------------------------
if S > 1
  if S^2 > 1
    cova=(S^2)*cova;
     sta=(S)*sqrt(diag(cova));

    vvv=(S^2)*vv;
  end
        'true1'
end
if S < 1
  if 1/S^2 > 1
    cova=(S^2)*cova;
    sta=(S)*sqrt(diag(cova));
    vvv=(S^2)*vv;
  end
    'true2'
end
end


%-------------------------------------------------------------------------
```

```
% saving the output data
%-------------------------------------------------------------------------
save c:\proje.dat X /ascii;
save c:\proje1.dat stand /ascii;
save c:\f.dat f /ascii;
save c:\sta.dat sta /ascii;
%-------------------------------------------------------------------------------
end
```